NACA

RESEARCH MEMORANDUM

INVESTIGATION OF THE EFFECTS OF BOMB-BAY CONFIGURATION UPON THE AERODYNAMIC CHARACTERISTICS OF A BODY WITH CIRCULAR CROSS SECTION AT SUPERSONIC SPEEDS

By Robert W. Rainey

Langley Aeronautical Laboratory
Langley Field, Va.

NATIONAL ADVISORY COMMITTEE
FOR AERONAUTICS

WASHINGTON
August 18, 1955

NATIONAL ADVISORY COMMITTEE FOR AERONAUTICS

RESEARCH MEMORANDUM

INVESTIGATION OF THE EFFECTS OF BOMB-BAY CONFIGURATION UPON THE AERODYNAMIC CHARACTERISTICS OF A BODY WITH CIRCULAR CROSS SECTION AT SUPERSONIC SPEEDS

By Robert W. Rainey

SUMMARY

An investigation has been made in the Langley 9-inch supersonic tunnel to ascertain the lift, drag, and pitching moment associated with typical body—bomb-bay combinations with and without bomb. The body had a fineness ratio of 10, and tests were made of the isolated body and the body in combination with eight bomb-bay or bomb plus bomb-bay configurations. The bomb had a closed body with fineness ratio of 5 and cruciform fins.

Measurements were made at angles of attack from -4° to 10° for the isolated body and from -4° to 6° for all the combinations of components at Mach numbers of 1.62, 1.94, and 2.40 and at Reynolds numbers of 9.0×10^6, 8.6×10^6, and 7.6×10^6, respectively, based on body length. Boundary-layer transition was induced artificially ahead of the bomb-bay location.

The results indicate that the addition of any bomb-bay or bomb plus bomb-bay configuration to the basic body at an angle of attack of 0° increased the drag and the slope of the lift curve, produced a negative lift except for the semiexternal bomb bay, and shifted the aerodynamic center rearward at all Mach numbers.

The internal-type configurations had the least drag penalty, the least aerodynamic-center shift, and, in general, the least incremental lift of the configurations envisioned to exist for a short period of time in the course of a typical mission. By adding a bomb internally, the drag penalty decreased and the lift increased.

The addition of external types of configurations to the basic body resulted in substantial drag penalties at all Mach numbers with the least drag penalty as well as the least change in lift noted for the semiexternal bomb-bay plus bomb installation.

The semiexternal bomb-bay plus bomb configuration had lower drag penalty at Mach numbers below about 2 and had incremental lift, shifts in center of pressure, and shifts in aerodynamic center at positive angles of attack throughout the Mach number range of the same order as the internal-type configurations.

INTRODUCTION

Increased attention is currently being given to the problems associated with the transport and release of bombs from aircraft operating at supersonic speeds. The release problems center on obtaining a combination of bomb and aircraft that will achieve satisfactory release characteristics with respect to both bomb and aircraft. It does not necessarily follow, however, that a combination suitable in this respect will also be free of prohibitive aerodynamic penalties during the transport phase. In the vicinity of the release point, the requirement of supersonic operation immediately before, during, and just after bomb release may greatly accentuate aerodynamic penalties. The necessity for considering the aerodynamic characteristics in addition to the release characteristics is, therefore, apparent.

A recent investigation has indicated the importance of bomb location and method of installation from the standpoint of release characteristics (ref. 1). Other investigations have shown that the location and type of installation are important to the buffet, drag, and trim characteristics (refs. 2 to 7). All of the references except references 1 and 7, however, are limited to near 0° angle of attack.

The purpose of the present investigation is to obtain information on the incremental forces associated with typical body—bomb-bay combinations with and without bomb, throughout an angle-of-attack range. Force tests were made in the Langley 9-inch supersonic tunnel using a bomb having a fineness ratio of 5 and several of the bomb-bay combinations reported in reference 1, in combination with a body having a fineness ratio of 10. Lift, drag, and pitching moments were measured at angles of attack from -4° to 10° for the isolated body and from -4° to 6° for all the combinations of components. Test Mach numbers were 1.62, 1.94, and 2.40 at Reynolds numbers of 9.0×10^6, 8.6×10^6, and 7.6×10^6, respectively, based on the body length. Boundary-layer transition was induced artificially. Some of the aerodynamic characteristics of the bomb used in this investigation were previously presented in reference 8 for a Mach number of 1.62.

SYMBOLS

C_D drag coefficient, Drag/qS

C_L lift coefficient, Lift/qS

C_{L_0} lift coefficient at $\alpha = 0^\circ$

C_m pitching-moment coefficient (referenced to 50 percent of basic body length), Pitching moment/qSl

C_{m_0} pitching-moment coefficient at $\alpha = 0^\circ$

ΔC_D incremental drag coefficient due to configuration change

ΔC_L incremental lift coefficient due to configuration change

ΔC_m incremental pitching-moment coefficient due to configuration change

$C_{L_\alpha} = \partial C_L/\partial\alpha$

$C_{m_\alpha} = \partial C_m/\partial\alpha$

$C_{m_{C_L}} = \partial C_m/\partial C_L$

l basic-body length

M free-stream Mach number

q free-stream dynamic pressure

S basic-body frontal area

x_{ac} aerodynamic-center location referenced to basic-body nose, $0.50 - C_{m_{C_L}}$

x_{cp} center-of-pressure location referenced to basic-body nose, $0.50 - C_m/C_L$

Δx_{ac} change in aerodynamic-center location due to configuration change

Δx_{cp} change in center-of-pressure location due to configuration change

α angle of attack, positive when bomb-bay location is on windward side

APPARATUS AND MODELS

Wind Tunnel

All tests were made in the Langley 9-inch supersonic tunnel which is a continuous-operation complete-return type of tunnel in which the stagnation pressure may be varied and controlled from about 1/10 atmosphere absolute to about 4 atmospheres absolute. The stagnation temperature and dewpoint may also be varied and controlled. The Mach number is varied by interchanging nozzle blocks which form test sections approximately 9 inches square.

Models

Both the basic body and the bomb were constructed of metal, and the finished exterior surfaces were smooth. The diameters of both bodies, the internal bomb-bay dimensions, and the thickness of the bomb fins were within ±0.001 inch of the specified dimensions. All other dimensions are believed to be within ±0.005 inch of the specified values.

Basic body.- The body was circular in cross section with a fineness ratio of 10 (see fig. 1(a)). This body consisted of a conical nose section to station 1.701, a circular arc of revolution to station 2.697, a cylinder to station 5.000, and a circular arc of revolution to the base. The nose had a semiapex angle of 10.32°.

A removable insert located $3\frac{1}{2}$ inches behind the apex of the nose section facilitated the interchange of the various bomb-bay and bomb configurations (figs. 1(b) and 1(c)). A transition strip 1/4 inch wide and about 0.015 inch thick was located with its rear edge 1/2 inch ahead of the bomb-bay-insert opening. The strip consisted of fairly evenly distributed, pulverized salt crystals.

Bomb and bomb bays.- The bomb model used in these tests (fig. 1(d)) was 0.375 times the size of one of those reported in reference 1. It had a fineness ratio of 5. The forebody and afterbody consisted of circular arcs of revolution joining with zero slope at the station of maximum diameter (40 percent of the bomb length). The leading edges of the fins were rounded.

Two pieces of 1/64-inch-diameter piano wire were used to attach the bomb to its particular bomb-bay insert; these wires were located at 25 and 75 percent of the bomb length. When attached, the bomb was always at a 45° roll attitude; since the fin span was equal to $\sqrt{2}$ times the bomb-body diameter, the fins required the same overall width as the bomb

body. When installed internally, the bomb was symmetrically located laterally, longitudinally, and vertically within the bomb bay. The same lateral and longitudinal bomb location was also used with the external bomb bays. In every case, the bomb was installed at an angle of incidence of 0°. As with the bomb, the bomb-bay configurations were 0.375 times the size of those reported in reference 1. In the plan view the internal bomb bays were rectangular with rounded corners having 1/8-inch radii. (For instance, see configuration 6, fig. 1(b).) The transverse baffles of configurations 3 and 6 divided the bay into four compartments of equal longitudinal dimensions. In the case of configuration 7, a close fit between bomb and cavity was maintained, and no seal was used. It is believed that little flow took place between the mating parts.

Model Installation

The basic body was sting mounted to the model support of the external balance system. The sting was shielded by a movable windshield which was equipped with four pressure tubes open at the snout of the windshield to measure the model base pressure (see fig. 2). The gap between the model base and the snout of the windshield was about 0.020 inch for all tests. Once the basic body with transition strip was installed at each Mach number, it was not removed until tests of all configurations were completed. During the model installation, the model angle of attack and angle of roll were set at 0°, and a 1/16-inch-diameter mirror near the base of the model was oriented for use with an optical angle-of-attack system.

Balance System

The balance system used in these tests was a six-component, external type which utilized mechanical self-balancing beams for force measurements. In the present tests, only three of the six components were used. A detailed description of this relatively new balance system is presented in the appendix.

TESTS

The tests were conducted at Mach numbers of 1.62, 1.94, and 2.40 and at Reynolds numbers of 9.0×10^6, 8.6×10^6, and 7.6×10^6, respectively, based on body length, with boundary-layer transition induced artificially by a transition strip. Tests were also conducted using configuration 1 (basic body) without the transition strip.

As mentioned previously, the body with transition strip installed was alined in the test section at the start of a series of tests at each Mach number and was not removed until all tests for that Mach number with transition strip installed were completed. This means that any extraneous forces due to initial misalinement, arbitrary flow inclinations, or model symmetry are about constant for all tests at a particular Mach number.

Additional corrections, which have been standardized and considered routine for all sting-mounted-model tests in the Langley 9-inch supersonic tunnel, were applied to the drag of each configuration to account for the difference between free-stream pressure and (1) the measured pressure on the base annulus of the basic body and (2) the measured pressure in the fixed-windshield—shield—balance-box enclosure.

At Mach numbers of 1.62 and 2.40, after the scheduled tests had been completed, the basic body with transition was rerun. It was found that the measured drags of the repeat test checked the drag values of the initial test within the limits of experimental accuracy. This indicates that little, if any, change in the condition of the transition strip took place while tests at each Mach number were made.

Drag measurements at $M = 1.94$ and 2.41 were made of the isolated bomb at $\alpha = 0^\circ$ using the same model and apparatus reported in reference 8. This bomb model was 8.11 inches long. An internal strain-gage balance was used. These tests were conducted throughout a Reynolds number range from a value less than that of the bomb used in conjunction with the bomb bays to a value of 7.65×10^6.

PRECISION OF DATA

All models were initially referenced with respect to the tunnel walls within $\pm 0.06^\circ$; angles of attack with respect to each other were accurate to within $\pm 0.01^\circ$. Surveys of the test section indicate maximum flow inclinations of the order of $1/4^\circ$.

A summary of the estimated maximum probable errors for the tests of models using the external balance system is presented in the following table:

Test Mach number	Maximum probable errors in -				
	M	R	C_L	C_m	C_D
1.62	±0.010	$\pm 0.11 \times 10^6$	±0.003	±0.003	±0.002
1.94	±.010	±.18	±.003	±.003	±.002
2.40	±.015	±.21	±.004	±.004	±.002

A summary of the estimated probable errors for the tests of the isolated bomb model is presented in the following table:

Test Mach number	Maximum probable errors in -		
	M	R	C_D
1.62	±0.010	$\pm 0.02 \times 10^6$	±0.0005
1.94	±.010	±.02	±.0009
2.40	±.015	±.02	±.0011

PRESENTATION OF RESULTS

The measured aerodynamic characteristics are presented in figures 3, 4, and 5. The basic-body results (with and without artificial transition) are compared in figures 3(a), 4(a), and 5(a). The results of only the basic body (with artificial transition) were used.

The C_L and C_m curves of each configuration were displaced by an amount equal to that required to displace the basic-body results for C_L and C_m to zero at $\alpha = 0^\circ$ for the particular test Mach number. The magnitudes of the displacements were small as indicated below:

Test Mach number	Magnitude of displacements in -	
	C_L	C_m
1.62	-0.001	-0.002
1.94	.006	-.006
2.40	-.009	-.008

The sources of these displacements were discussed in the section entitled "Tests." Included in figures 4 and 5 (indicated as dashed lines) are small portions of the corrected C_L and C_m curves near $\alpha = 0^\circ$ in order that C_{L_0} and C_{m_0} may be correctly indicated. These are not included in figure 3 at $M = 1.62$ because the magnitudes of the corrections were within the experimental accuracy of the measurements.

The incremental results, ΔC_L, ΔC_m, and ΔC_D, as a function of α are presented in figures 6, 7, and 8. Also included are the isolated-bomb values of C_D at the same Reynolds number of the bomb used in conjunction with the bomb bays of the present tests and $\frac{1}{2} C_D$ of the isolated bomb at a Reynolds number of 7.65×10^6. This was the highest Reynolds number of the isolated-bomb tests and should be more indicative of the C_D of the semiexternal bomb (configuration 7) which is in the presence of a turbulent boundary layer. From the corrected C_L and C_m results, x_{cp} and Δx_{cp} were calculated and are presented in figures 9, 10, and 11 as a function of α. Likewise, x_{ac} and Δx_{ac} are presented in figures 12, 13, and 14. Cross plots of the aforementioned results which indicate their variation with Mach number at specified angles of attack are presented in figures 15 to 20.

In the figures of the analysis, whenever any increments are presented "due to the addition of bomb to bomb bay," the manner in which they were obtained is as follows:

Box type = Configuration 5 - Configuration 2

Box type + Baffles = Configuration 6 - Configuration 3

Semiexternal = Configuration 7 - Configuration 4

External + Cavity = Configuration 8 - Configuration 4

External = Configuration 9 - Configuration 1

DISCUSSION

Basic Data

The drag results of configuration 1 (basic body), (figs. 3(a), 4(a), and 5(a)), indicated that the addition of the transition strip removed the laminar drag "bucket" in the low angle-of-attack range. Also, at angles of attack, only minor changes were evident in the lift and pitching-moment results which indicated that the total lift, as well as the distribution of lift was only slightly changed as a result of adding the transition strip. It is believed that, for the body without the transition strip installed, the angle-of-attack effects in combination with the test Reynolds number were sufficient to cause natural transition to occur, probably at least as far forward as the forward portion of the afterbody.

This would probably result in about the same lift distribution over the afterbody with and without artificial transition, as the force data indicated.

It is of interest to note that, particularly at M = 1.62, the drag of configurations utilizing the internal types of configurations (nos. 2, 3, 5, and 6) increased more rapidly at the positive angles of attack than at the negative angles (see, for example, fig. 3(b)). This is believed to have occurred partly as a result of the flow more readily impinging on the forward facing surfaces within the bomb bays at positive angles of attack. The difference between the pressure distributions over the afterbody at the same positive and negative angles of attack and its effects upon drag are unknown.

Configuration Considerations

Before discussing the penalties involved in using a particular bomb-bay configuration, it must be noted that, from an operational standpoint, the bomb-bay configurations would not be in use for the same length of time nor for the same portion of a flight in order to accomplish a particular mission. The time for which the aerodynamic penalties of configurations 2, 3, 5, and 6 (designated in the present paper as the internal types) might be imposed upon the aircraft would be short. In the most time-consuming sequence of operation, this duration would ordinarily be, at the most, a matter of minutes. These configurations should be considered as short-duration configurations.

It must be emphasized that the short-duration configurations may be equally if not more important than the long-duration configuration from simple considerations of the essential, so-called "supersonic-dash" requirement. This requirement calls for a specific minimum supersonic speed just prior to and during release and for a short period of time thereafter. Therefore, the aircraft must be designed so that it experiences no large aerodynamic penalties during the various phases of the supersonic dash which might result in a substantial reduction in speed.

The duration for which configuration 7 might be used could be of the order of one-half of the total flight time of the mission. This configuration should be considered as a long-duration configuration. If configuration 7 were used as the release configuration, immediately upon release the aircraft would be subjected to the penalties of configuration 4. Doors might then be used to convert the aircraft back to its clean condition; under these conditions, configuration 4 should be considered as a configuration with a very short duration.

Likewise, configuration 8 might be an interim configuration used to convert from configuration 7 (used from take-off to just prior to

release) to configuration 9 (used solely for release) by lowering the bomb on struts. Therefore, configurations 8 and 9 might be considered as short-duration configurations also.

It is apparent that the total aircraft drag must be considered jointly with aircraft weight in a final analysis in view of their close relation to aircraft performance. There are so many obvious complexities involved in total-drag considerations that no attempt has been made within this paper to consider effects other than those of the bomb bay or bomb plus bomb bay upon the fuselage-alone characteristics.

The effects of additional aircraft components, such as wing, tail, or engine nacelle, were not considered to be within the scope of the present investigation in view of the dependence of these effects upon such parameters as geometry, location, and attitude of the particular components involved.

The analyses have been grouped into the internal types (configurations 2, 3, 5, and 6) and the external types (configurations 4, 7, 8, and 9) of installations. The former group consisted entirely of short-duration bomb-bay configurations that might require greater fuselage volumes than those configurations included in the latter group, which consisted of both short- and long-duration configurations.

Incremental Results

Internal types.- At $M = 1.62$ (fig. 6(a)), the values of ΔC_D for the internal types are all positive with larger magnitudes at positive values of α due partly to the flow impinging more readily on the forward-facing surfaces of the bomb bay. In the low angle-of-attack range the additional pressure drag of baffles produced a higher ΔC_D. The effect of adding the bomb was to reduce the level of the ΔC_D as a result of decreasing the flow into the bomb bay and reducing the pressure increase on the rear surface of the bay (see fig. 6(b)). This decrease of flow into the bay was also noted in reference 1 as a reduction of circulation within the bomb bay as the bomb diameter was increased.

The circulation and flow within the internal configurations probably resulted in negative pressure coefficients acting within and in the vicinity of the bomb bay to contribute to the negative ΔC_L indicated in figure 6(a). Also, it appears possible that some interference pressures might have been carried over onto the afterbody although this is believed to have been small in view of the small magnitude of ΔC_m. The effect of adding a bomb was to produce a positive ΔC_L (see fig. 6(b)) probably through the reduction of the negative pressures on the top of the bomb bay.

The results at $M = 1.94$ and $M = 2.40$ (figs. 7(a) to 8(b)) are, in general, similar to those noted at $M = 1.62$ with the primary exception of the negative ΔC_L due to the addition of the bomb at $M = 2.40$ at low negative values of α (fig. 8(b)).

External types.- At all Mach numbers the drag penalty of configuration 4 at $\alpha = 0^\circ$ was relatively high (see figs. 6(a), 7(a), and 8(a)). The expansion of the flow into the forward portions of the cavity followed by compressions within the afterportions resulted in additive incremental drags for configuration 4 (see ref. 6). The effects of the positive incremental pressures were believed to have been predominant and to have resulted in comparatively large values of ΔC_L at all Mach numbers. Small interference pressures may have been felt on the afterbody at $\alpha = 0^\circ$ as indicated by the small values of ΔC_m.

The addition of the bomb within the cavity changed configuration 4 to configuration 7. The incremental drag at $\alpha = 0^\circ$ is compared with $\frac{1}{2} C_D$ of the isolated bomb in figures 6(a), 7(a), and 8(a). The interference drag, which is the difference between the ΔC_D of configuration 7 and $\frac{1}{2} C_D$ of the isolated bomb, was favorable at $M = 1.62$ and $M = 1.94$; this favorable interference drag was also reported in reference 5 at supersonic Mach numbers up to $M = 1.8$, the limit of the tests. At $M = 2.40$, the present results indicated that the interference drag was unfavorable. This will be discussed further in the section entitled "Effects of Mach Number Variation at $\alpha = 0^\circ$." The insertion of the bomb into the cavity reduced the incremental drags at $M = 1.62$ and 1.94 by magnitudes greater than the isolated C_D of the bomb (see figs. 6(b), 7(b), and 8(b), curves labeled semiexternal). At each Mach number the reduction was greatest near $\alpha = 0^\circ$ and nearly constant at $\alpha > 2^\circ$. For configuration 7, the incremental lifts ΔC_L and the incremental pitching moments ΔC_m were small (see figs. 6(a), 7(a), and 8(a)), again indicating that the interference pressures on the afterbody of the basic body probably were small.

The drag of configuration 8 was the highest drag encountered. The incremental drags were nearly constant throughout the angle-of-attack range (figs. 6(a), 7(a), and 8(a)). The total drag of configuration 8 was less than the sum of the drags of configuration 4 plus that of the isolated bomb, indicating that the sum of the interference drags was negative. As mentioned previously, in the absence of a bomb, an expansion fan probably originated as the flow turned into the forward portion of the cavity and was followed by a series of shock waves originating throughout

the length of the cavity. The location of the bomb of configuration 8 was such that, excluding mutual-interference effects, a portion of the forebody of the bomb probably was submerged within the negative-pressure-increment flow field. Also, it is probable that a portion of the afterbody and fins of the bomb were submerged within a positive-pressure-increment flow field. Both factors would have reduced the drag of the bomb. Similarly, with the presence of the bomb, it appears that, neglecting mutual interference again, the effect of the bomb could have been such so as to reduce the drag of the cavity. The inclusion of mutual-interference effects undoubtedly altered the local flow conditions in the region between bomb and cavity; however, it is believed that a portion of the negative interference drag may be attributed to the preceding interference effects. The breakdown of the lift interference is not fully understood; but the lift is undoubtedly affected by the shock and flow phenomenon between the bomb and cavity as well as the interference-pressure field which is caused by the bomb and cavity and wraps around the fuselage in a helical fashion.

The ΔC_D of configuration 9 was nearly constant with α and was substantially greater than the C_D of the isolated bomb. As α increased, ΔC_L increased and ΔC_m decreased because of the addition of the bomb (see figs. 6(b), 7(b), and 8(b)); it appears that the changes of distribution of interference pressures upon the fuselage with variation in α were sufficient to make these changes in ΔC_L and ΔC_m and, at the same time to maintain a nearly constant ΔC_D.

In general, as α increased ΔC_L increased and ΔC_m decreased because of the addition of any external-type bomb bay or bomb plus bomb bay.

Center-of-Pressure Locations

Presented in figures 9, 10, and 11 are the center-of-pressure locations and changes. These results have been omitted at angles of attack from -1° to 1° because the accuracy of x_{cp}/l in the low range of α was poor.

Internal types.- The center-of-pressure locations at positive values of α were predominantly forward of that of the basic body probably because of the negative ΔC_L associated with these internal configurations (see figs. 9(a), 10(a), and 11(a)); this is indicated as a negative $\Delta x_{cp}/l$ in figures 9(b), 10(b), and 11(b). At values of α greater than 4°, $\Delta x_{cp}/l$ was, in every case, less than 0.05. Therefore, it is believed that the interference pressures carried over onto the afterbody were small or compensating in this angle-of-attack range.

Because these bomb bays were located on the leeward side of the body at negative values of α and were internally located, the spread in $\Delta x_{cp}/l$ was less at each Mach number than for positive values of α (figs. 9(b), 10(b), and 11(b)).

The addition of the bomb to the bomb bays (figs. 9(c), 10(c), and 11(c)) at positive values of α shifted the center of pressure rearward in every case except for configuration 6 at $M = 2.40$.

External types.- At every Mach number, the center-of-pressure locations of the body—bomb-bay combinations were predominantly rearward of that of the basic body (figs. 9(a), 10(a), and 11(a)) at angles of attack greater than $2\frac{1}{2}^\circ$. For configuration 4 the rearward shift was believed to have been the result of the positive lift and drag increments in the region of the cavity.

For configuration 7 the contribution of the incremental drag of the semiexternal bomb (excluding interference drags) to the basic body would produce a negative ΔC_m. This would contribute to the positive $\Delta x_{cp}/l$ indicated in figures 9(b), 10(b), and 11(b). The addition of the bomb to change configuration 4 to configuration 7 actually produced a forward shift in the center of pressure (figs. 9(c), 10(c), and 11(c), labeled semiexternal). The major contribution to this shift was probably the negative ΔC_L noted previously; a secondary contribution was believed to have been the decrease in C_D. The values of x_{cp}/l of configuration 8 were within 0.05 of those for configuration 7 for α greater than 2°. A similar shift in x_{cp}/l due to the addition of the bomb was again noted (figs. 9(c), 10(c), and 11(c), labeled external plus cavity).

The addition of the bomb to the basic body (configuration 9) shifted the center of pressure rearward at positive angles of attack. The drag of the bomb contributed to the stabilizing C_m and the corresponding rearward movement in center-of-pressure locations (figs. 9(b), 10(b), and 11(b)).

Aerodynamic-Center Locations

Internal types.- At positive, low angles of attack at $M = 1.62$ and 1.94, the aerodynamic-center locations of configurations 2, 3, 5, and 6 were, in general, slightly behind those of the basic body (figs. 12(b) and 13(b)); at $M = 2.40$, no decided change is evident (fig. 14(b)). The effects of increasing angle of attack were to produce a general forward movement of aerodynamic center at $M = 1.94$ and 2.40.

The effects of adding the bomb are presented in figures 12(c), 13(c), and 14(c); the angle-of-attack effects were a function of Mach number.

External types.- At low angles of attack the addition of the external types of bomb bays or bombs plus bomb bays moved the aerodynamic-center locations rearward (figs. 12(b), 13(b), and 14(b)). The effect of increasing α to 6° was generally to decrease $\Delta x_{ac}/l$. This became more pronounced as Mach number increased.

Effects of Mach Number Variation at $\alpha = 0^\circ$

Lift.- The effects upon C_{L_α} of adding an internal type of configuration to the basic body were small at all Mach numbers (fig. 15(a)). The effect of increasing M was to increase C_{L_α}. The previously mentioned values of ΔC_L (fig. 15(b)) were fairly constant with change in M with small difference noted as a result of changing internal configurations. The positive ΔC_L due to the addition of the bomb was also nearly constant at all Mach numbers (fig. 15(c)).

The effect of adding an external type of configuration to the basic body was to increase C_{L_α}. The amount of increase was dependent upon the type of configuration. An increase in M resulted in an increase in C_{L_α}. The large ΔC_L noted for configuration 4 and the small ΔC_L noted for configuration 7 (fig. 15(b)) were apparent at all Mach numbers.

Drag.- For the internal types, the drag at $\alpha = 0^\circ$ for configuration 3 was the highest at all Mach numbers (fig. 15(a)). The baffles contributed an incremental drag to configuration 2 that was from about one-fourth to one-half of the ΔC_D of configuration 2 throughout the Mach number range (fig. 15(b)). It is believed that the baffle drag could be reduced if the "skin" of the fuselage were extended in order to completely enclose the baffles. From the bottom, the opening of the bomb bay would then appear as an enlarged plan form of the bomb with the baffles enclosed and protected from the impact of the airstream. The addition of the bomb reduced the C_D at all Mach numbers (fig. 15(c)) with the reduction becoming least at $M = 2.40$.

The variations of the drag with Mach number of the configurations having external types of configurations are presented in figure 15(a); the drag increments are compared with the drag of the isolated bomb in figure 15(b). For configuration 7, the interference C_D changed from negative at $M = 1.62$ to positive at $M = 2.40$. The increase in M (and the accompanying decrease in Mach angle) swept the interference helices further rearward so that the interference pressures over the

afterbody were distributed differently at each test Mach number. It is believed that this was the primary cause of the large variation in interference drags. The high drag of configuration 8 was present at all Mach numbers with its highest value near $M = 1.9$ as was also the case for configuration 9. The interference drag of configuration 9 was positive throughout the Mach number range with its highest value near $M = 1.9$ (fig. 15(c)). (Compare difference between C_D of isolated bomb and curve labeled external.) However, the interference drag of configuration 8 was negative (as previously discussed) throughout the Mach number range with its largest negative value at $M = 2.40$ (compare difference between C_D of isolated bomb and curve labeled external plus cavity).

Aerodynamic-center location.- The aerodynamic-center locations of the configurations equipped with internal types of configurations moved rearward as the Mach number increased, in keeping with the basic-body results (fig. 15(a)). The effect of the internal configurations was to shift the aerodynamic center rearward (fig. 15(b)) at all Mach numbers with the largest shift at about $M = 1.9$. The effects of adding the bomb were negligible at all Mach numbers (fig. 15(c)).

For the configurations utilizing external types of configurations, the aerodynamic-center locations were also rearward of that of the basic body at all Mach numbers (figs. 15(a) and (b)). Also, x_{ac}/l increased as M increased. Because of the addition of the bomb bay x_{ac}/l was also dependent upon Mach number. The effects of adding the bomb in the semiexternal and external positions were nearly constant throughout the test Mach number range (fig. 15(c)).

Effects of Mach Number Variation at $\alpha \neq 0^\circ$

The effects of a variation in Mach number upon the pertinent parameters of the configurations at five angles of attack are summarized in figures 16 to 20.

Lift, drag, and pitching moment.- The addition of an internal configuration at positive angles of attack resulted in relatively small negative values of ΔC_L at all Mach numbers (fig. 16(a)). In general, ΔC_L was least at $M = 1.94$. The addition of the bomb added a small positive ΔC_L at all Mach numbers (fig. 16(b)). It is of interest to note that little or no drag penalty is paid through the usage of baffles (no bomb installed) at $M = 1.62$ and 2.40 (compare configurations 2 and 3. fig. 17(a)). As was noted at $\alpha = 0^\circ$, the addition of the bomb reduced the drag (fig. 17(b)) at all Mach numbers with the least reduction at $M = 2.40$. Because of the addition of bomb bay or bomb plus bomb bay,

the effects of ΔC_L and ΔC_D as reflected upon ΔC_m were small throughout the Mach number range for positive values of α (fig. 18(a)). Again, the effect of adding the bomb was small (fig. 18(b)).

With regard to the negative angles of attack, the difference in ΔC_L, ΔC_D, and ΔC_m between configurations having internal types of configurations became substantially reduced at $\alpha = -4^\circ$ as a result of the "protuberance" having been located on the lee side of the basic body (figs. 16, 17, and 18).

The addition of the external types of configurations (fig. 16(a)) essentially produced a positive ΔC_L at positive values of α and a negative ΔC_L at negative values of α for most Mach numbers. The major exception was for configuration 4 which produced a positive ΔC_L at negative values of α; this was believed to be due to the pressure distribution on the cavity; however, this positive ΔC_L decreased as α decreased. There was no general trend of ΔC_L with Mach number for all the external types because of the variation in general profile of the configurations and the difference in their interference fields. The results indicated a reduction in ΔC_D as Mach number increased for configurations 8 and 9 (fig. 17(a)). General reductions were noted in the trends of ΔC_L and ΔC_D due to the addition of the bomb (figs. 16(b) and 17(b)), particularly at Mach numbers greater than 1.9 for ΔC_L. These reductions in ΔC_D were believed to have been associated with the reduction in the isolated C_D of the bomb as M increased (figs. 15(b) and 15(c)). With regard to the ΔC_m due to the addition of the external types (fig. 18(a)), with the exception of configuration 8, variation in M had little effect, and ΔC_m was positive at positive values of α and negative at negative values of α. Also, in general, the variation in M had little effect upon ΔC_m due to the addition of the bomb (fig. 18(b)).

Center of pressure and aerodynamic center.- As M increased, the center-of-pressure and aerodynamic-center locations, in general, moved rearward. This rearward movement would ordinarily be expected since it is true for slender bodies at supersonic speeds. The effects upon x_{cp}/l and x_{ac}/l (figs. 19(b) and 20(b)) were much less because of adding internal-type configurations as compared to adding the external-type configurations. This was also true as a consequence of adding the bomb (figs. 19(c) and 20(c)), particularly at the negative angles of attack.

CONCLUSIONS

The results of an experimental investigation at Mach numbers of 1.62, 1.94, and 2.40 of several bomb-bay and bomb plus bomb-bay configurations in combination with a body having a fineness ratio of 10 and a circular cross section indicate the following conclusions:

1. The addition of any bomb-bay or bomb plus bomb-bay configuration to the basic body at an angle of attack of 0° increased the drag and the slope of the lift curve, produced a negative lift except for the semi-external bomb bay, and shifted the aerodynamic center rearward at all Mach numbers.

2. The internal-type configurations had the least drag penalty, the least aerodynamic-center shift, and, in general, the least incremental lift of the configurations envisioned to be short-duration configurations. By adding a bomb internally, the drag penalty decreased and the lift increased.

3. The addition of external-type configurations to the basic body resulted in substantial drag penalties at all Mach numbers with the least drag penalty as well as the least change in lift noted for the semiexternal bomb-bay plus bomb installation.

4. The semiexternal bomb-bay plus bomb configuration, envisioned to be a long-duration configuration, had less drag penalty at Mach numbers less than about 2 and about the same order of incremental lift, shifts in center of pressure, and shifts in aerodynamic center at positive angles of attack throughout the Mach number range as the internal-type, short-duration configurations.

Langley Aeronautical Laboratory,
National Advisory Committee for Aeronautics,
Langley Field, Va., May 2, 1955.

APPENDIX

Description of the Six-Component Balance System at the Langley 9-Inch Supersonic Tunnel

The balance system used in these tests is an external, six-component system which utilizes mechanical, self-balancing beams as force-measuring devices. The rigid frame of the balance is attached to the bottom of the tunnel side walls (fig. 21(a)). This frame contains pads to which the six balance beams are attached by flex-link assemblies. A floating balance frame is also located beneath the tunnel side walls and is supported by six pin-mounted systems of links and bell cranks (fig. 21(b)). Each link system is connected to a separate balance beam.

Three of the link systems support the floating frame in the lift-drag (horizontal) plane, two parallel to the lift axis and one parallel to the drag axis. The upstream lift-link system was not completely installed at the time the photographs were made. The position of the upstream lift bell crank is indicated in figure 21(b) and appears in figure 21(e). These three systems supply force measurements for calculating lift, pitching moment, and drag. The other three links support the floating frame in the side-force (vertical) plane; the upstream link is located in the vertical plane passing through the tunnel center line (see figs. 21(d) and 21(e)). The two downstream links are located symmetrically opposite of this plane and are designated as the east and west side-force links in figures 21(a) and 21(e). Therefore, it is possible to obtain side force, yawing moment, and rolling moment.

The various parts of the downstream lift-link system are labeled in figures 21(b) and 21(e). A component of the resultant load on the model is transmitted into the lift link connected to the floating frame, then, into the bell crank, and, from there, into the link connected to the downstream balance beam. The upstream lift-link system and the drag-link system are similar. All joints were pin mounted.

Each side-force link system consists of a vertical column which transmits that component of the side-force load from the floating frame to the particular side-force beam. Each end of the vertical columns is pin mounted.

Attached to the top surface of the floating frame are two bar guide mounts, one on each side of the tunnel. Each mount contains a guide through which the lateral translating bar slides (figs. 21(c) and 21(e)). This bar is located in the lift-drag plane and is parallel to the lift axis. The model support (fig. 21(d)) attaches to this bar; thus, it is possible to translate the model laterally and at each angle of attack

keep the model boxed within the reflected nose disturbances. A translating motor, which was not installed at the time the photographs were made (fig. 21(d)), furnishes the torque through a magnetic clutch to a drive screw to translate the bar. The same motor simultaneously translates the shield which surrounds the bar (fig. 21(b)) and the hood and movable wind shield which surround the model mount and sting (fig. 2). A mass counterbalance (fig. 21(d)) geared to the translating-bar drive system moves laterally in a direction opposite to the direction of the bar. This offsets most of the effect of the change in the lateral center-of-gravity location upon the side-force beams. The rest of these changes are accounted for by a calibration with a particular model installed.

As stated previously, the beams are the self-balancing type. The beam flex-link assembly functions as the fulcrum of the beam. (See sketch.)

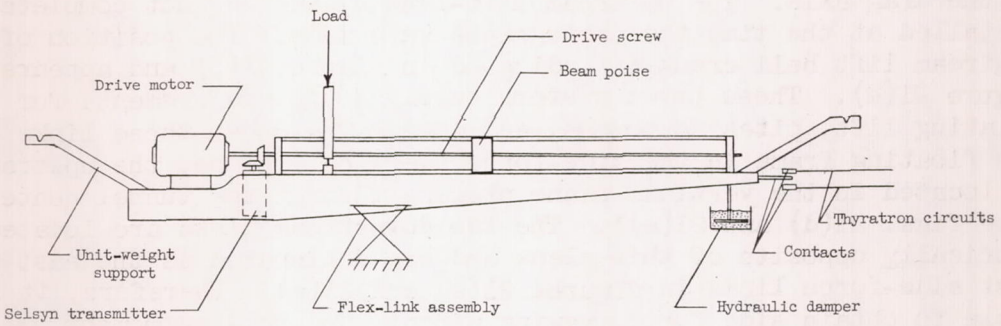

Sketch

An applied load causes the beam to become unbalanced and rotate, thereby completing the circuit to a thyratron tube which directs the beam motor to shift the poise and again balance the beam. The poise position is indicated at the control panel by use of a pair of selsyns and a counter. The calibration constant was determined by the ratio of applied load to change in poise position. The aforementioned beam rotation is very small as the total gap between the contacts in the two thyratron circuits is of the order of 0.005 inch.

Each balance beam is equipped with two sets of unit weights (three unit weights for each end of the beam) which extend the range of the beam by a factor of 7. (See fig. 21(d).) These are loaded and unloaded from the beam electrically by a 1-revolution-per-minute motor which is controlled from the tunnel drive-control panel. A unit-weight indicating panel is also located at the tunnel drive-control panel. Attached to each beam is a hydraulic damper. Located on the translating bar is an electric motor which provides power to the angle-of-attack system.

The pressure within the box which houses the balance system is controlled automatically with respect to a reference pressure which, for the present tests, was the stream static pressure.

During the construction of the balance, extreme efforts were made to aline the various link systems in their respective planes. The calibration indicates negligible interactions of one component with another. Also, the test section to which the balance is mounted is easily detached within the tunnel circuit and can be interchanged with a second test section whenever this balance is not to be used.

REFERENCES

1. Rainey, Robert W.: A Wind-Tunnel Investigation of Bomb Release at a Mach Number of 1.62. NACA RM L53L29, 1954.

2. Smith, Norman F., Bielat, Ralph P., and Guy, Lawrence D.: Drag of External Stores and Nacelles at Transonic and Supersonic Speeds. NACA RM L53I23b, 1953.

3. Jacobsen, Carl R.: Effects of Size of External Stores on the Aerodynamic Characteristics of an Unswept and a 45° Sweptback Wing of Aspect Ratio 4 and a 60° Delta Wing at Mach Numbers of 1.41, 1.62, and 1.96. NACA RM L52K20a, 1953.

4. Mason, Homer P.: Effects of External Store Mounting on the Buffet, Trim, and Drag Characteristics of Rocket-Powered Fuselage and Store Combinations Between Mach Numbers of 0.7 and 1.4. NACA RM L53J22, 1953.

5. Hoffman, Sherwood, and Wolff, Austin L.: Effect on Drag of Longitudinal Positioning of Half-Submerged and Pylon-Mounted Douglas Aircraft Stores on a Fuselage With and Without Cavities Between Mach Numbers 0.9 and 1.8. NACA RM L54E26, 1954.

6. Mason, Homer P., and Henning, Allen B.: Effects of Some External-Store Mounting Arrangements and Store Shapes on the Buffet and Drag Characteristics of Wingless Rocket-Powered Models at Mach Numbers From 0.7 to 1.4. NACA RM L54I20a, 1954.

7. Smith, Norman F., and Carlson, Harry W.: The Origin and Distribution of Supersonic Store Interference From Measurement of Individual Forces on Several Wing-Fuselage-Store Configurations. I.- Swept-Wing Heavy-Bomber Configuration With Large Store (Nacelle). Lift and Drag; Mach Number, 1.61. NACA RM L55A13a, 1955.

8. Rainey, Robert W.: Effect of Variations in Reynolds Number on the Aerodynamic Characteristics of Three Bomb or Store Shapes at a Mach Number of 1.62 With and Without Fins. NACA RM L53D27, 1953.

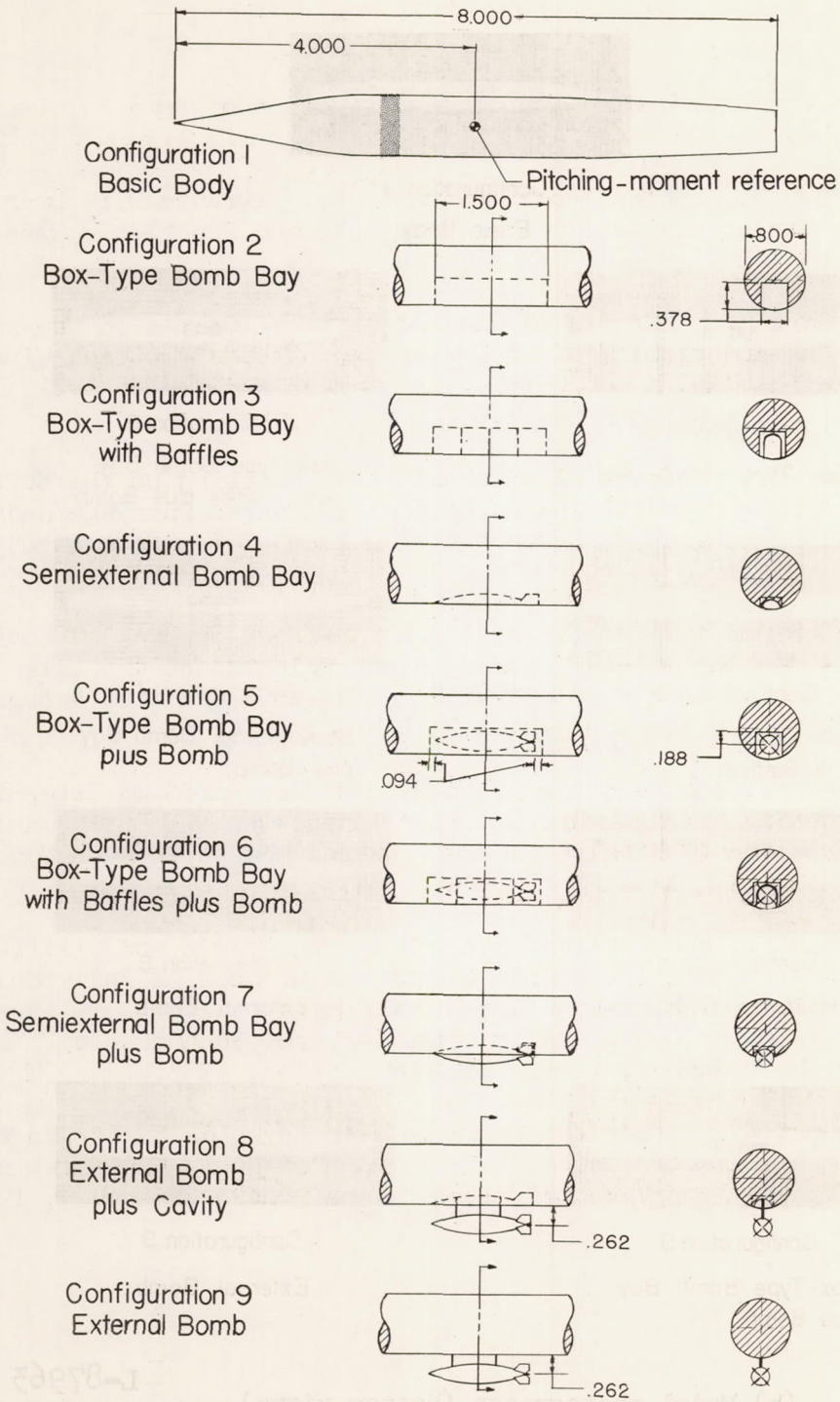

(a) Dimensional drawing.

Figure 1.- Model dimensions and designations. All dimensions are in inches.

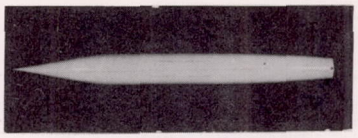

Configuration 1
Basic Body

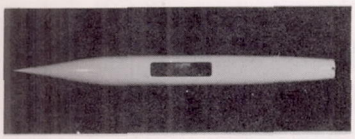

Configuration 2
Box-Type Bomb Bay

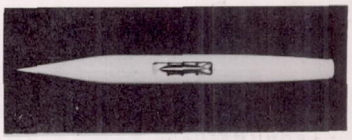

Configuration 6
Box-Type Bomb Bay
with Baffles plus Bomb

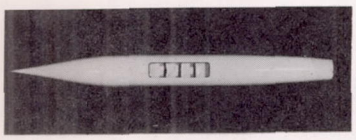

Configuration 3
Box-Type Bomb Bay
with Baffles

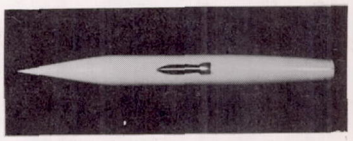

Configuration 7
Semiexternal Bomb Bay
plus Bomb

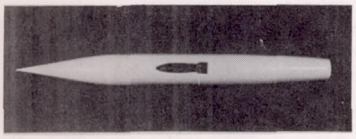

Configuration 4
Semiexternal Bomb Bay

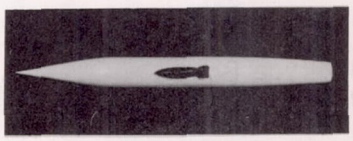

Configuration 8
External Bomb
plus Cavity

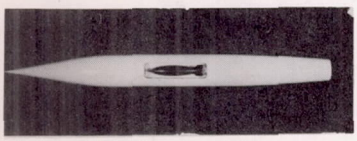

Configuration 5
Box-Type Bomb Bay
plus Bomb

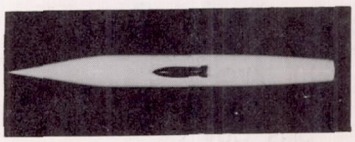

Configuration 9
External Bomb

L-87963

(b) Model photographs (bottom views).

Figure 1.- Continued.

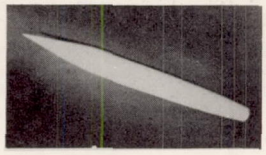

Configuration 1
Basic Body

Configuration 2
Box-Type Bomb Bay

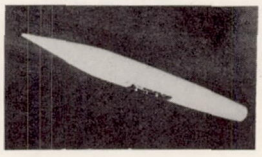

Configuration 6
Box-Type Bomb Bay
with Baffles plus Bomb

Configuration 3
Box-Type Bomb Bay
with Baffles

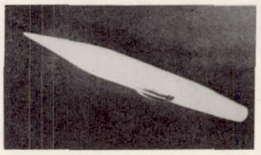

Configuration 7
Semiexternal Bomb Bay
plus Bomb

Configuration 4
Semiexternal Bomb Bay

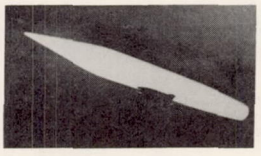

Configuration 8
External Bomb
plus Cavity

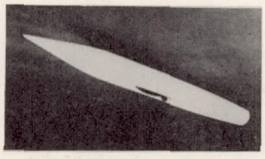

Configuration 5
Box-Type Bomb Bay
plus Bomb

Configuration 9
External Bomb

L-87964

(c) Model photographs (front three-quarter views).

Figure 1.- Continued.

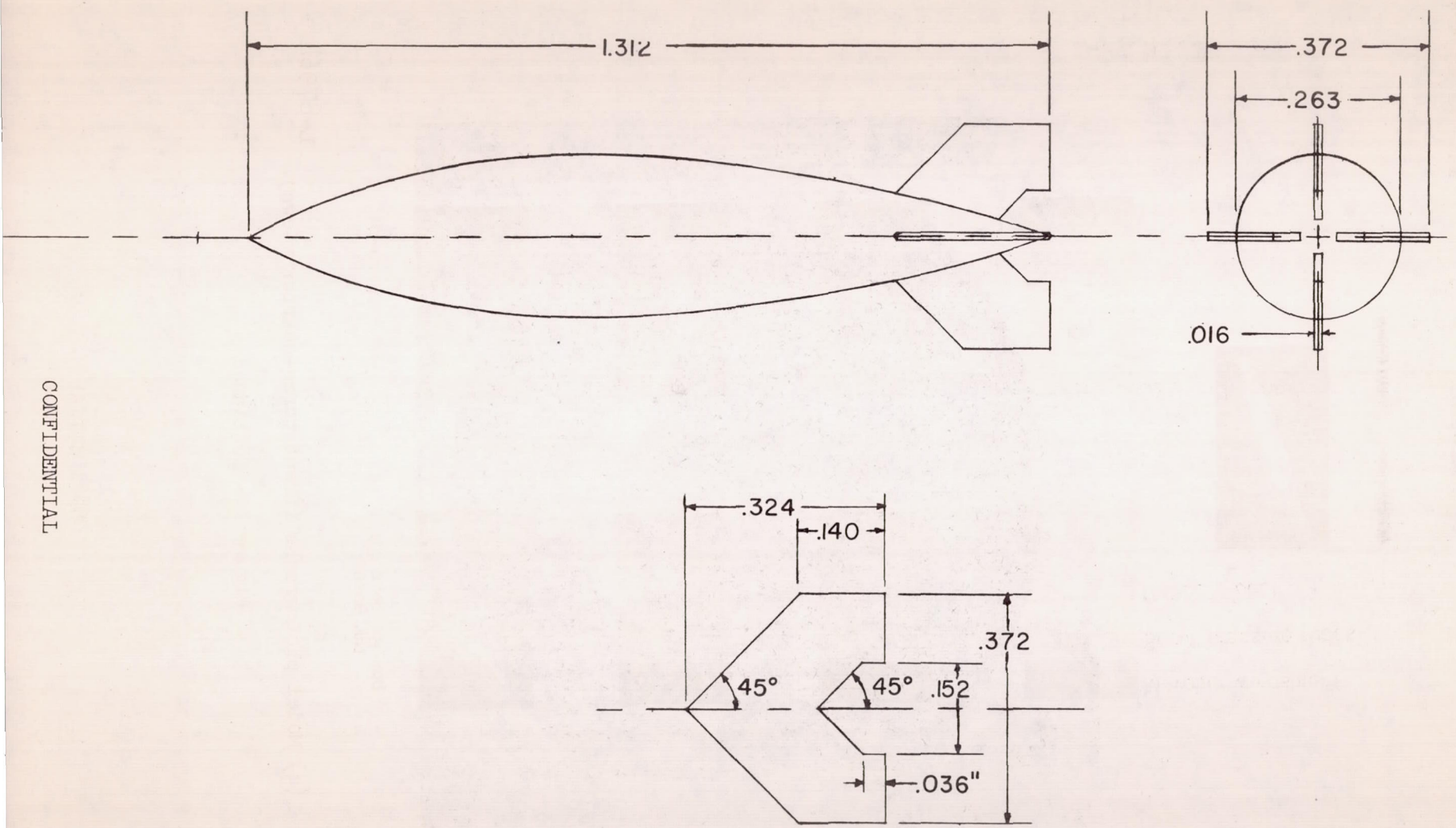

(d) Bomb configuration (maximum diameter at 40 percent length).

Figure 1.- Concluded.

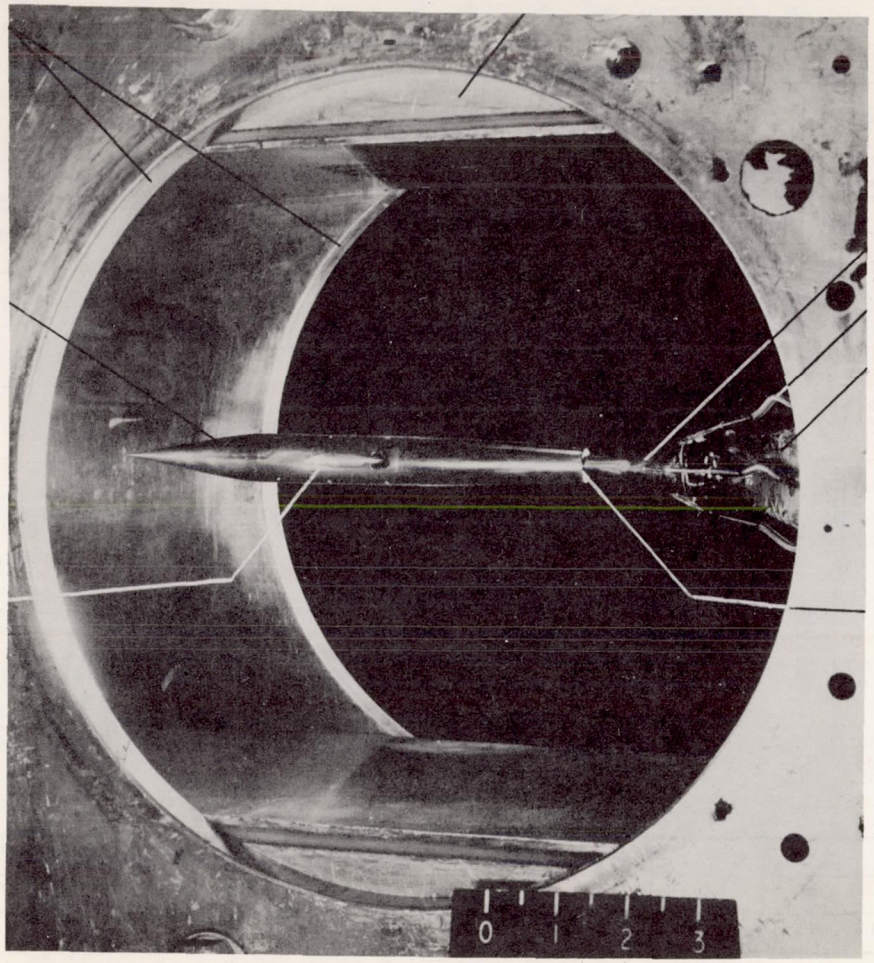

L-87441.1

Figure 2.- Model installation in Langley 9-inch supersonic tunnel.

CONFIDENTIAL

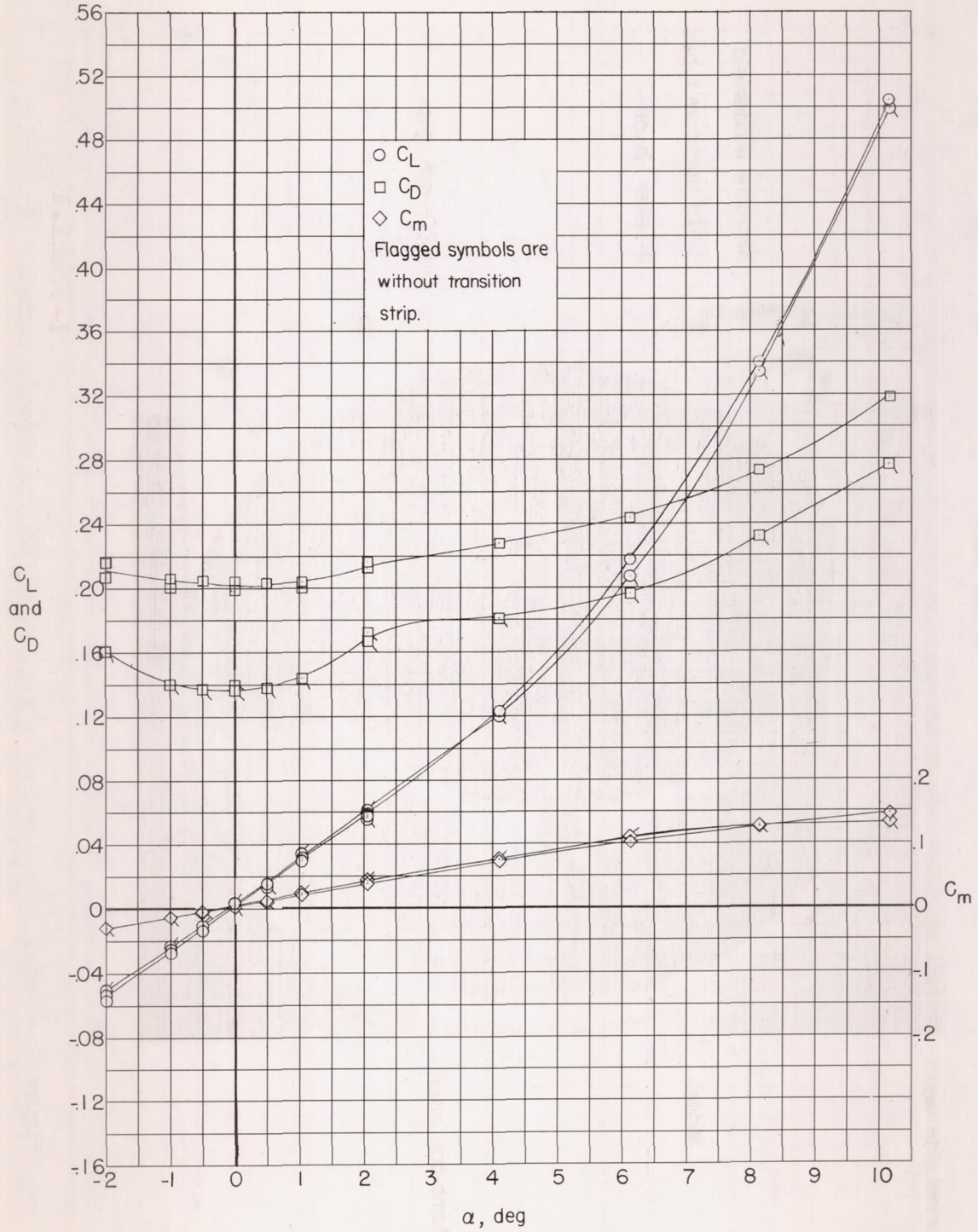

(a) Configuration 1 (basic body).

Figure 3.- Measured aerodynamic characteristics at M = 1.62.

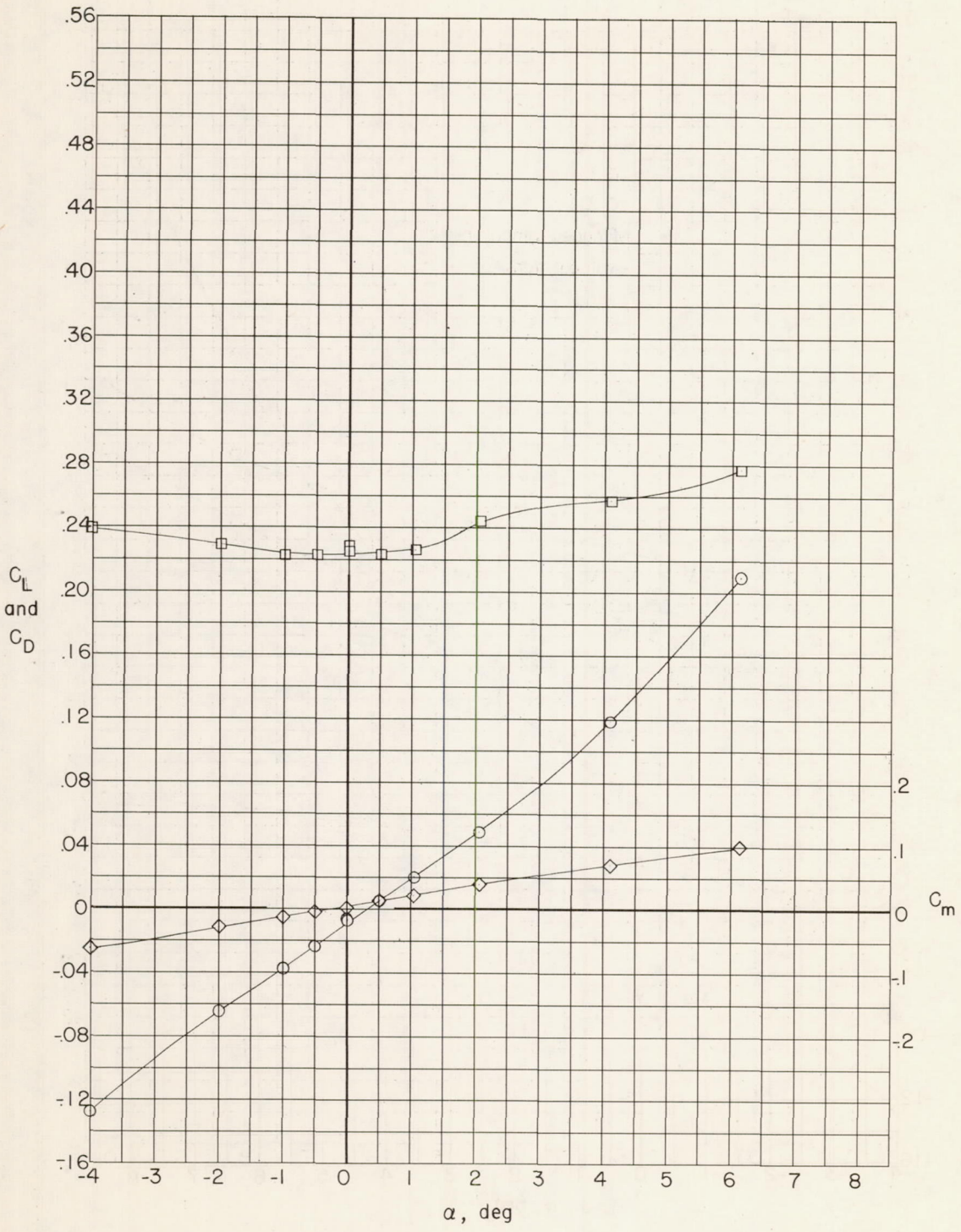

(b) Configuration 2.

Figure 3.- Continued.

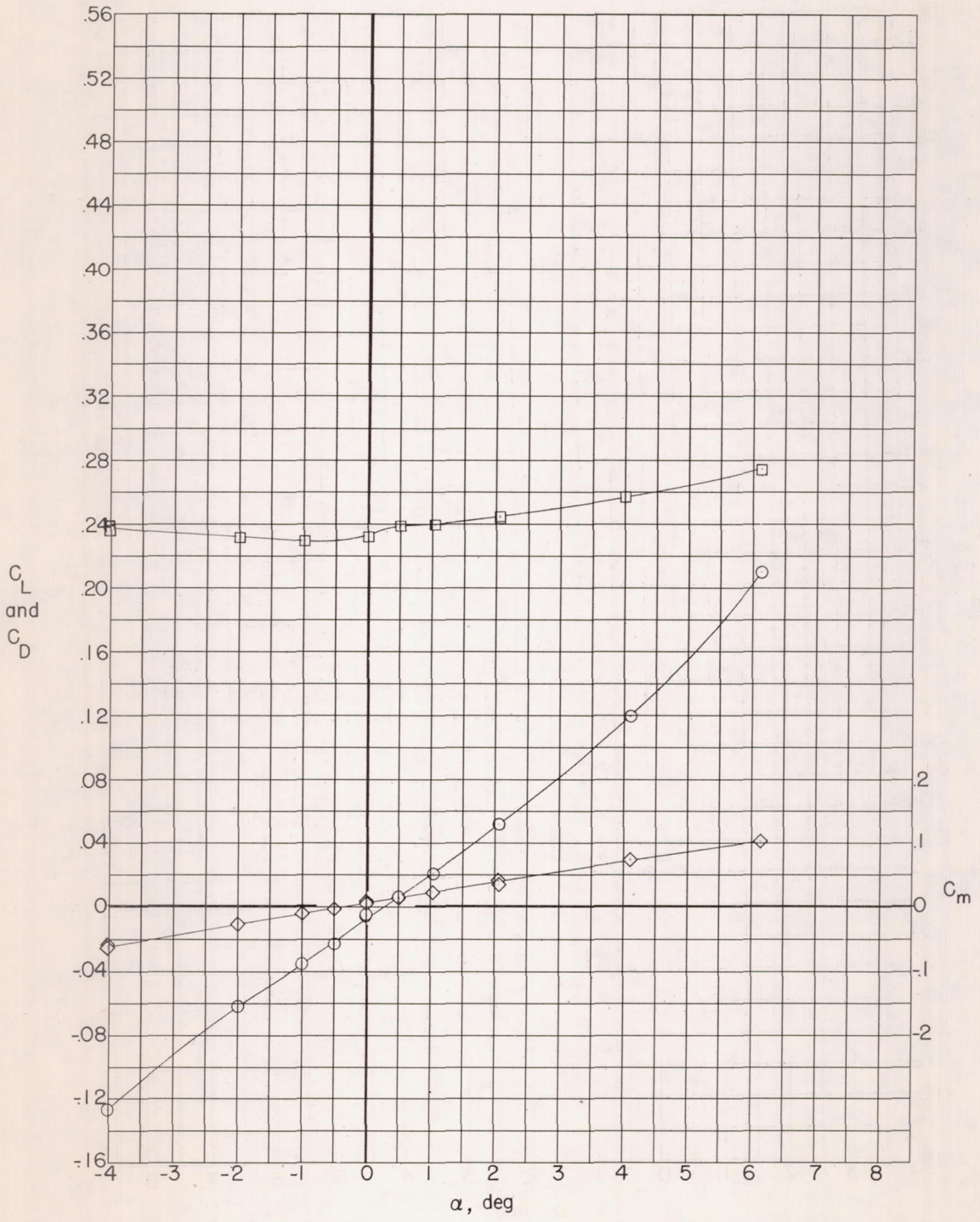

(c) Configuration 3.

Figure 3.- Continued.

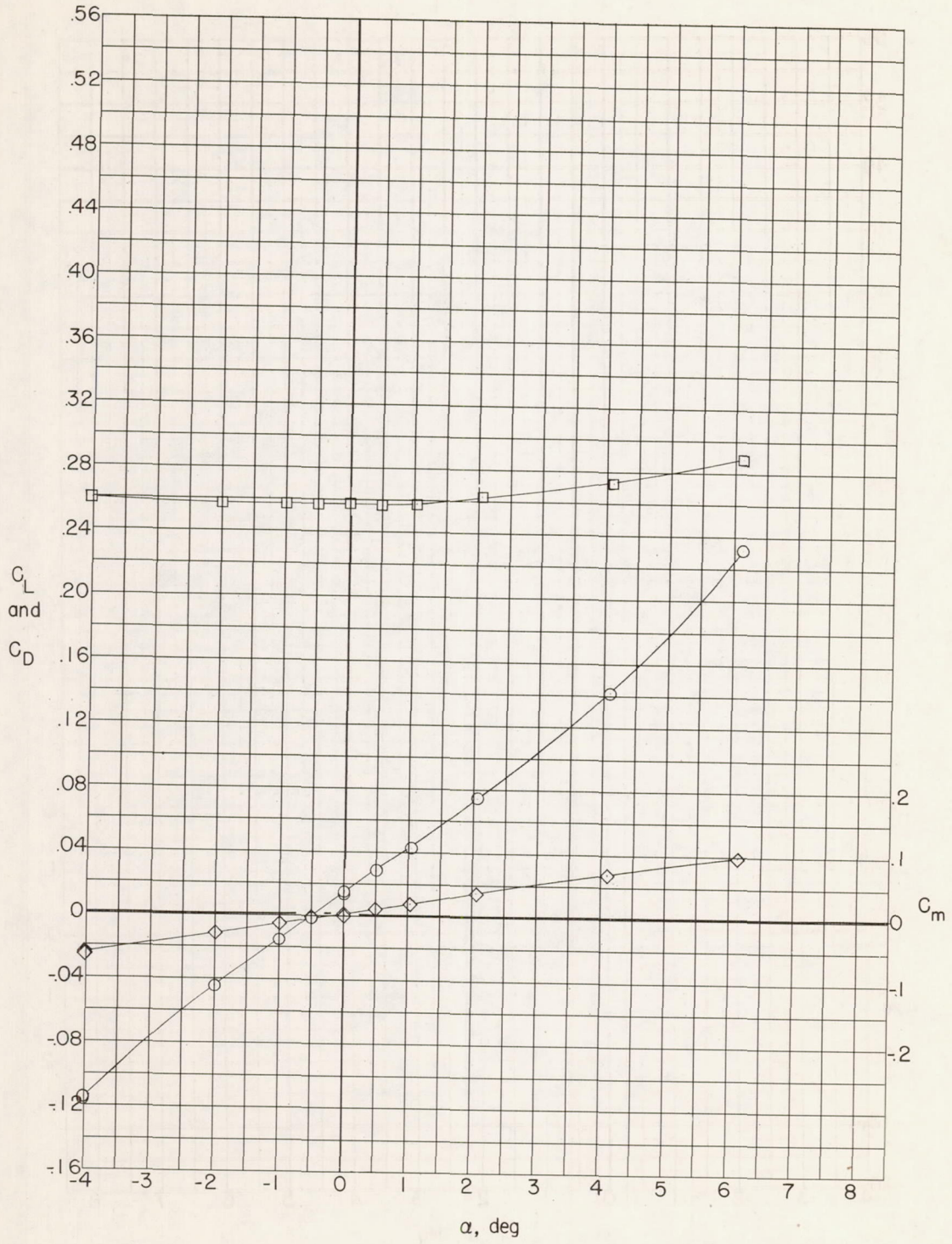

(d) Configuration 4.

Figure 3.- Continued.

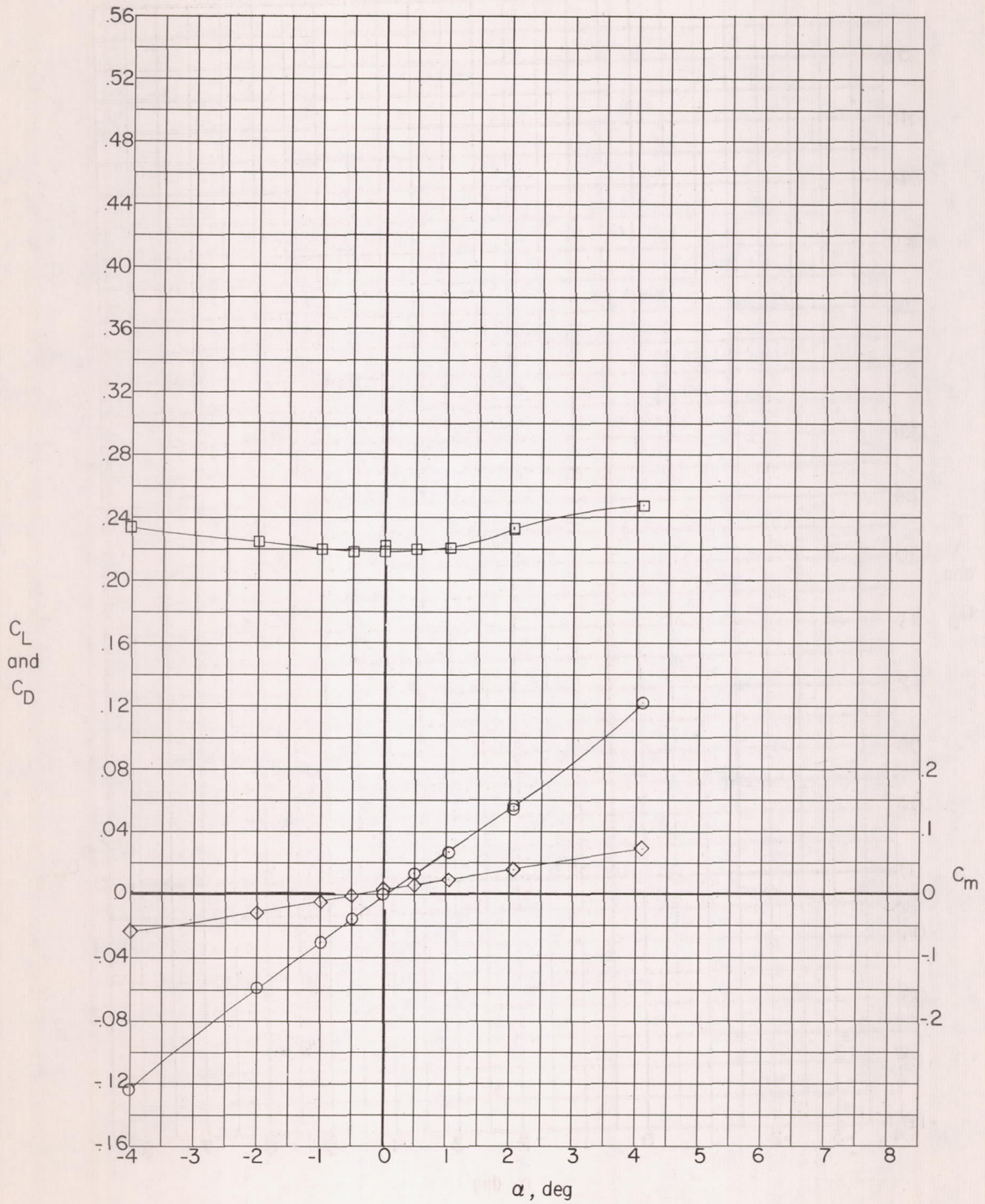

(e) Configuration 5.

Figure 3.- Continued.

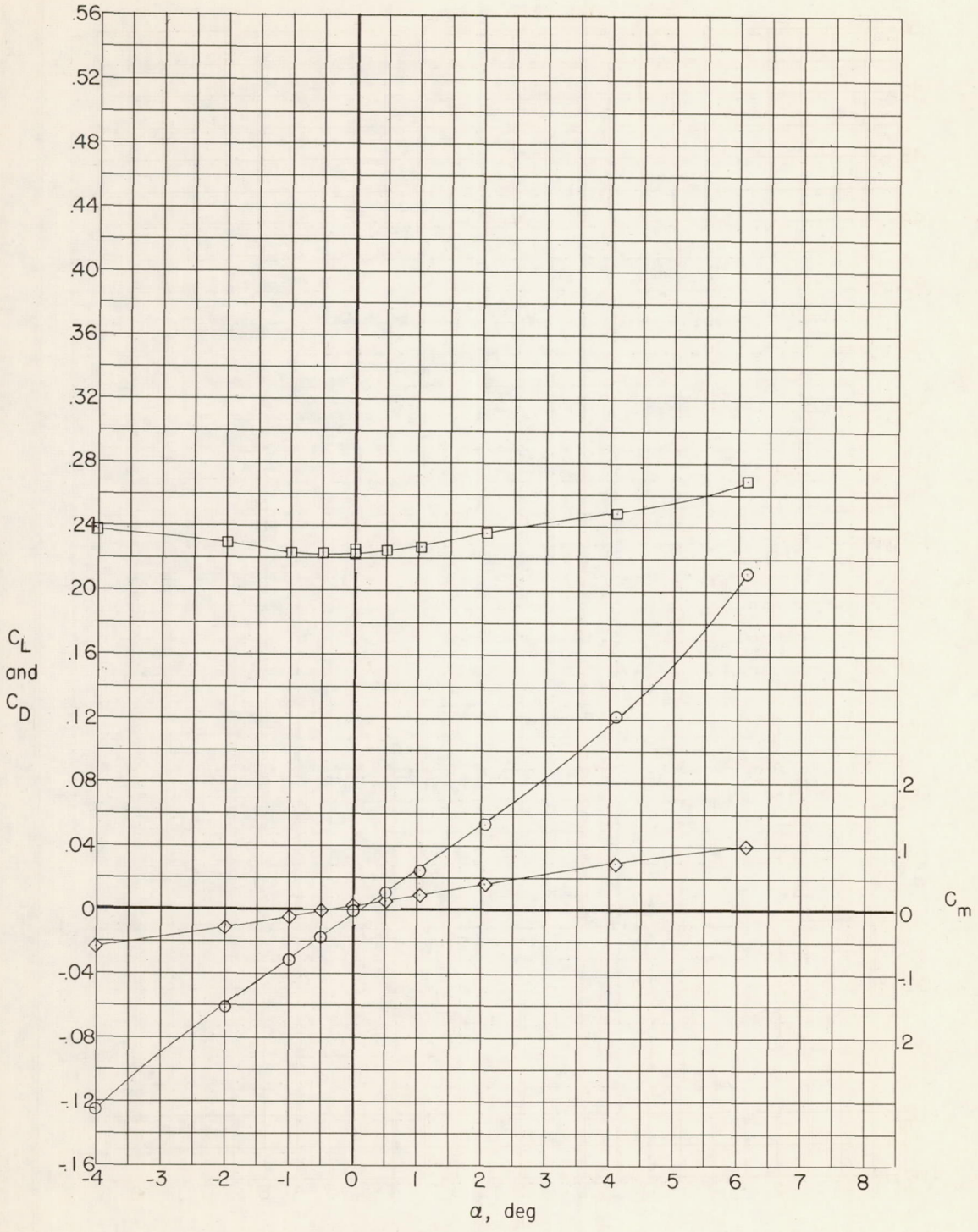

(f) Configuration 6.

Figure 3.- Continued.

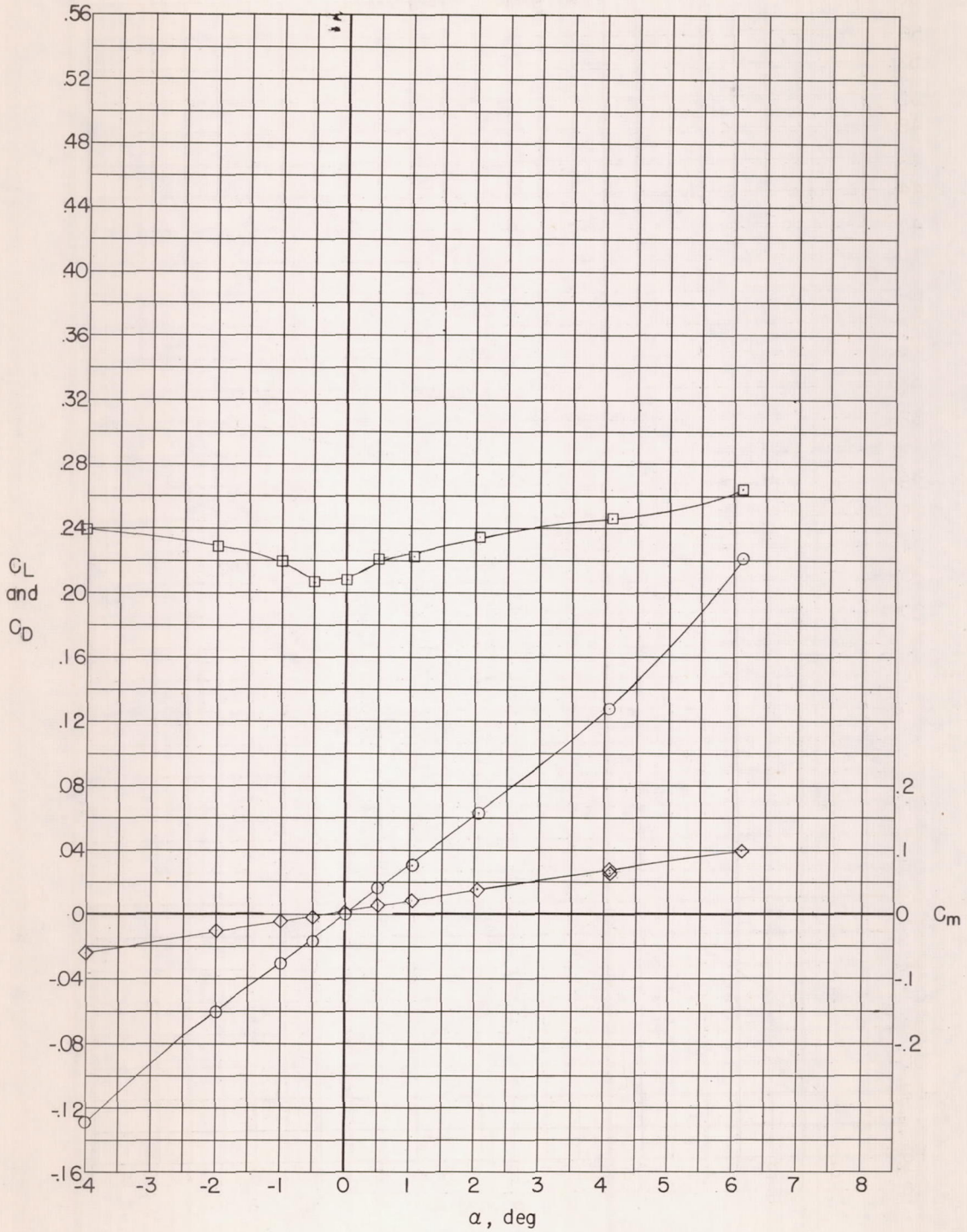

(g) Configuration 7.

Figure 3.- Continued.

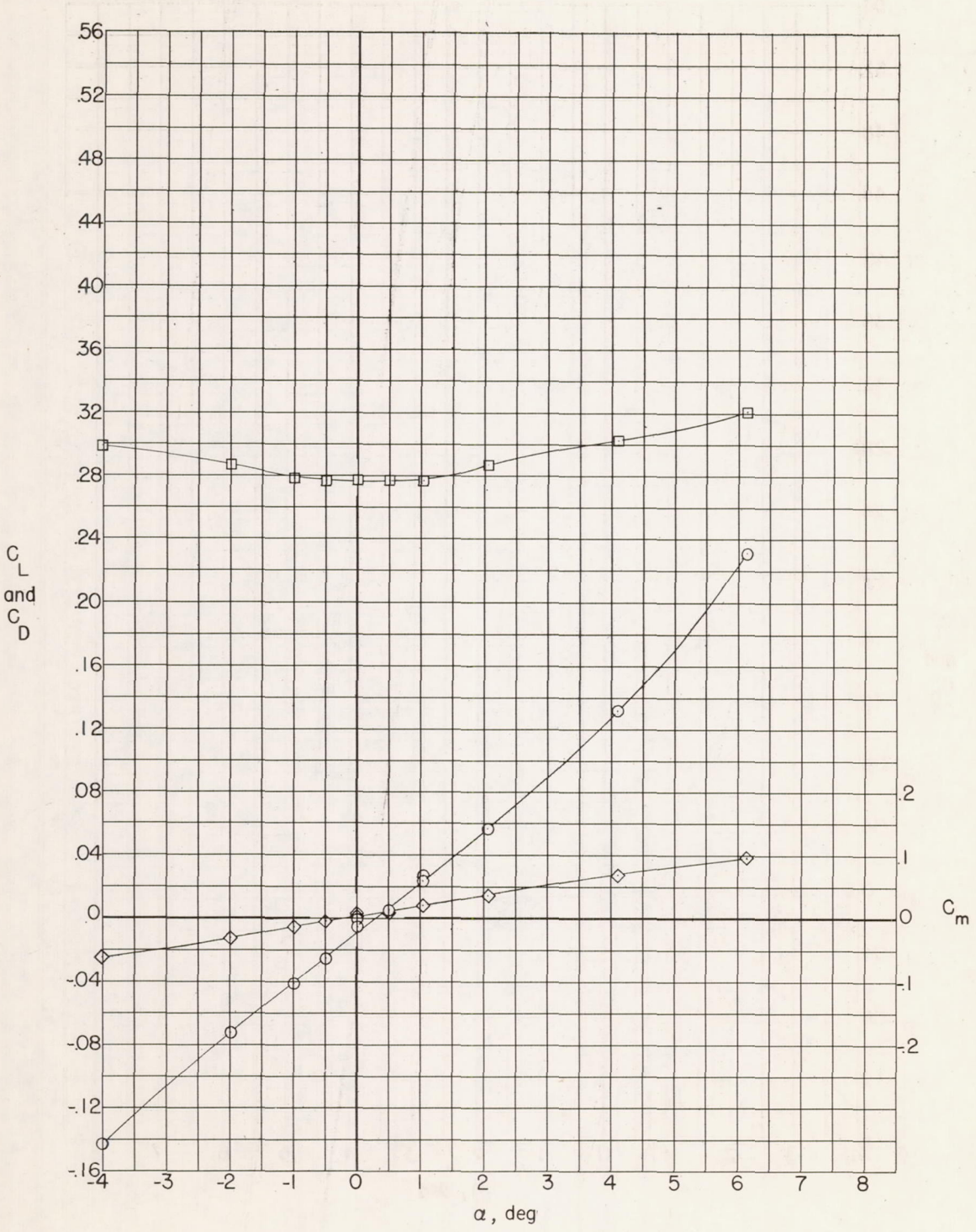

(h) Configuration 8.

Figure 3.- Continued.

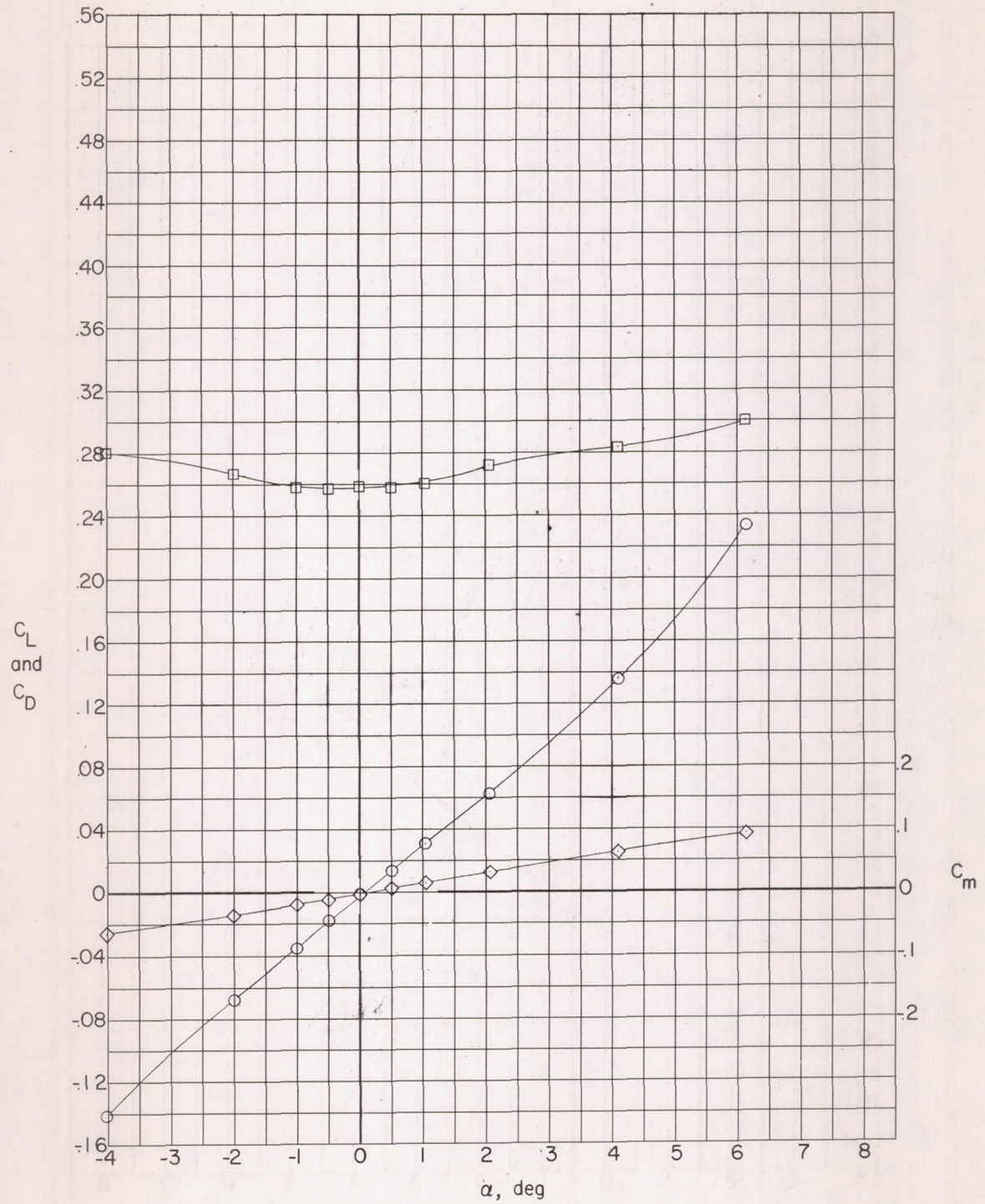

(i) Configuration 9.

Figure 3.- Concluded.

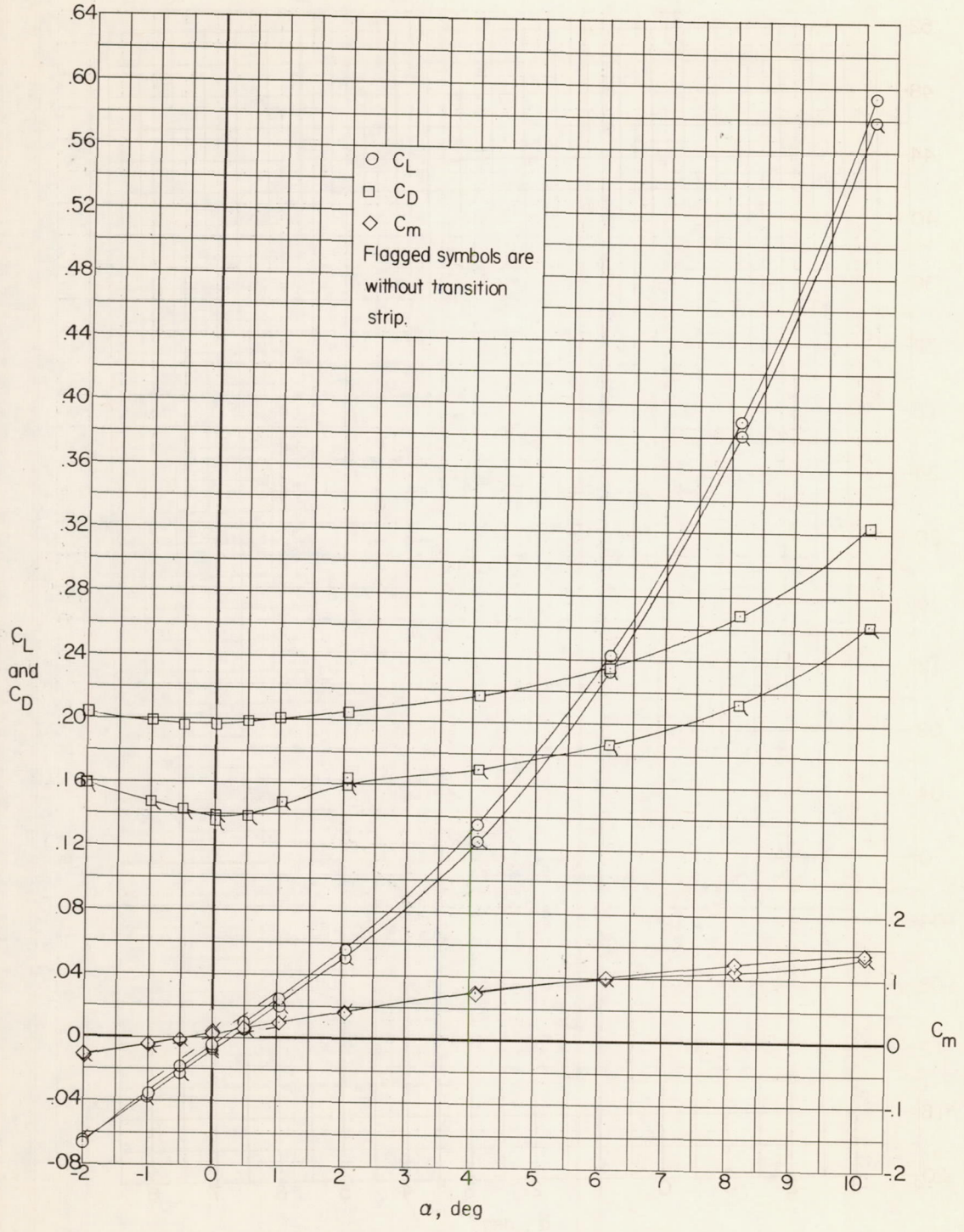

(a) Configuration 1 (basic body).

Figure 4.- Measured aerodynamic characteristics at M = 1.94. (Dashed curves are corrected C_L and C_m results.)

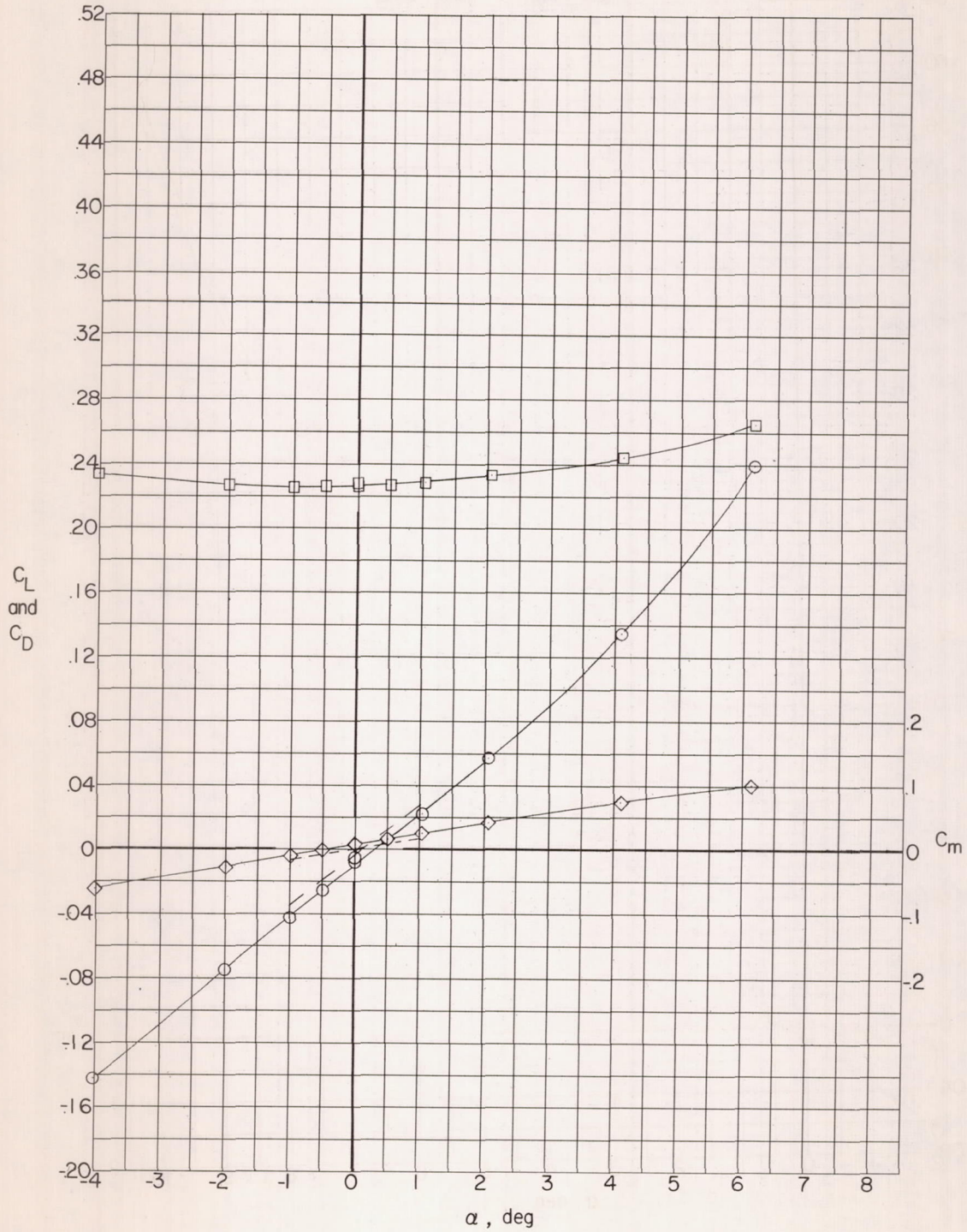

(b) Configuration 2.

Figure 4.- Continued.

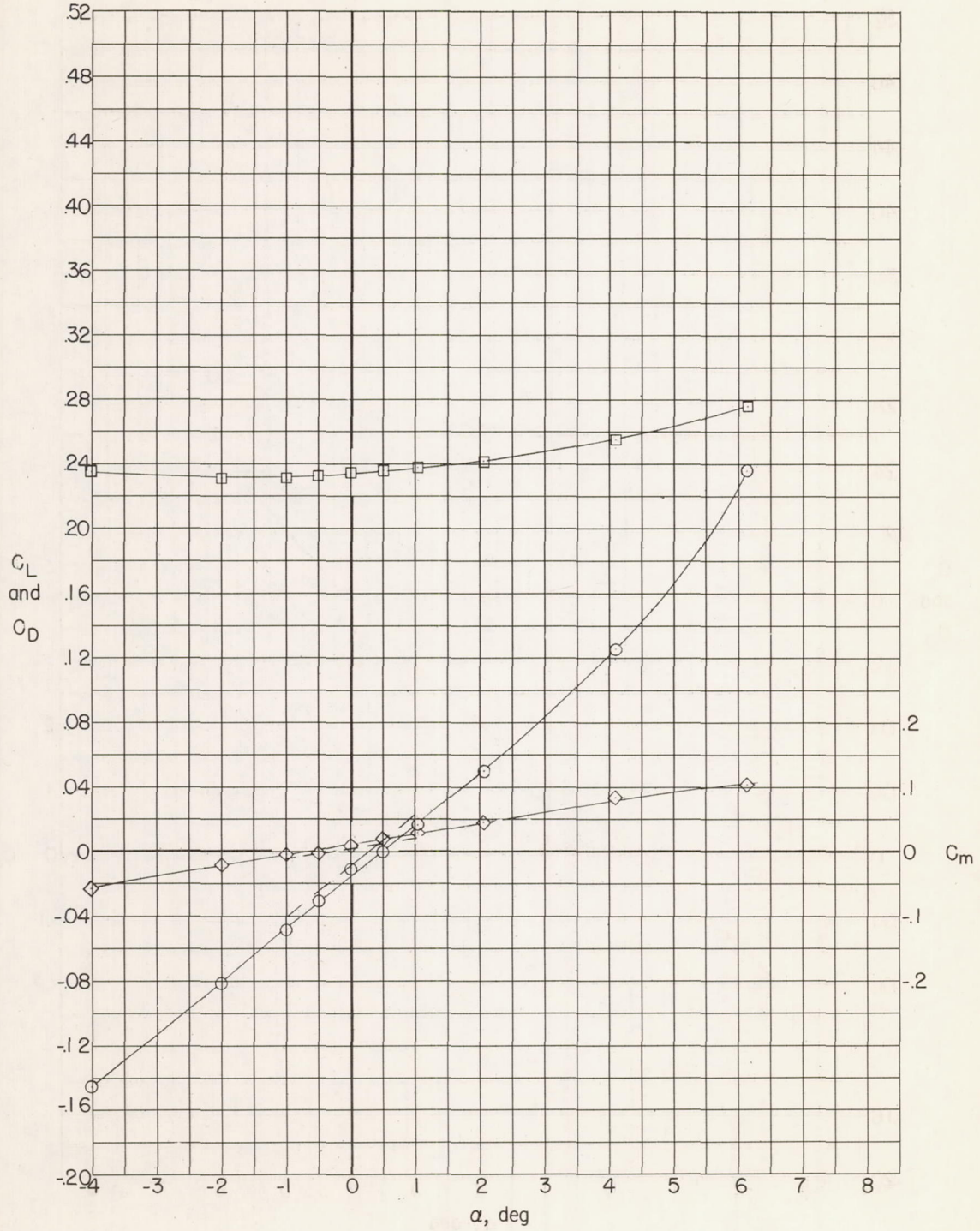

(c) Configuration 3.

Figure 4.- Continued.

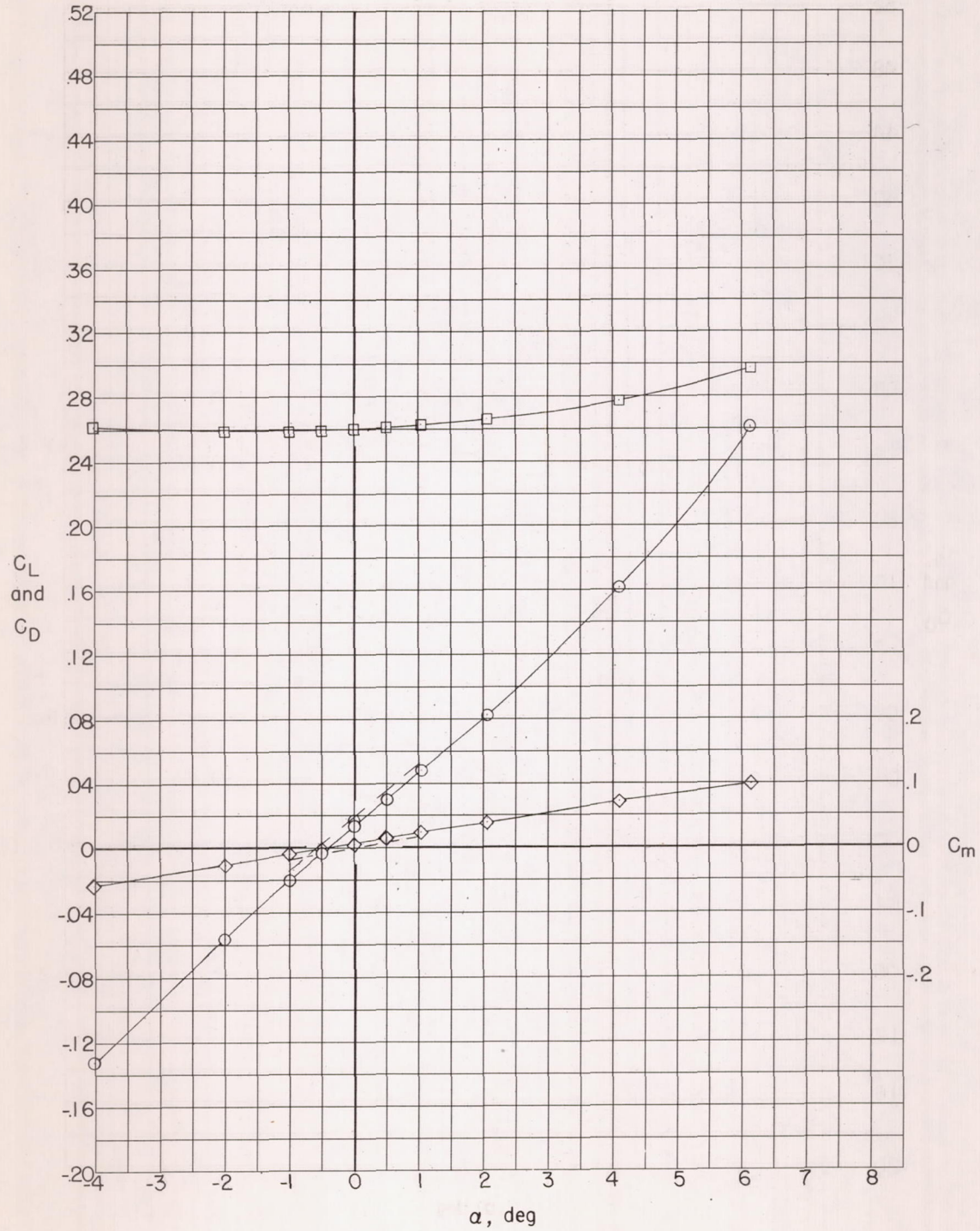

(d) Configuration 4.

Figure 4.- Continued.

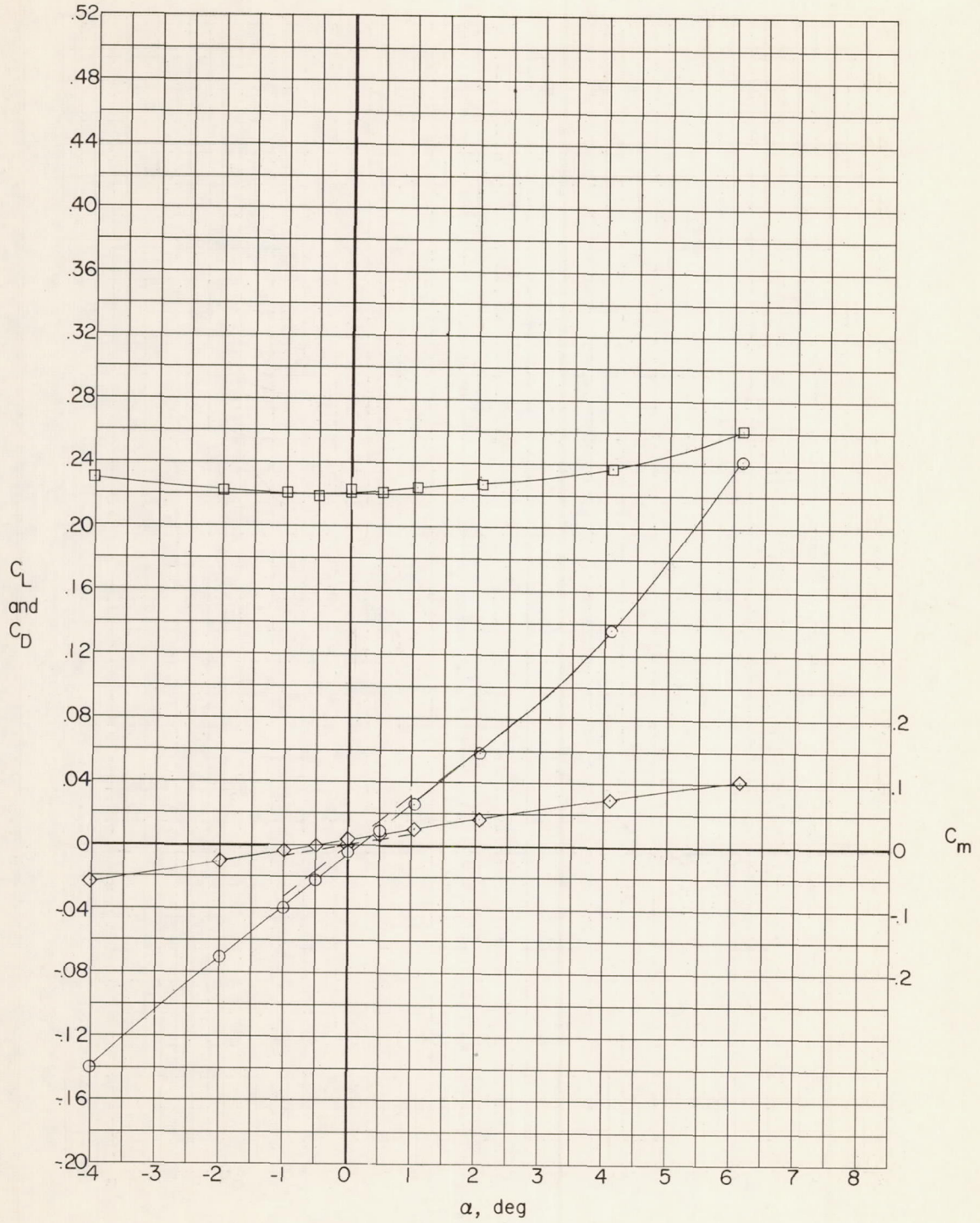

(e) Configuration 5.

Figure 4.- Continued.

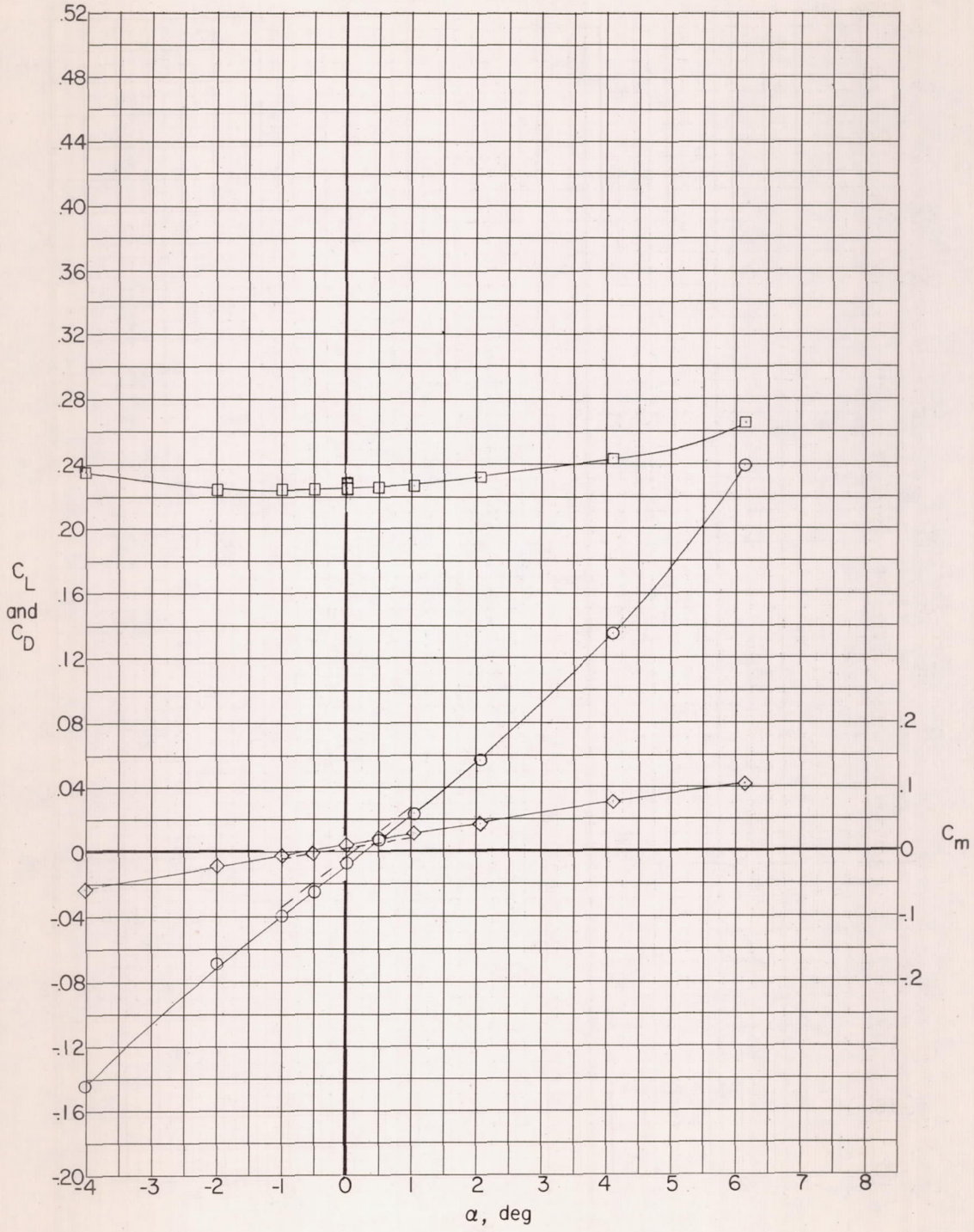

(f) Configuration 6.

Figure 4.- Continued.

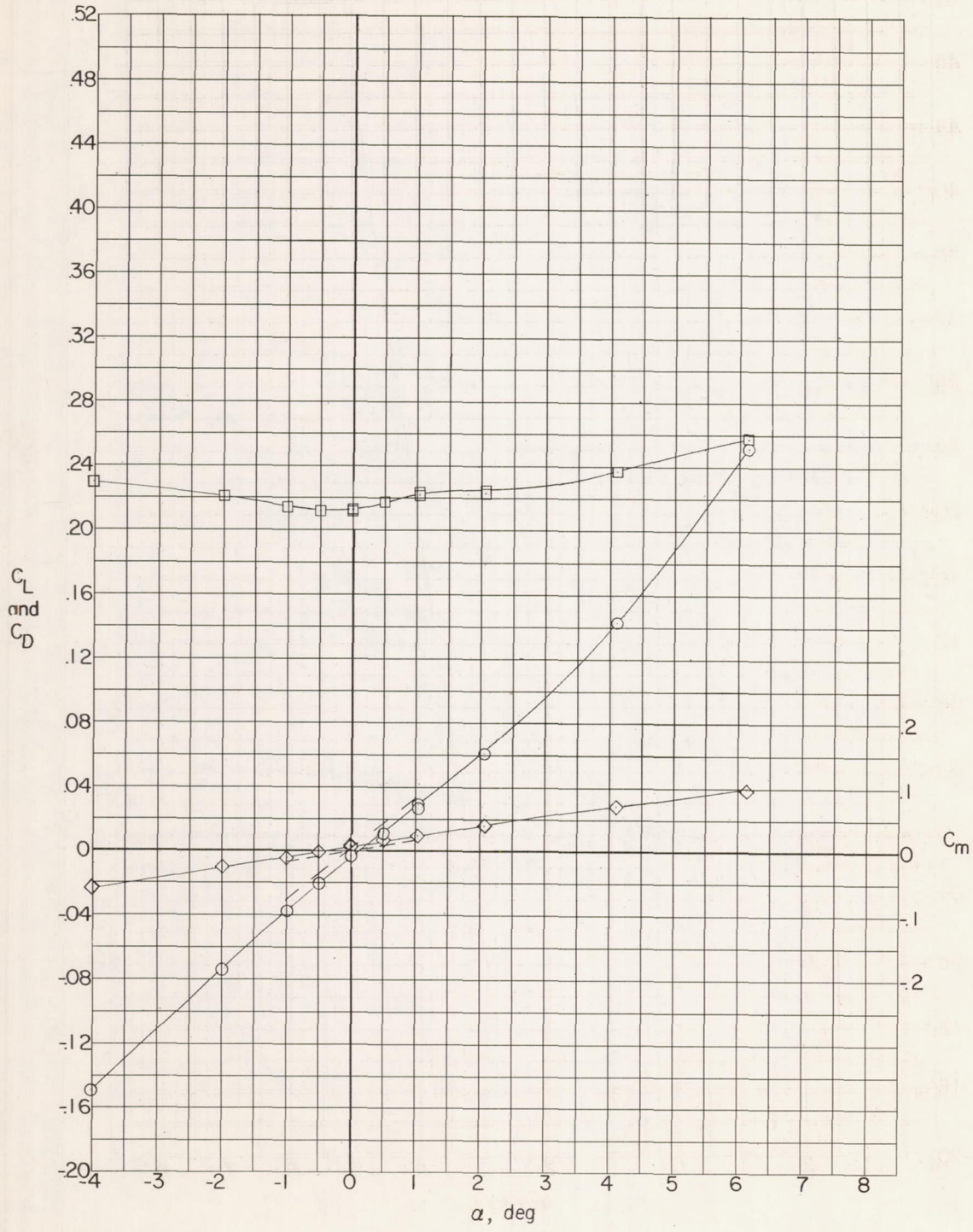

(g) Configuration 7.

Figure 4.- Continued.

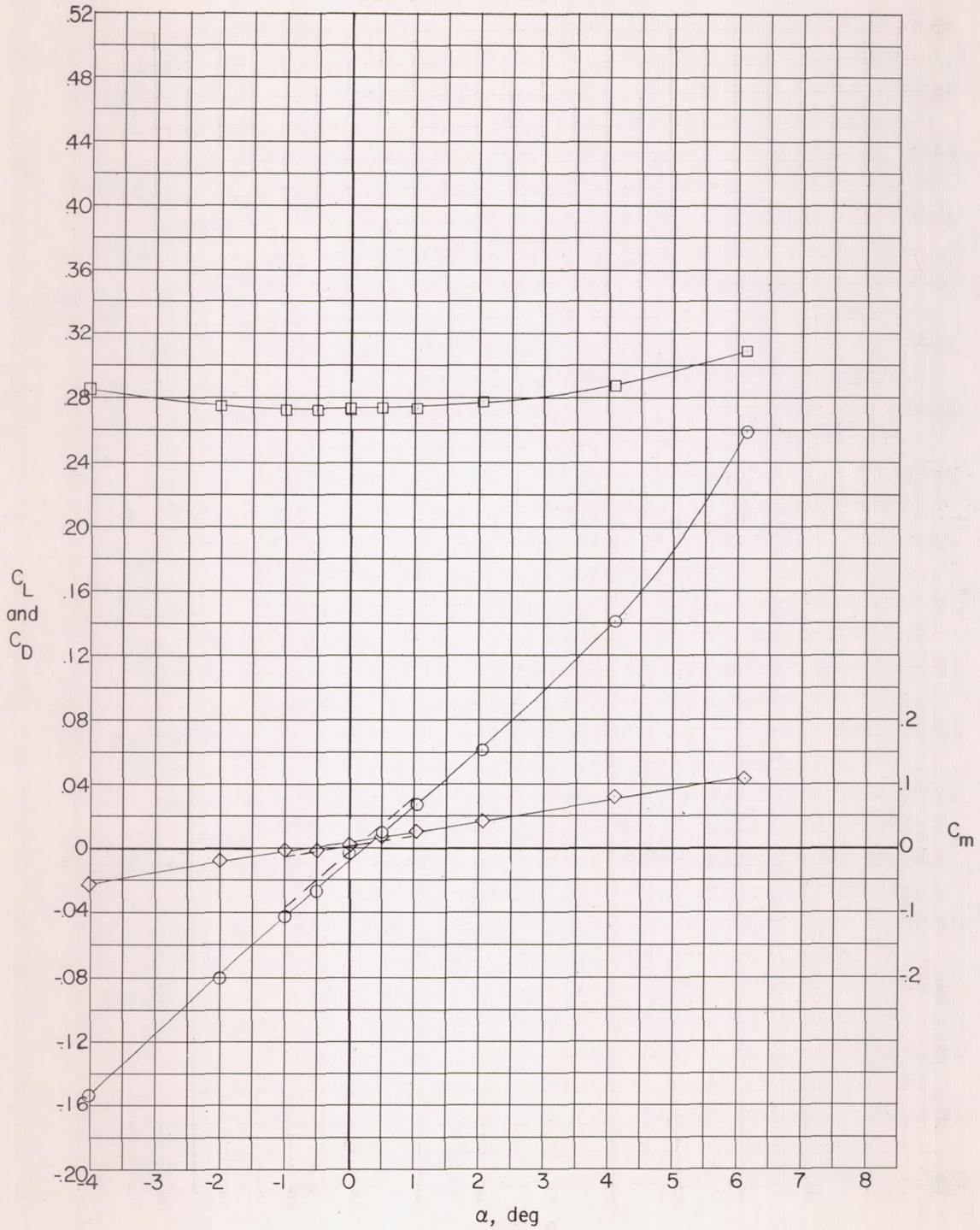

(h) Configuration 8.

Figure 4.- Continued.

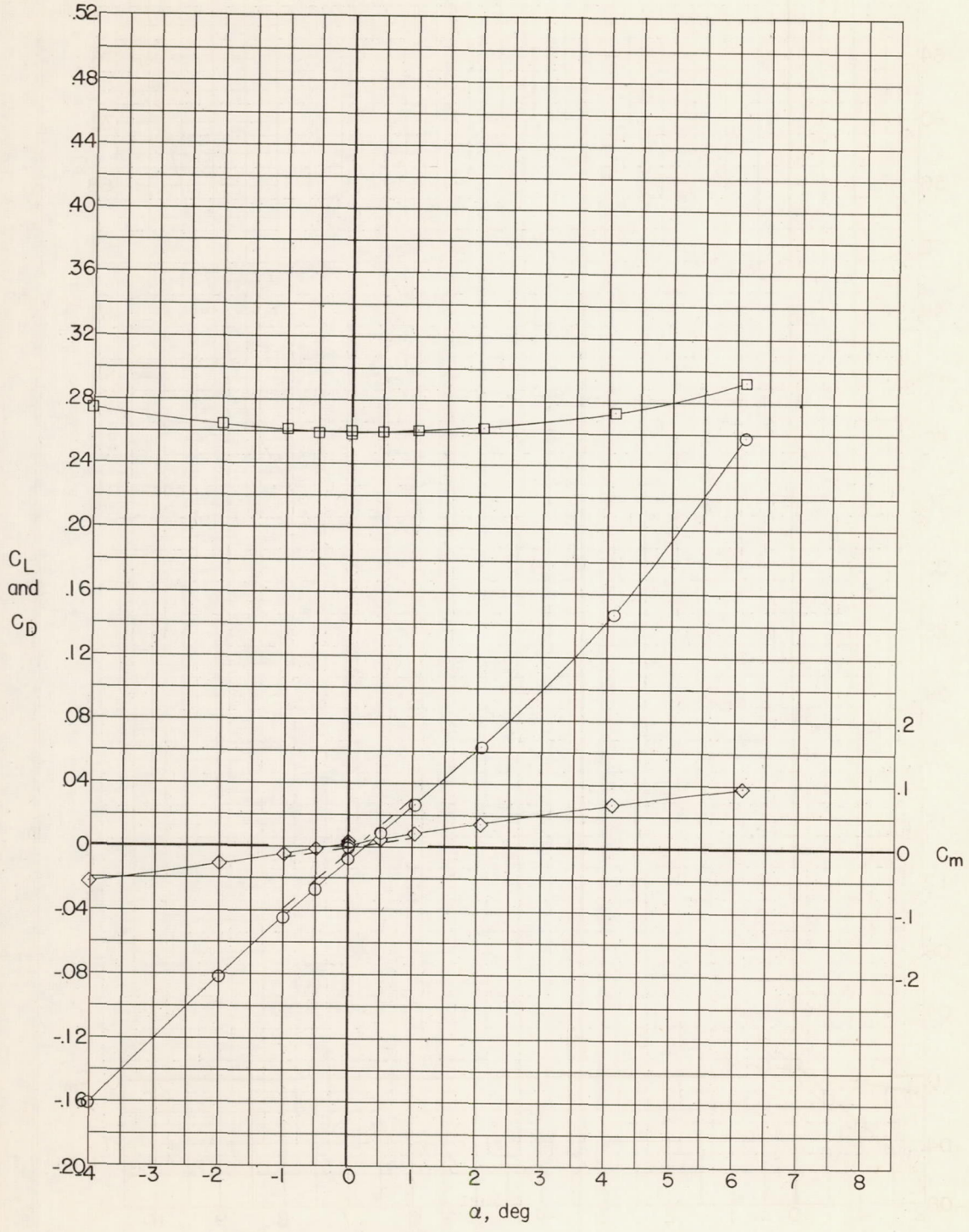

(i) Configuration 9.

Figure 4.- Concluded.

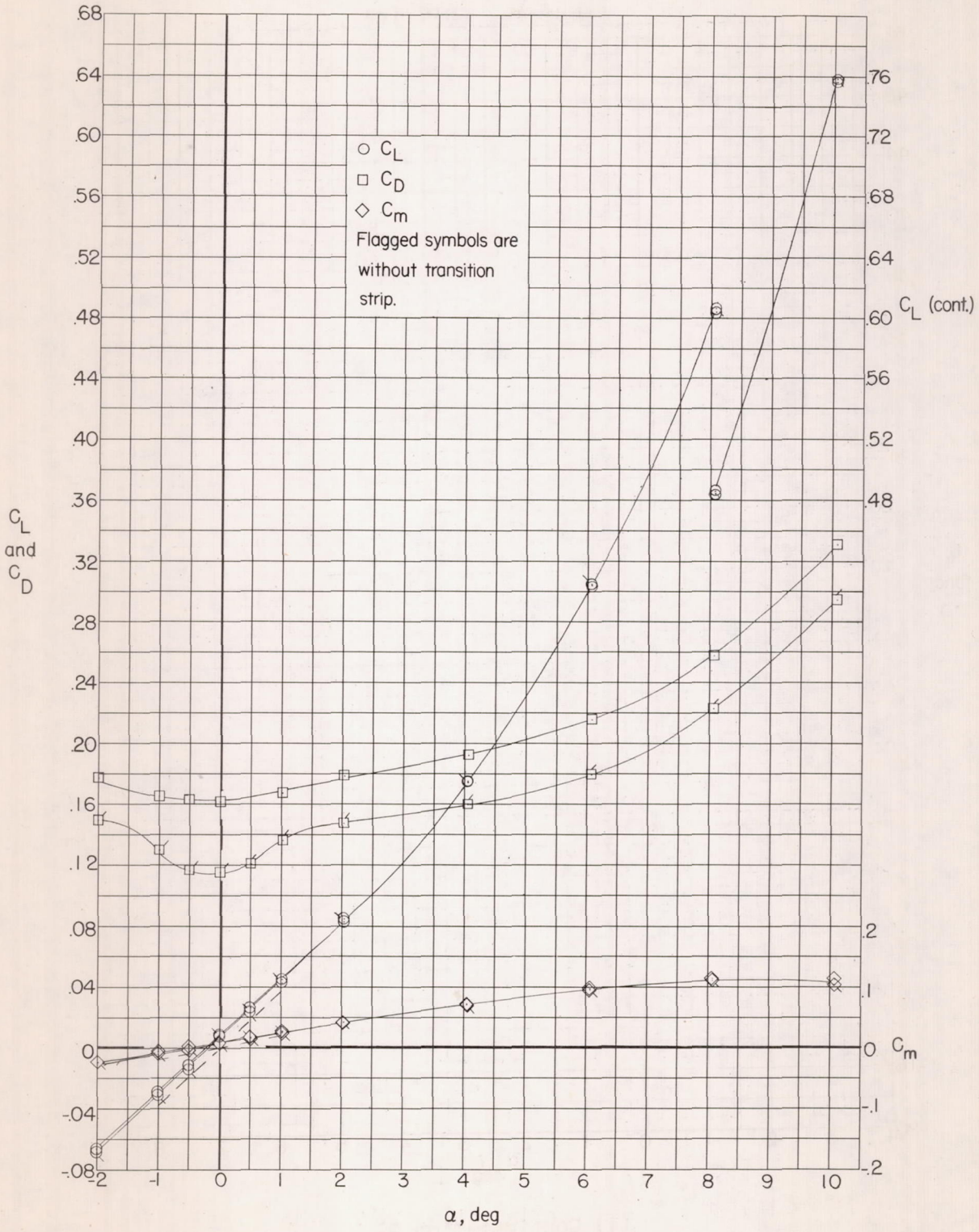

(a) Configuration 1 (basic body).

Figure 5.- Measured aerodynamic characteristics at M = 2.40. (Dashed curves are corrected C_L and C_m results.)

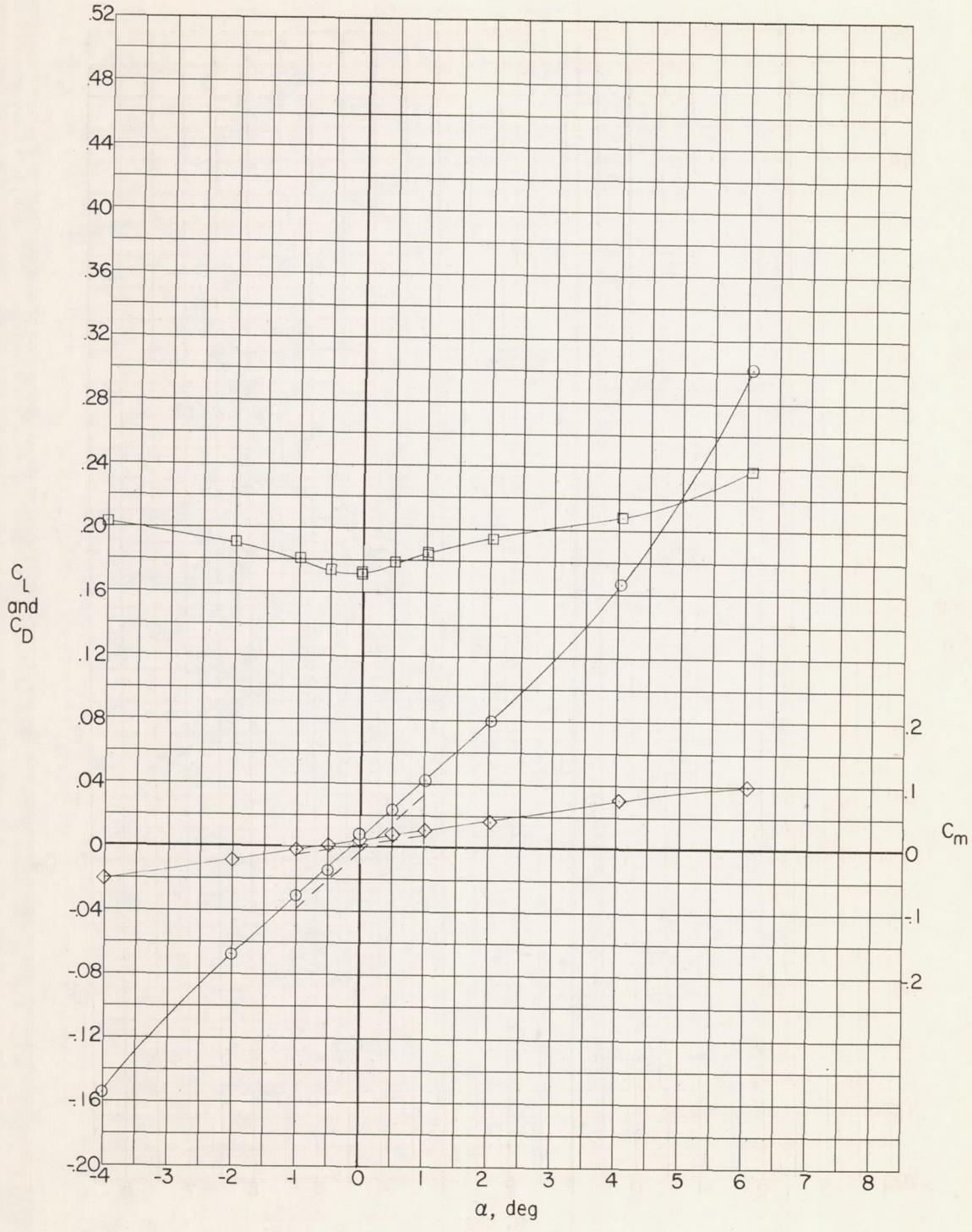

(b) Configuration 2.

Figure 5.- Continued.

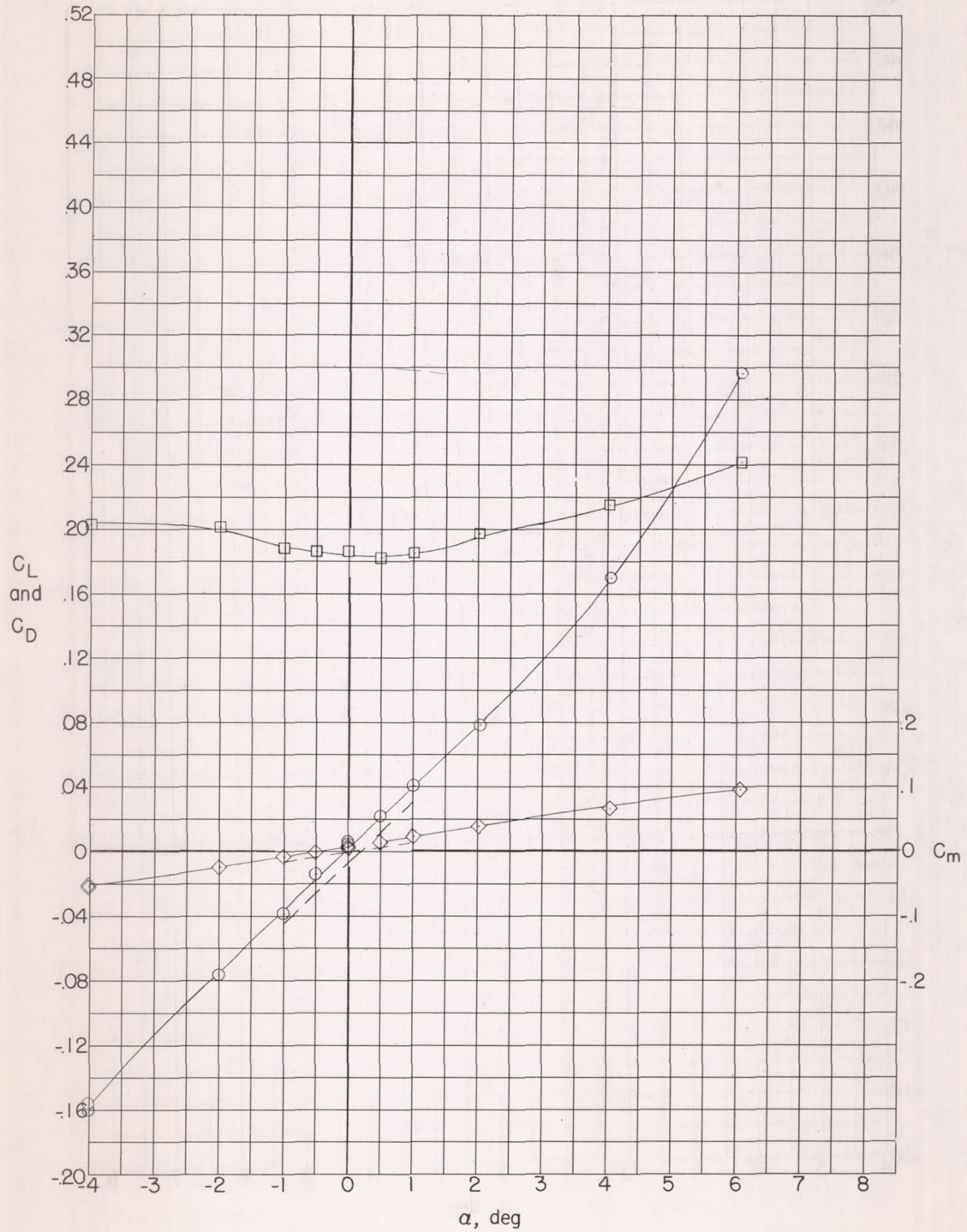

(c) Configuration 3.

Figure 5.- Continued.

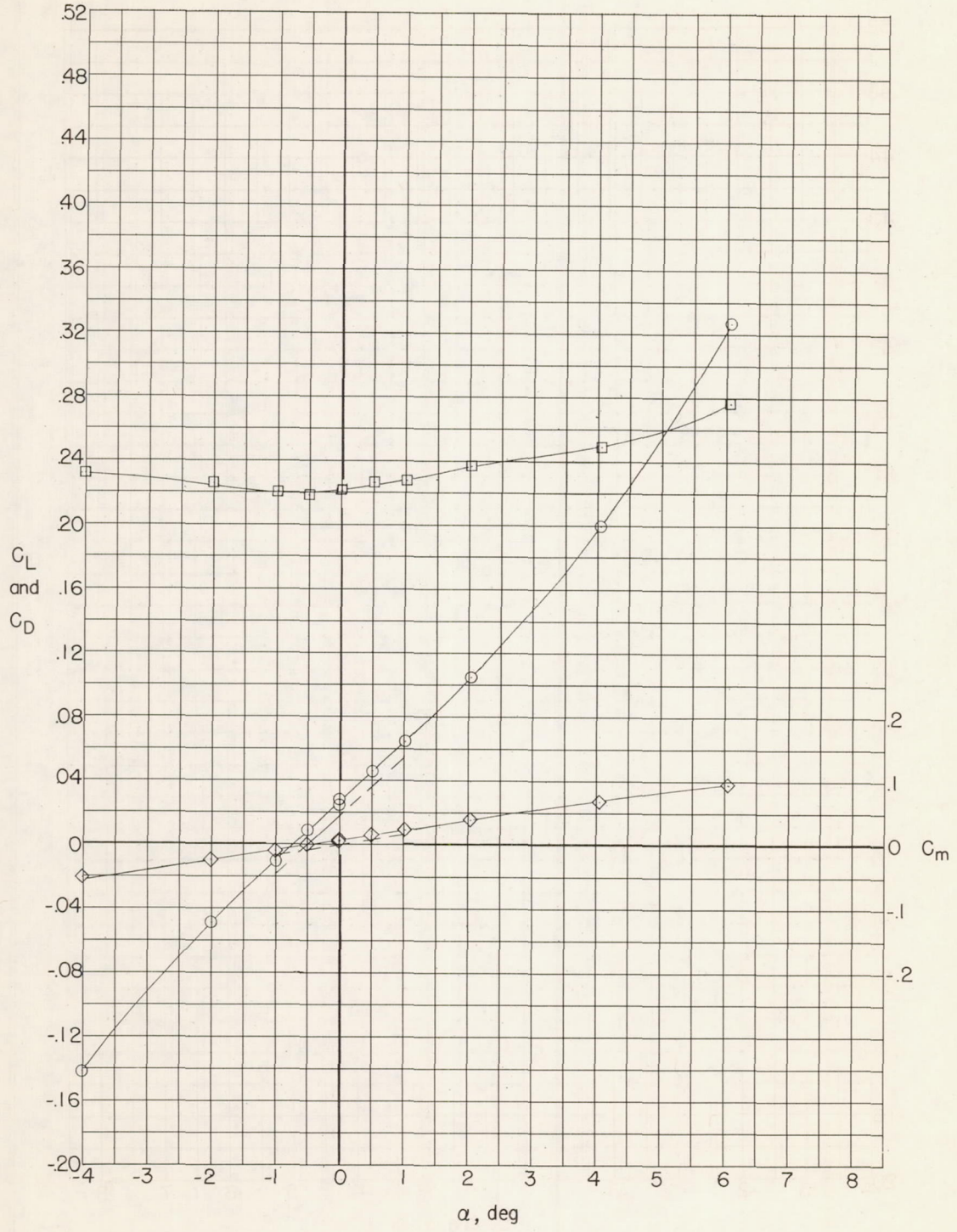

(d) Configuration 4.

Figure 5.- Continued.

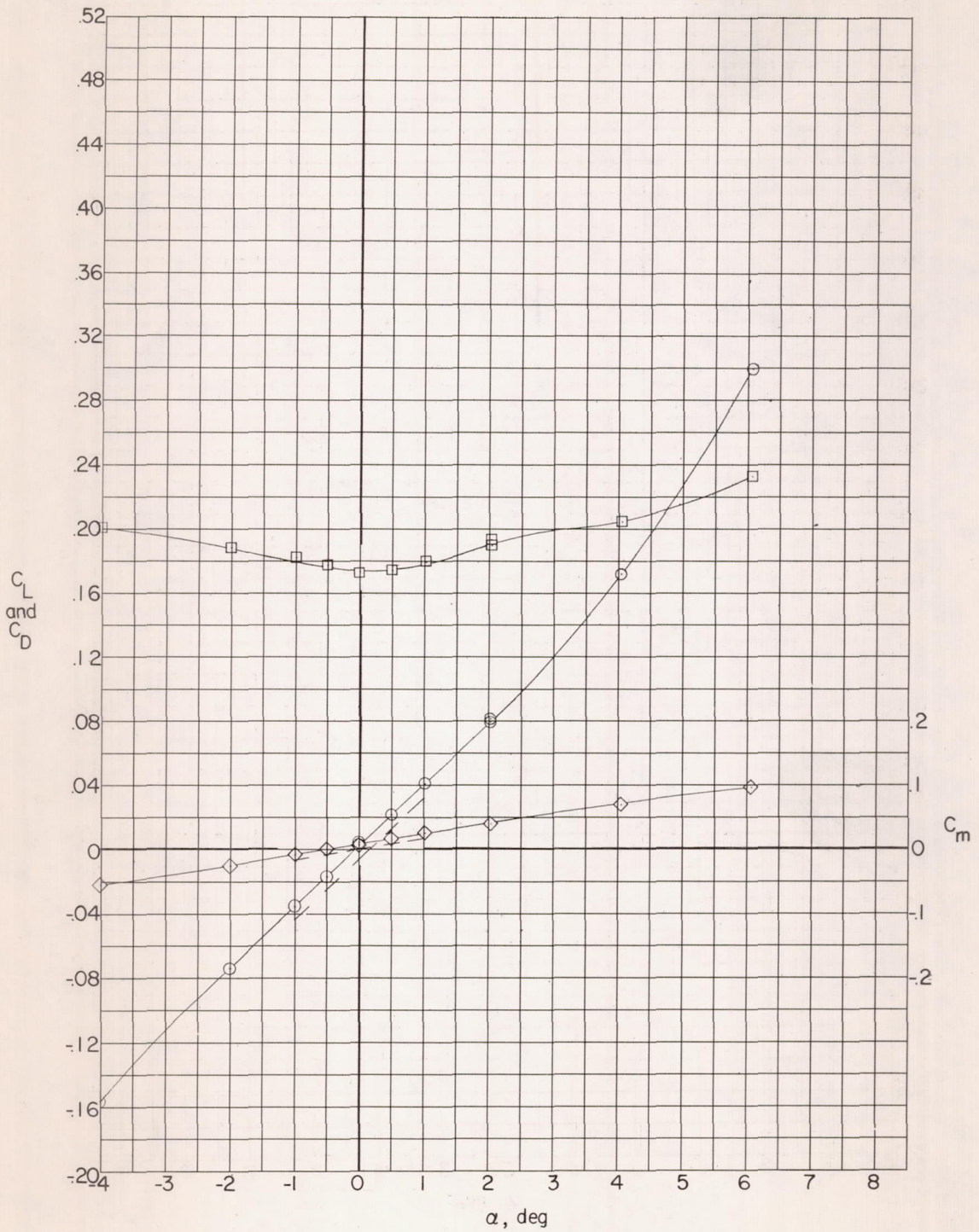

(e) Configuration 5.

Figure 5.- Continued.

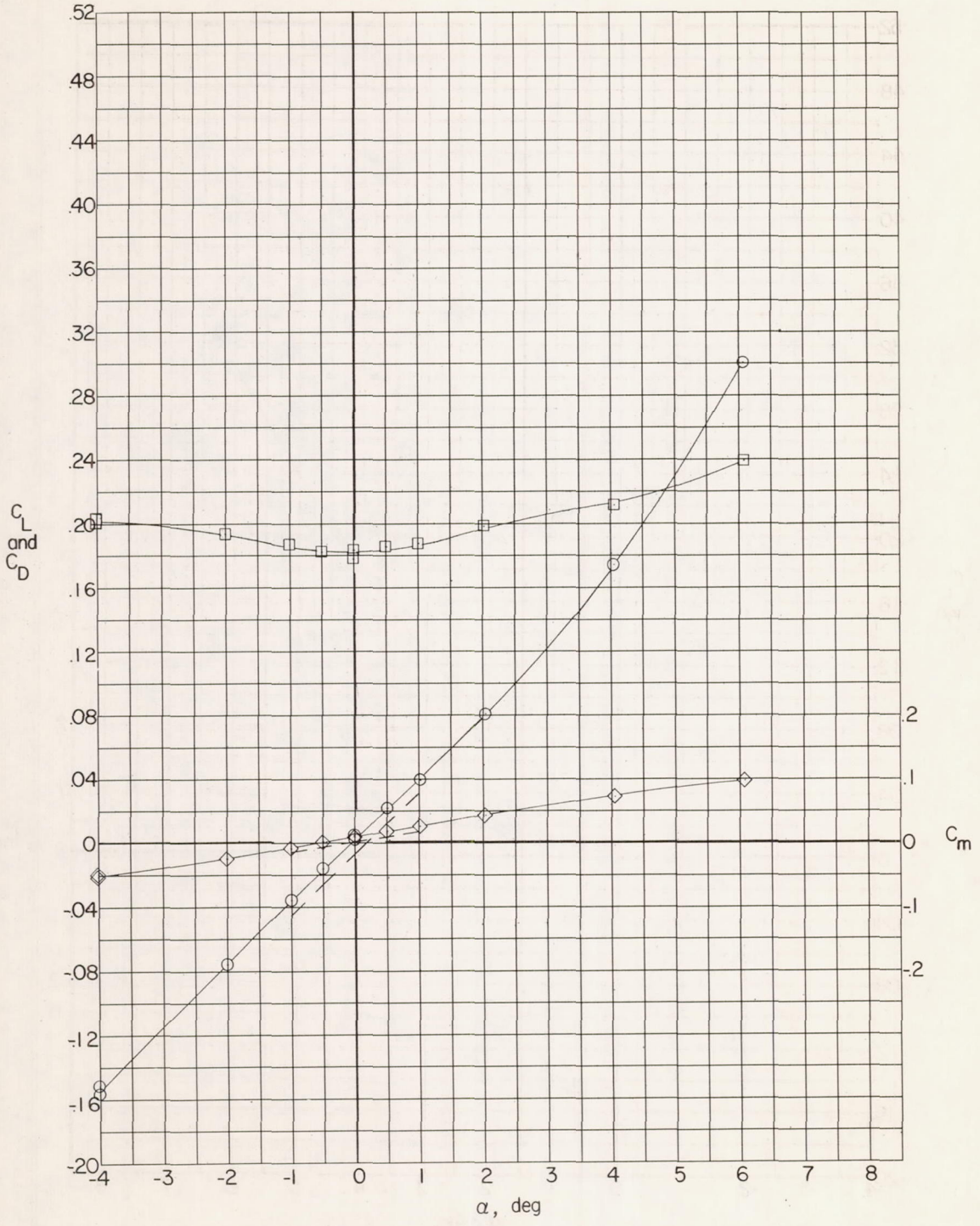

(f) Configuration 6.

Figure 5.- Continued.

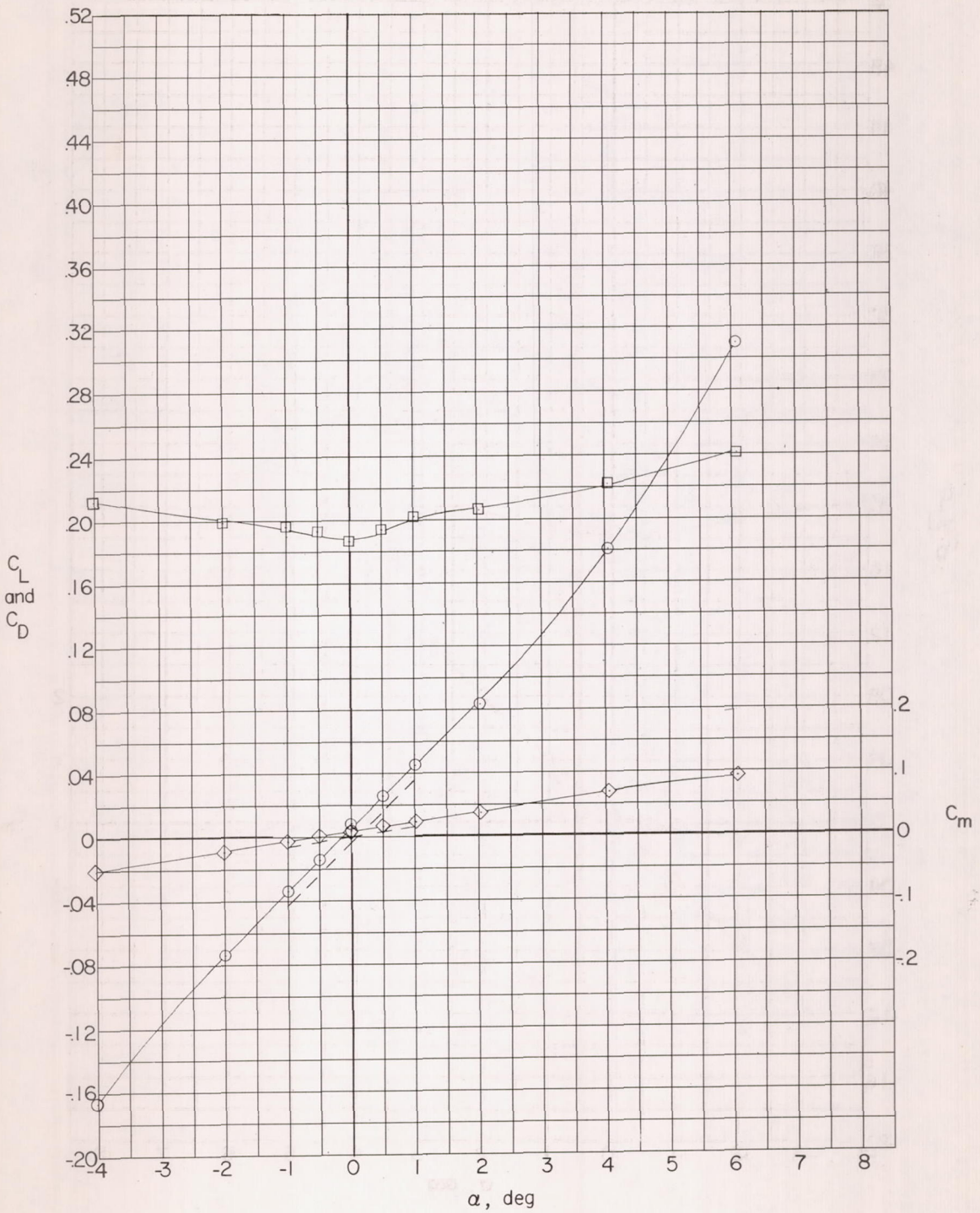

(g) Configuration 7.

Figure 5.- Continued.

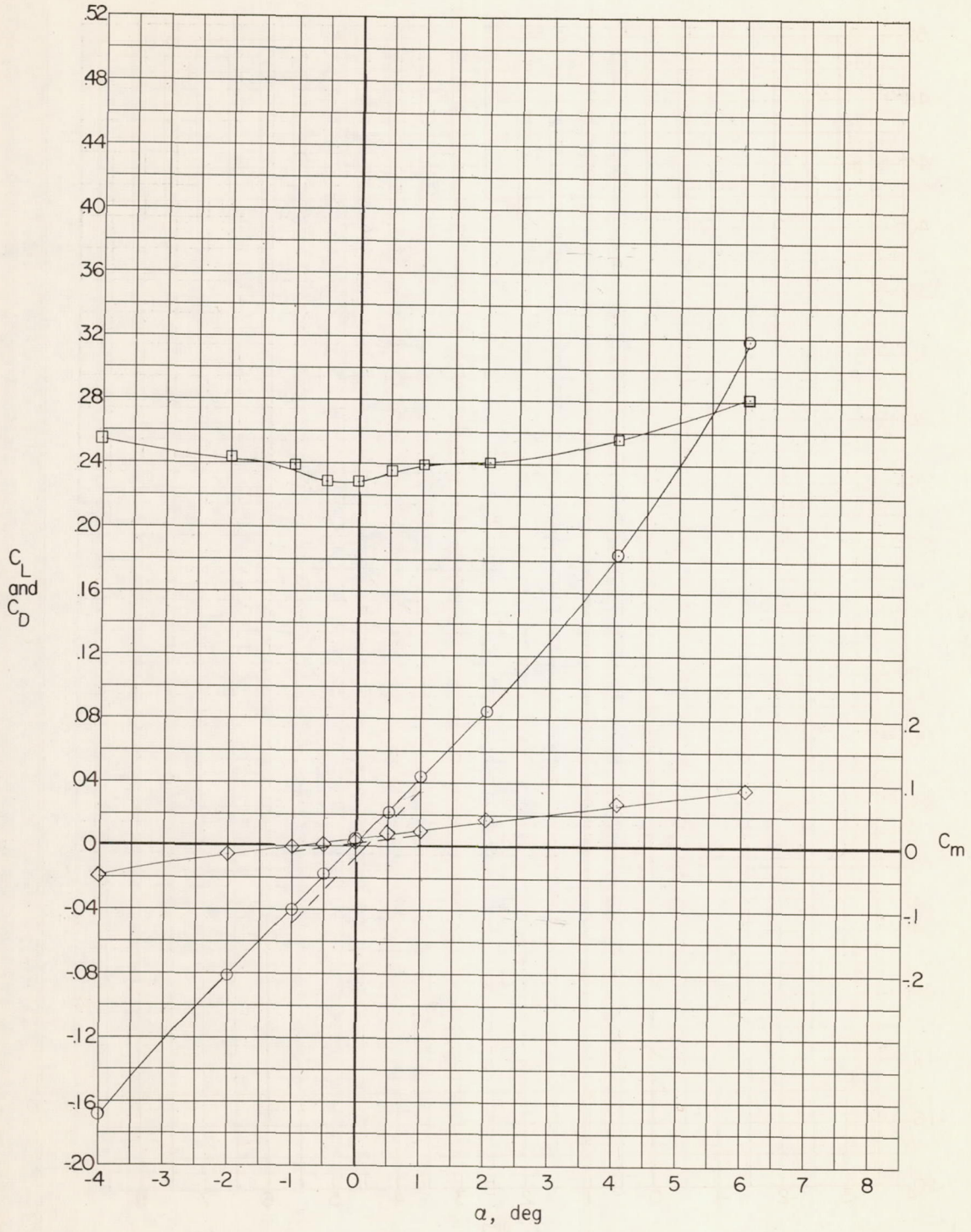

(h) Configuration 8.

Figure 5.- Continued.

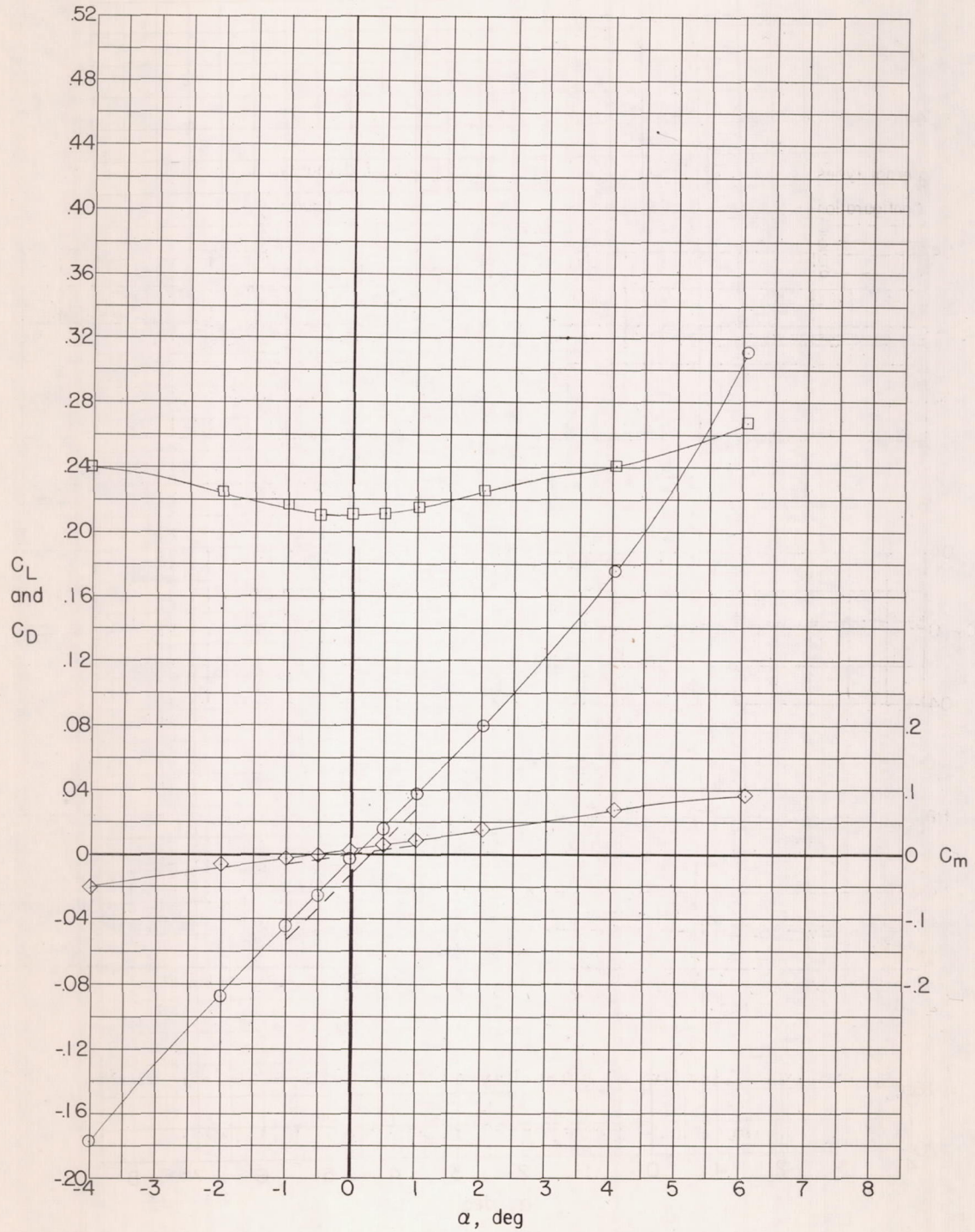

(i) Configuration 9.

Figure 5.- Concluded.

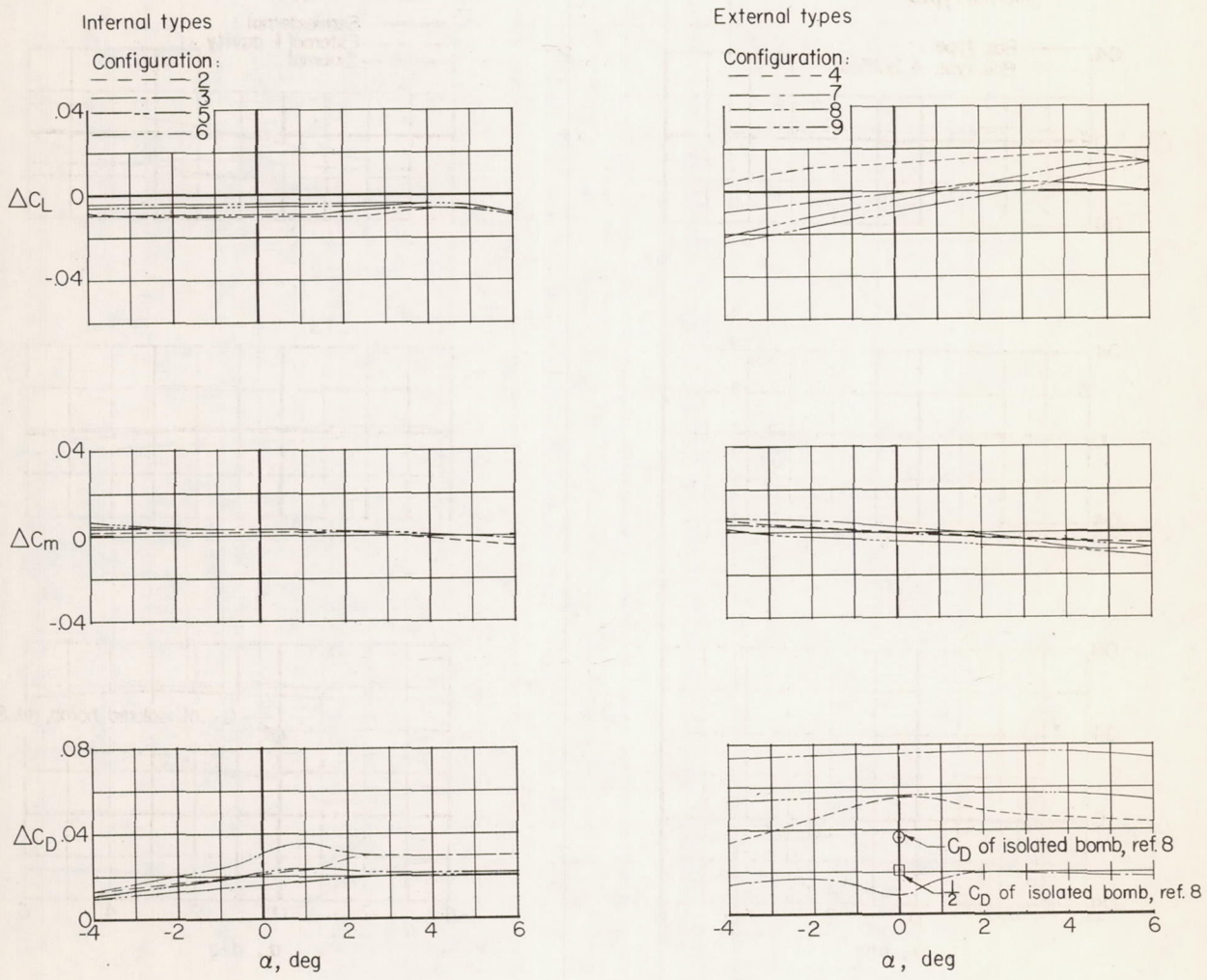

(a) Due to installation of bomb bay or bomb plus bomb bay to basic body.

Figure 6.- Incremental results at M = 1.62.

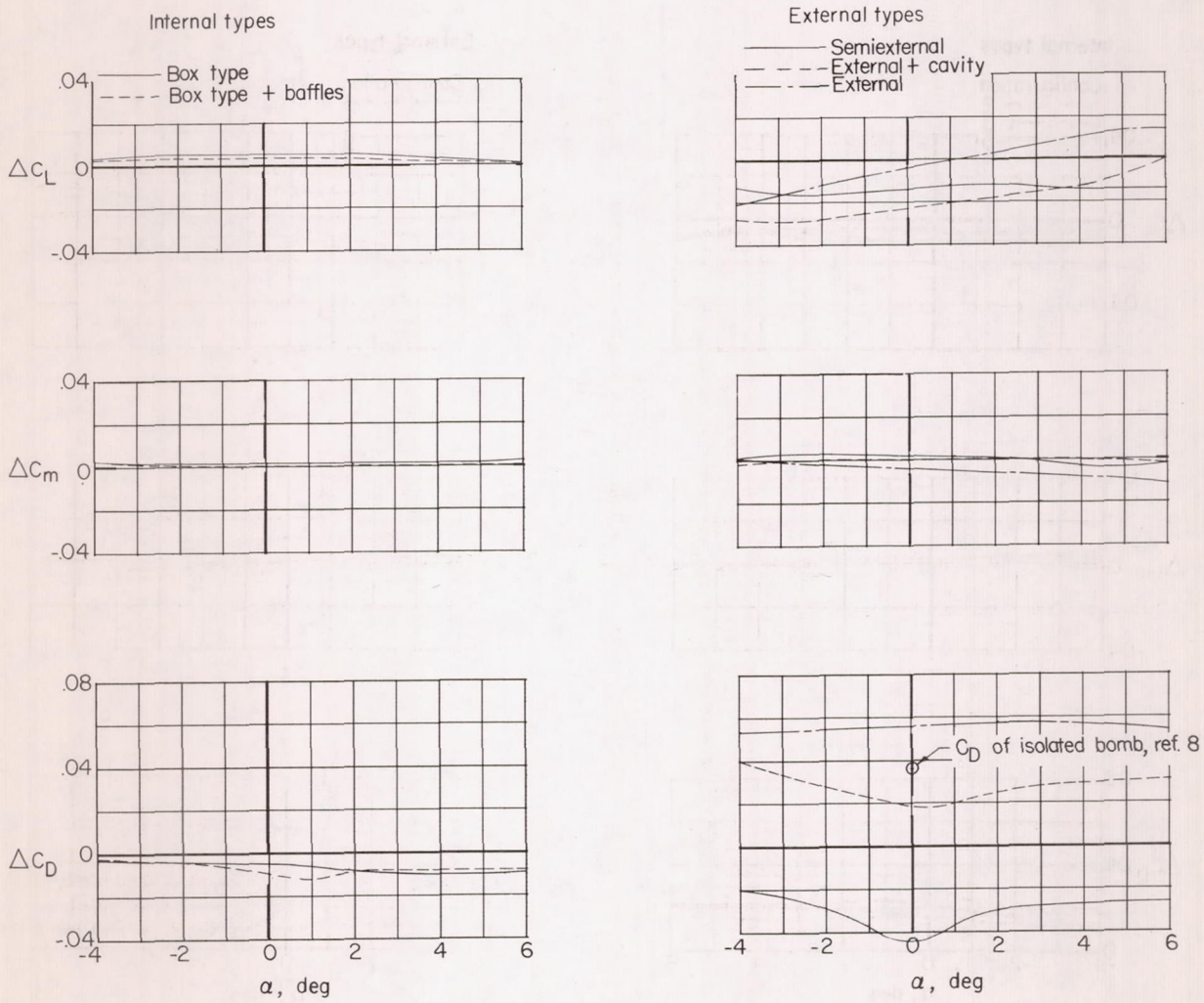

(b) Due to addition of bomb to bomb bay.

Figure 6.- Concluded.

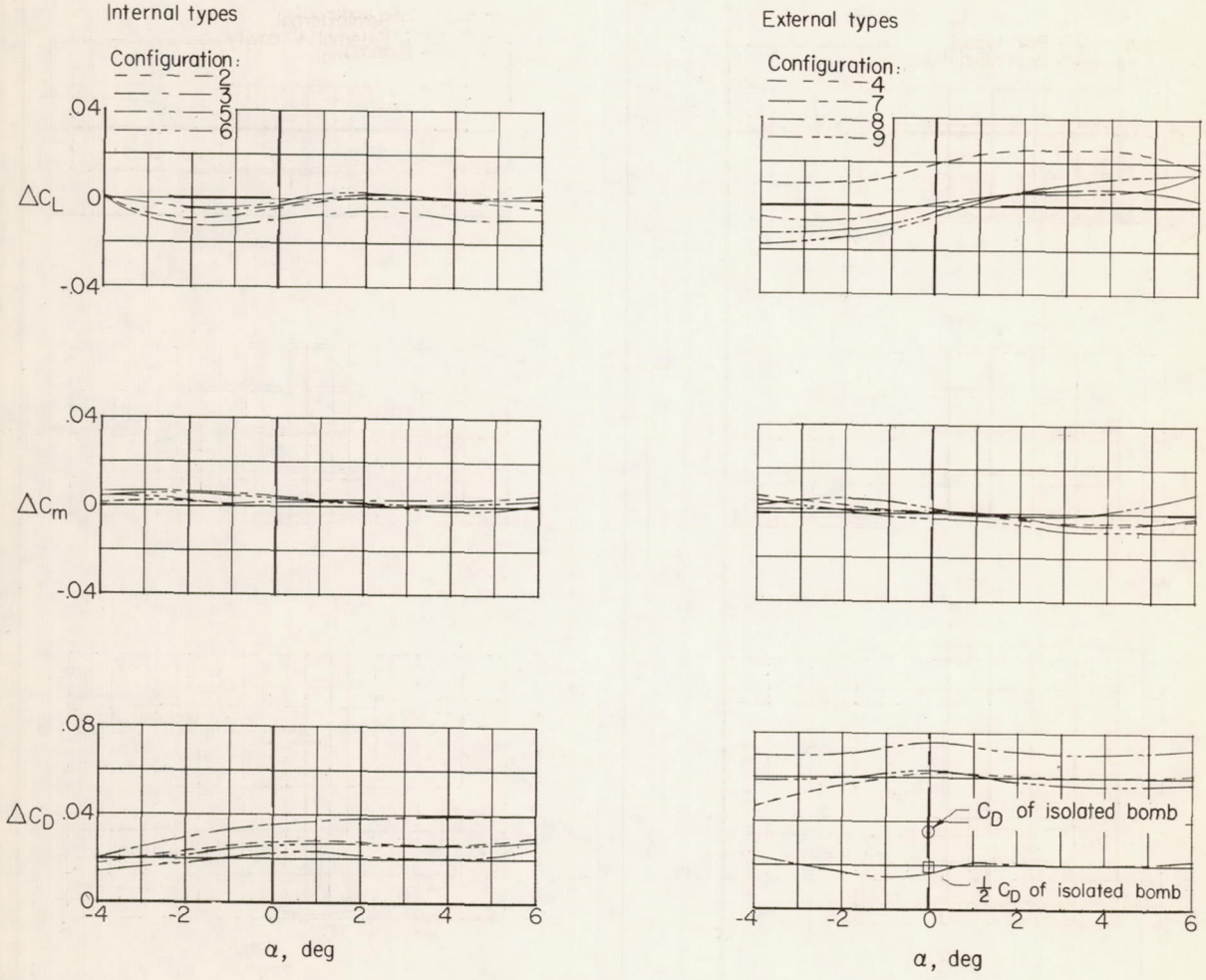

(a) Due to installation of bomb bay or bomb plus bomb bay to basic body.

Figure 7.- Incremental results at M = 1.94.

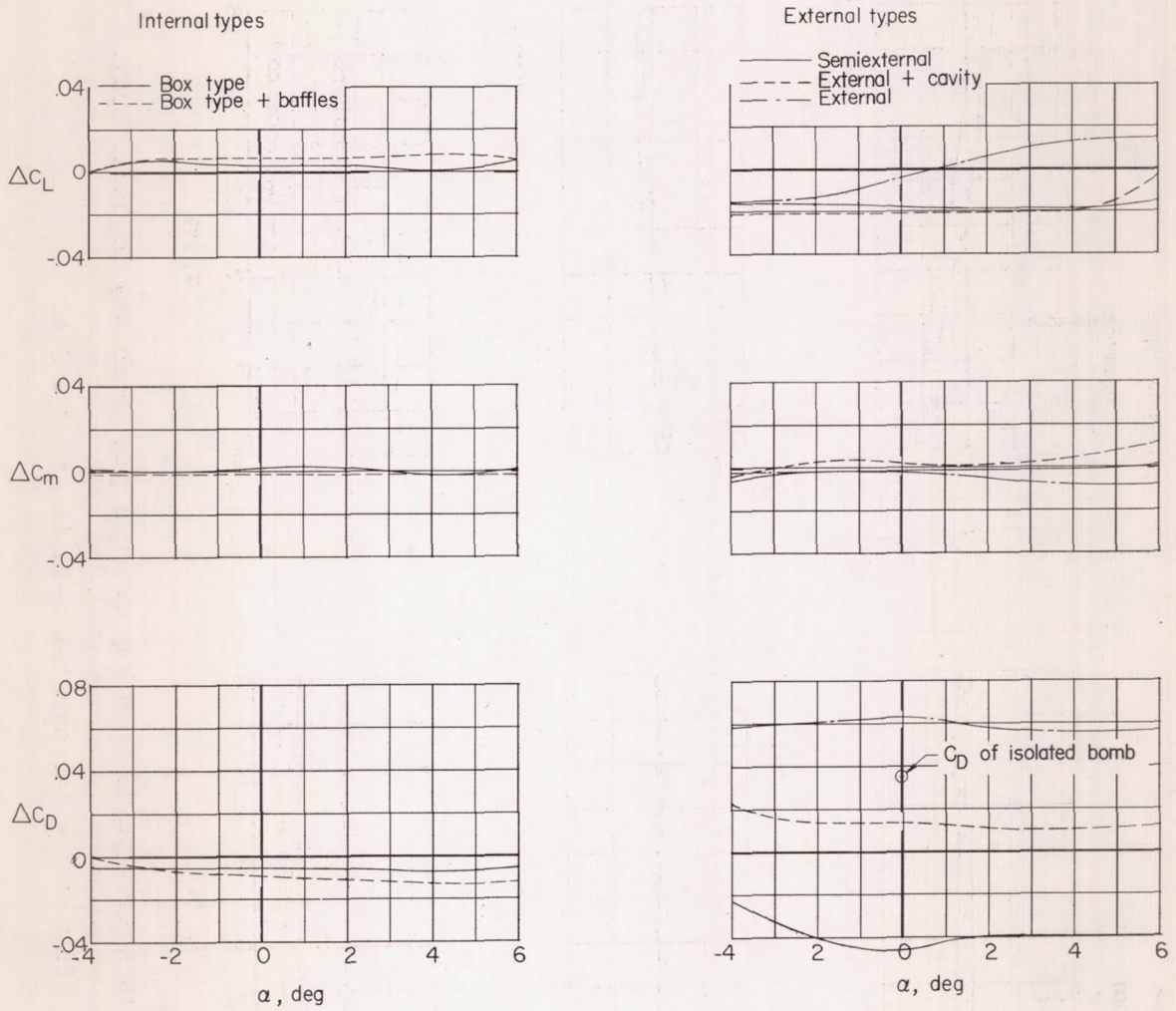

(b) Due to addition of bomb to bomb bay.

Figure 7.- Concluded.

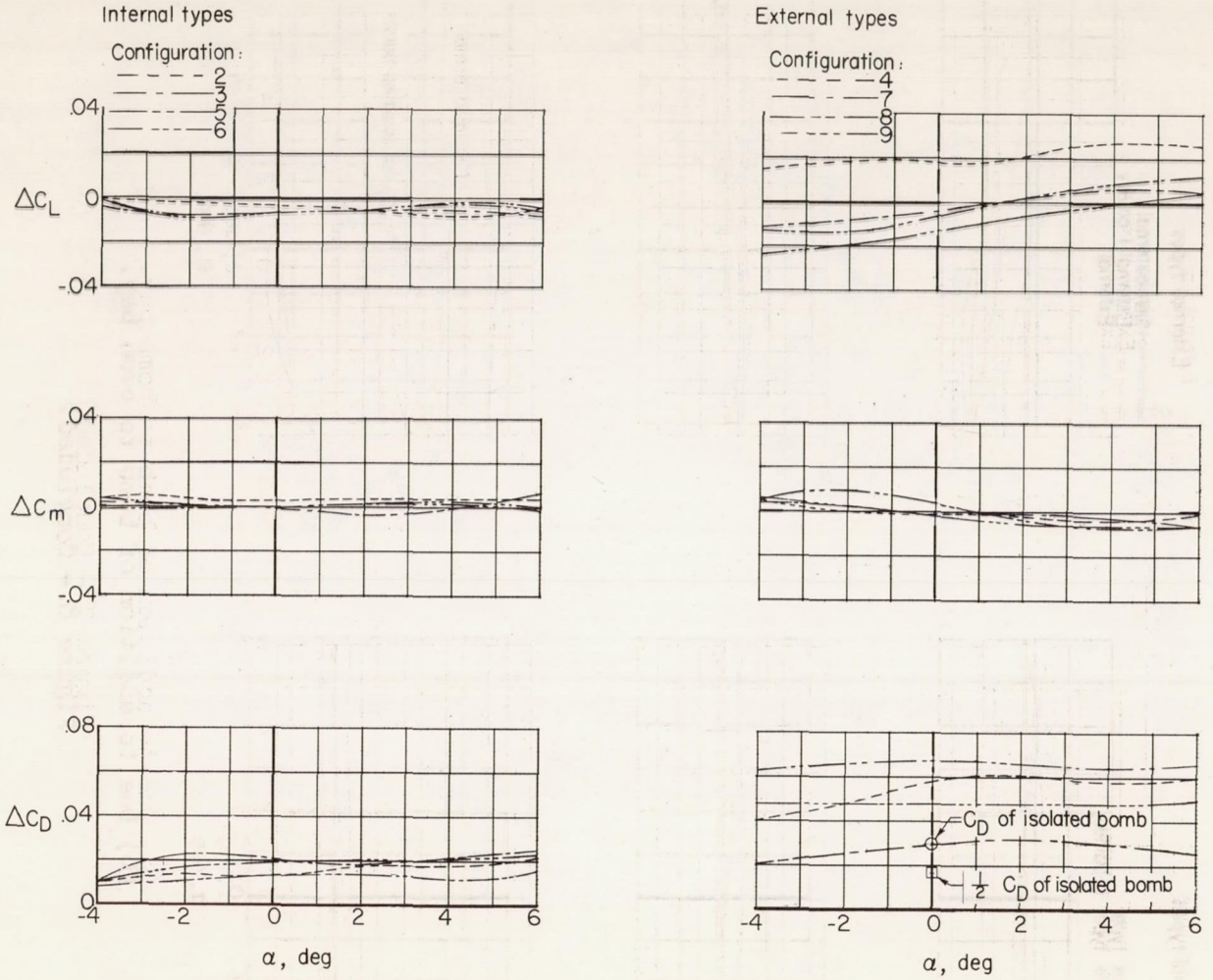

(a) Due to installation of bomb bay or bomb plus bomb bay to basic body.

Figure 8.- Incremental results at M = 2.40.

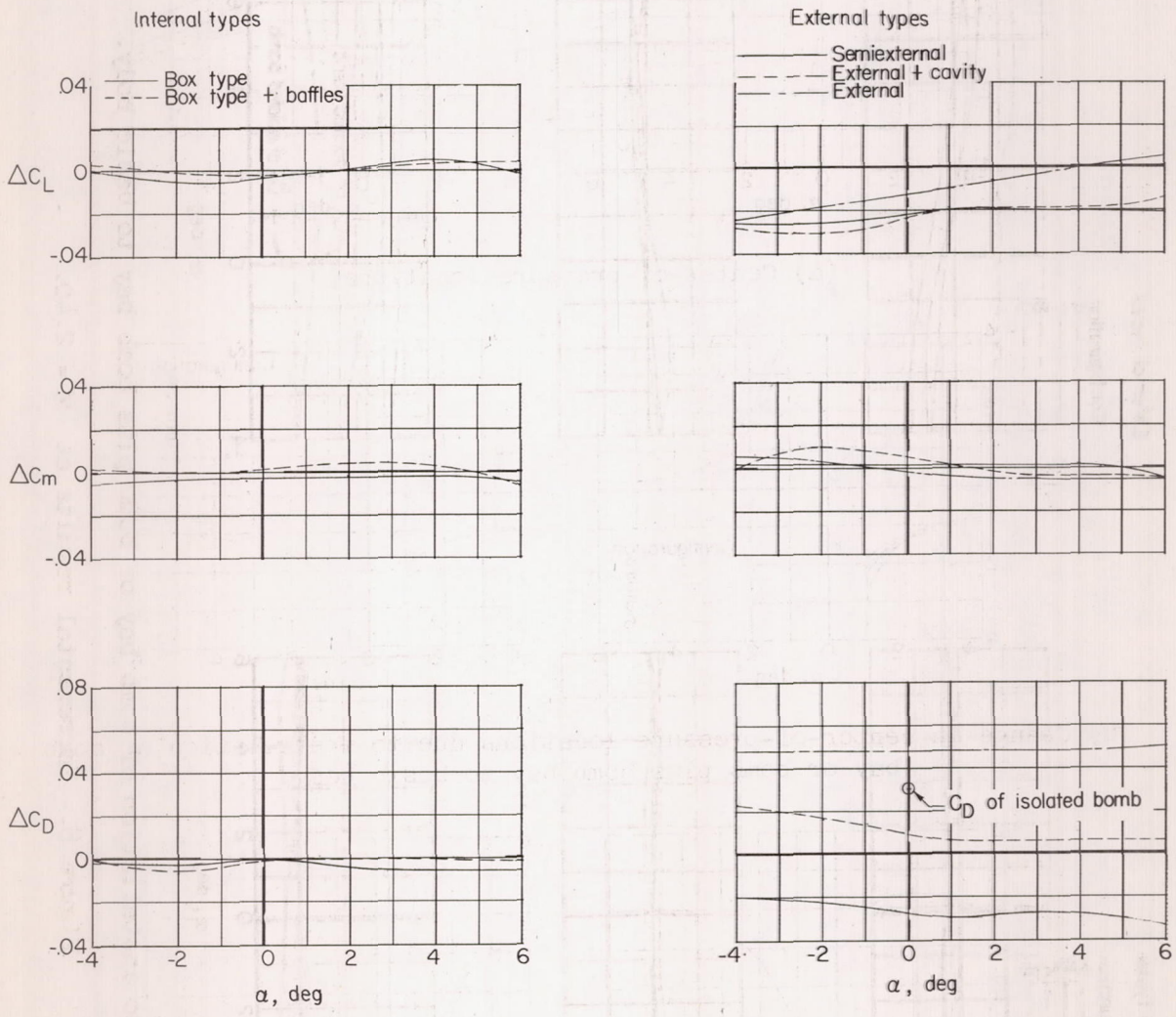

(b) Due to addition of bomb to bomb bay.

Figure 8.- Concluded.

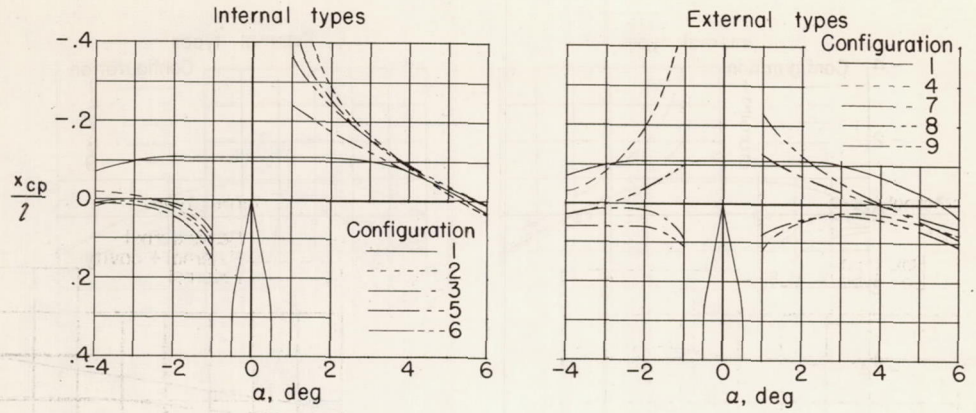

(a) Center-of-pressure locations.

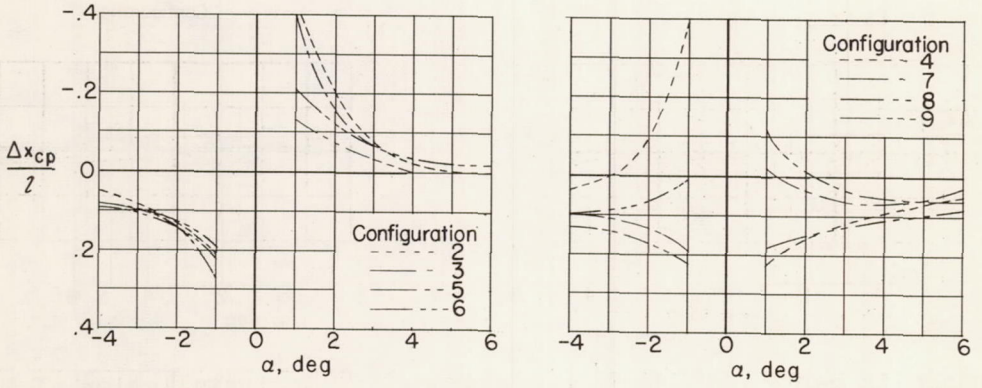

(b) Change in center-of-pressure locations due to installation of bomb bay or bomb plus bomb bay to basic body.

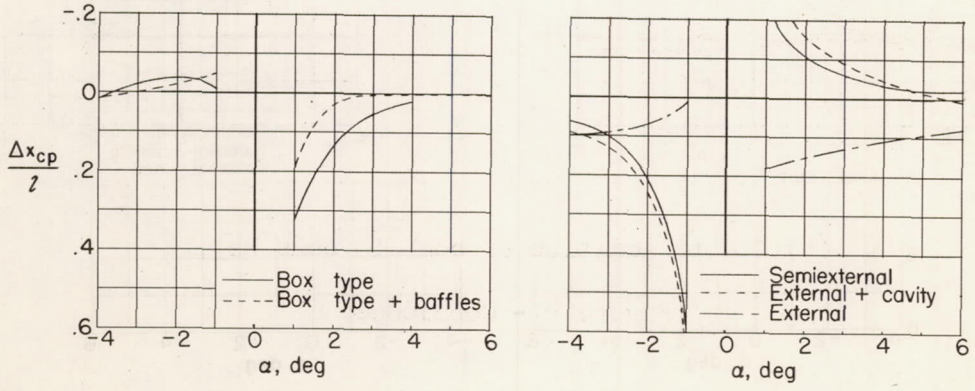

(c) Change in center-of-pressure locations due to addition of bomb to bomb bay.

Figure 9.- Center-of-pressure locations and changes at M = 1.62.

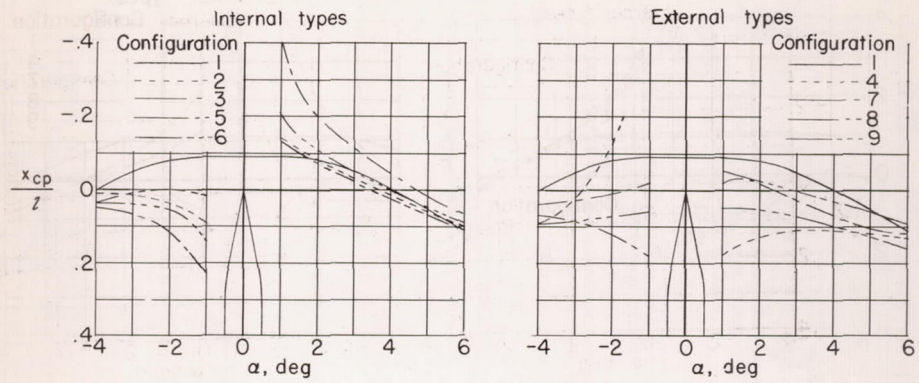

(a) Center-of-pressure locations.

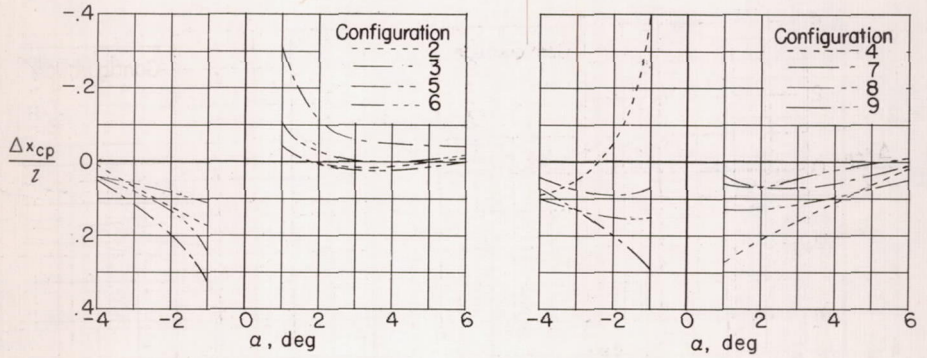

(b) Change in center-of-pressure locations due to installation of bomb bay or bomb plus bomb bay to basic body.

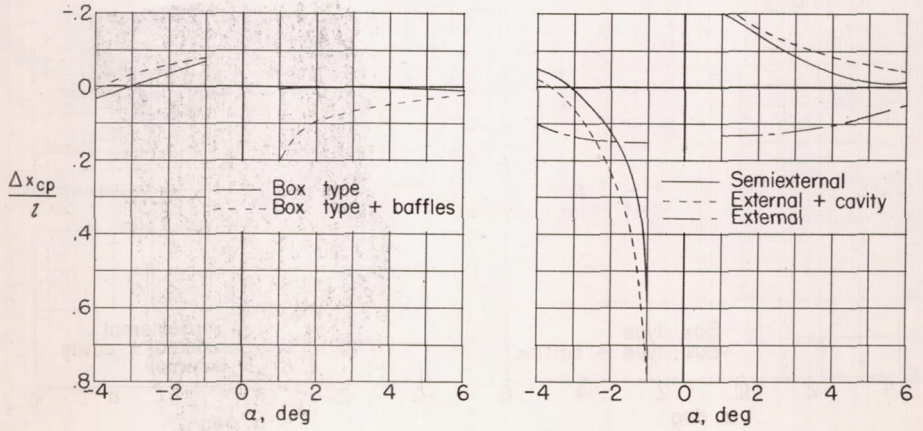

(c) Change in center-of-pressure locations due to addition of bomb to bomb bay.

Figure 10.- Center-of-pressure locations and changes at M = 1.94.

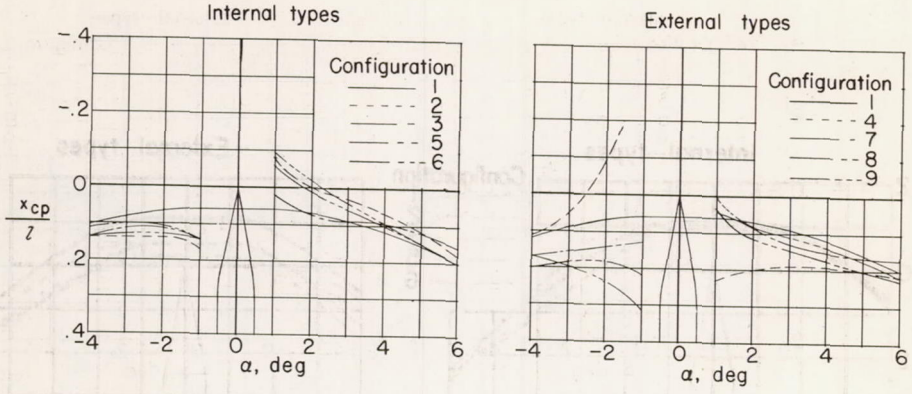

(a) Center-of-pressure locations.

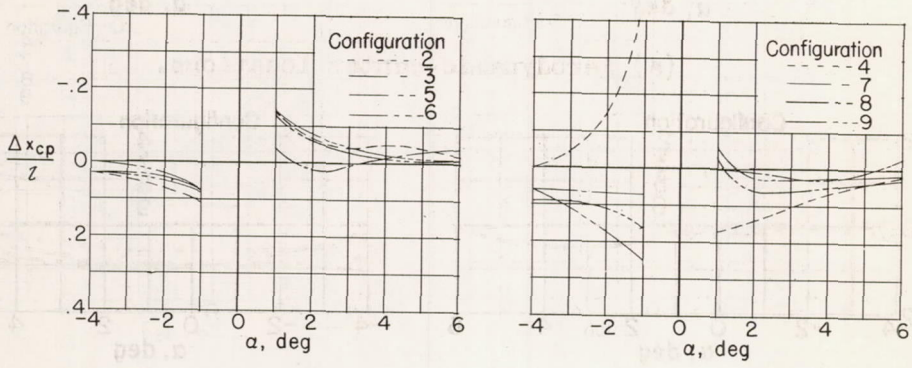

(b) Change in center-of-pressure locations due to installation of bomb bay or bomb plus bomb bay to basic body.

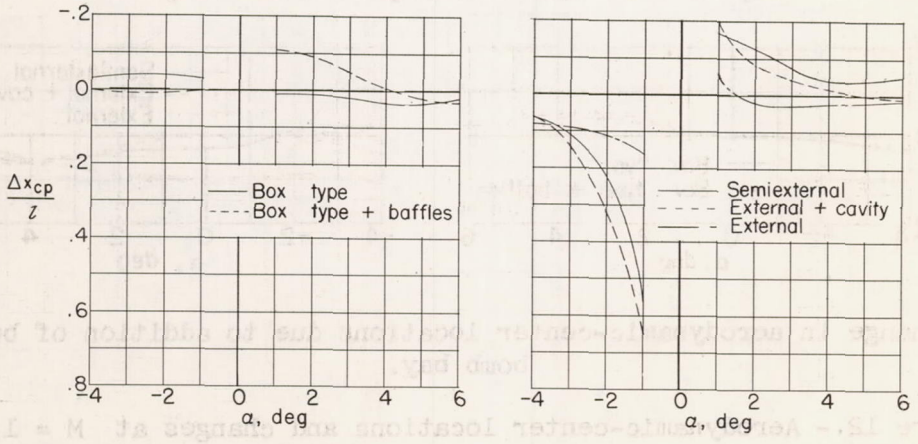

(c) Change in center-of-pressure locations due to addition of bomb to bomb bay.

Figure 11.- Center-of-pressure locations and changes at M = 2.40.

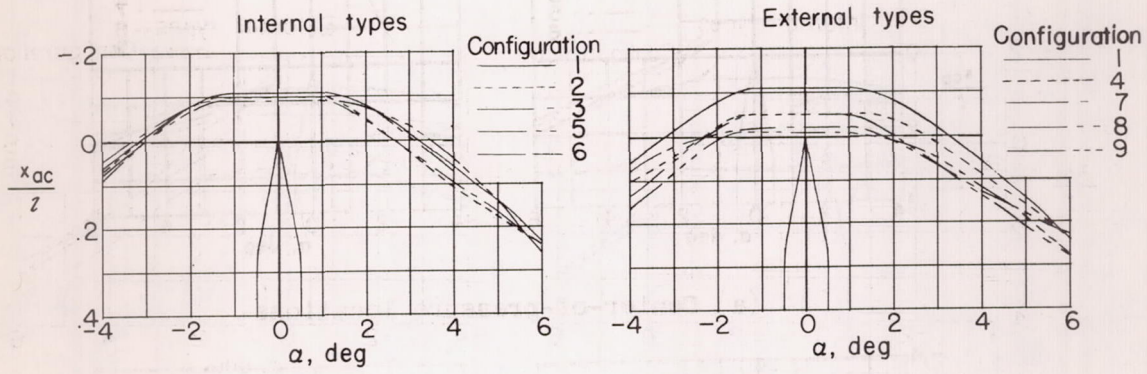

(a) Aerodynamic-center locations.

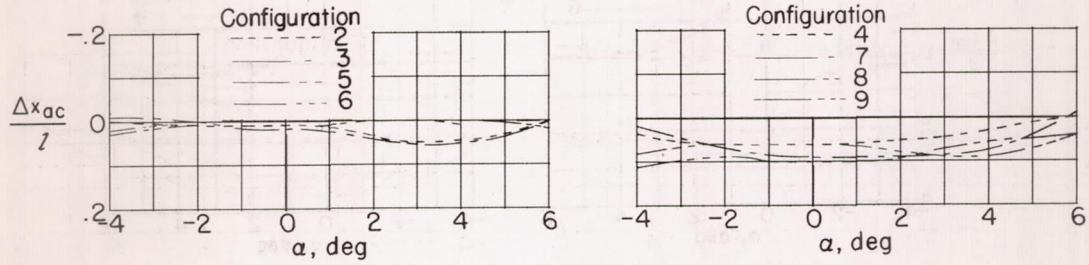

(b) Change in aerodynamic-center locations due to installation of bomb bay or bomb plus bomb bay to basic body.

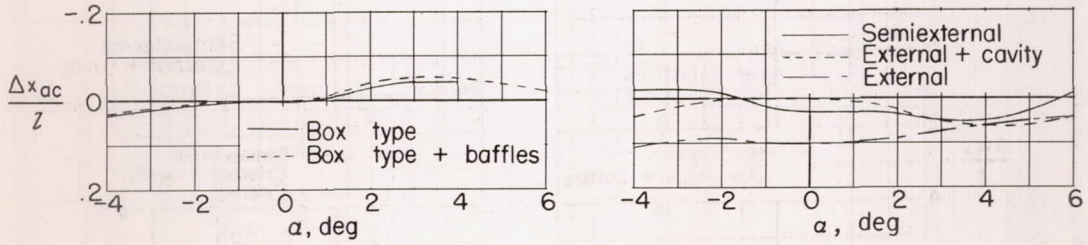

(c) Change in aerodynamic-center locations due to addition of bomb to bomb bay.

Figure 12.- Aerodynamic-center locations and changes at M = 1.62.

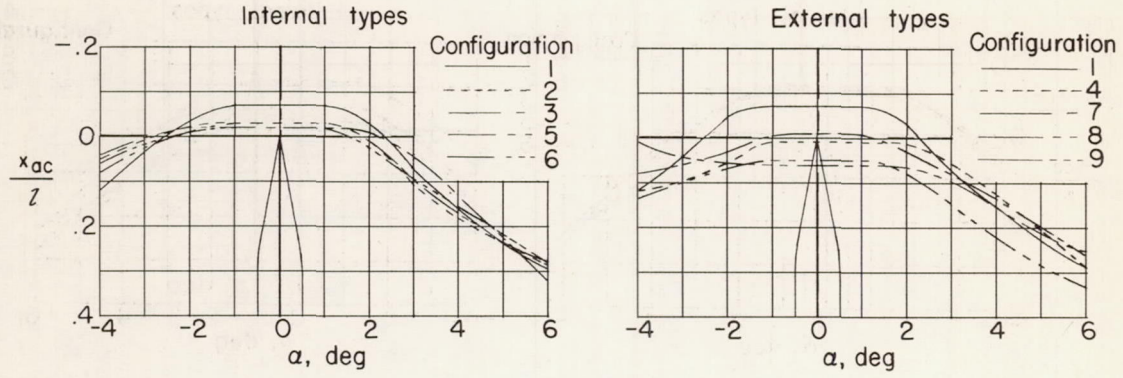

(a) Aerodynamic-center locations.

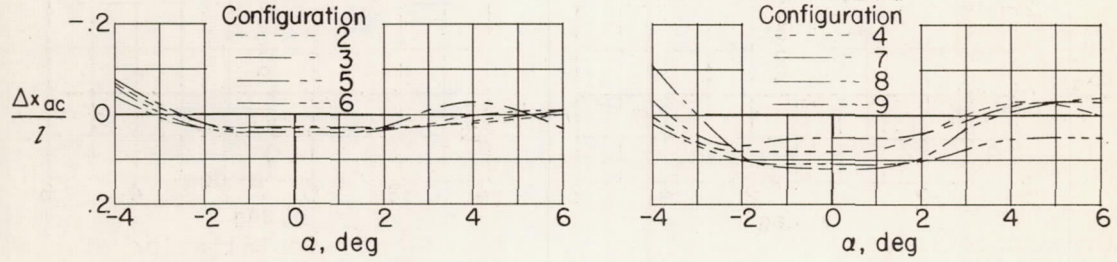

(b) Change in aerodynamic-center locations due to installation of bomb bay or bomb plus bomb bay to basic body.

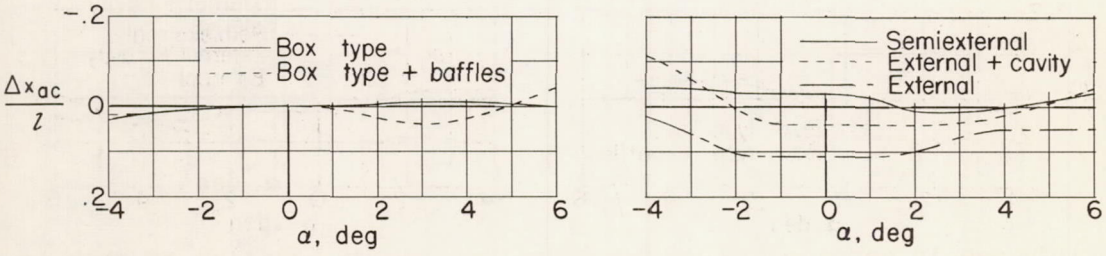

(c) Change in aerodynamic-center locations due to addition of bomb to bomb bay.

Figure 13.- Aerodynamic-center locations and changes at M = 1.94.

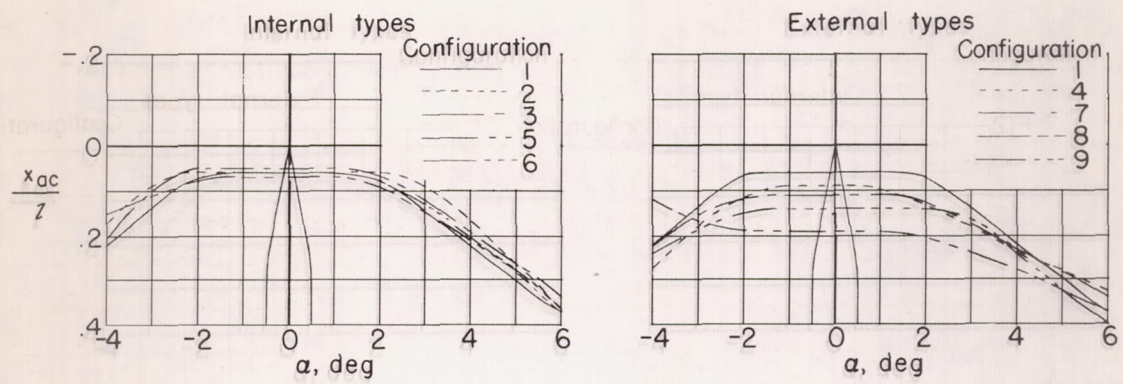

(a) Aerodynamic-center locations.

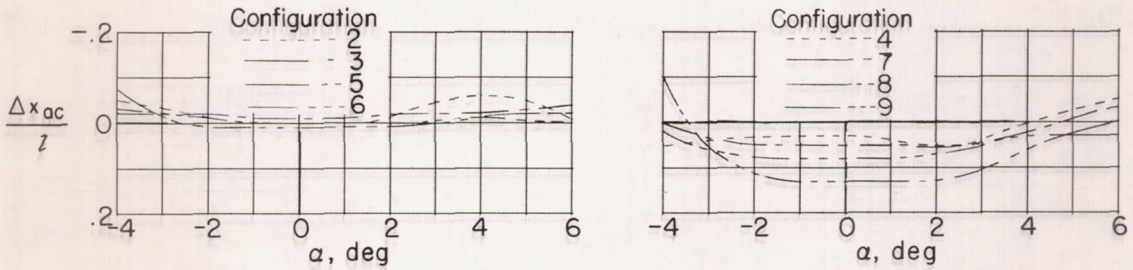

(b) Change in aerodynamic-center locations due to installation of bomb bay or bomb plus bomb bay to basic body.

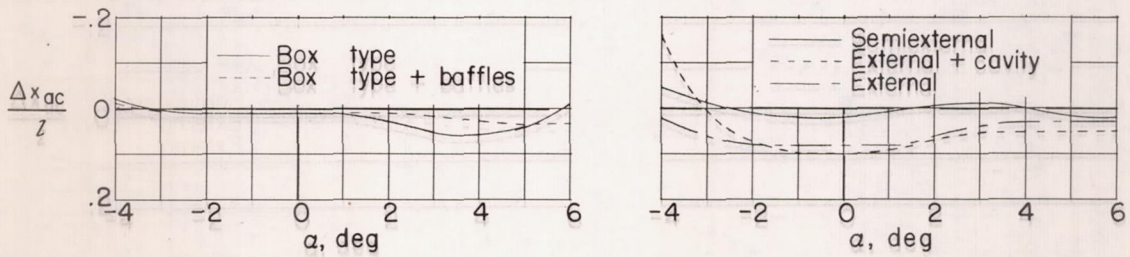

(c) Change in aerodynamic-center locations due to addition of bomb to bomb bay.

Figure 14.- Aerodynamic-center locations and changes at M = 2.40.

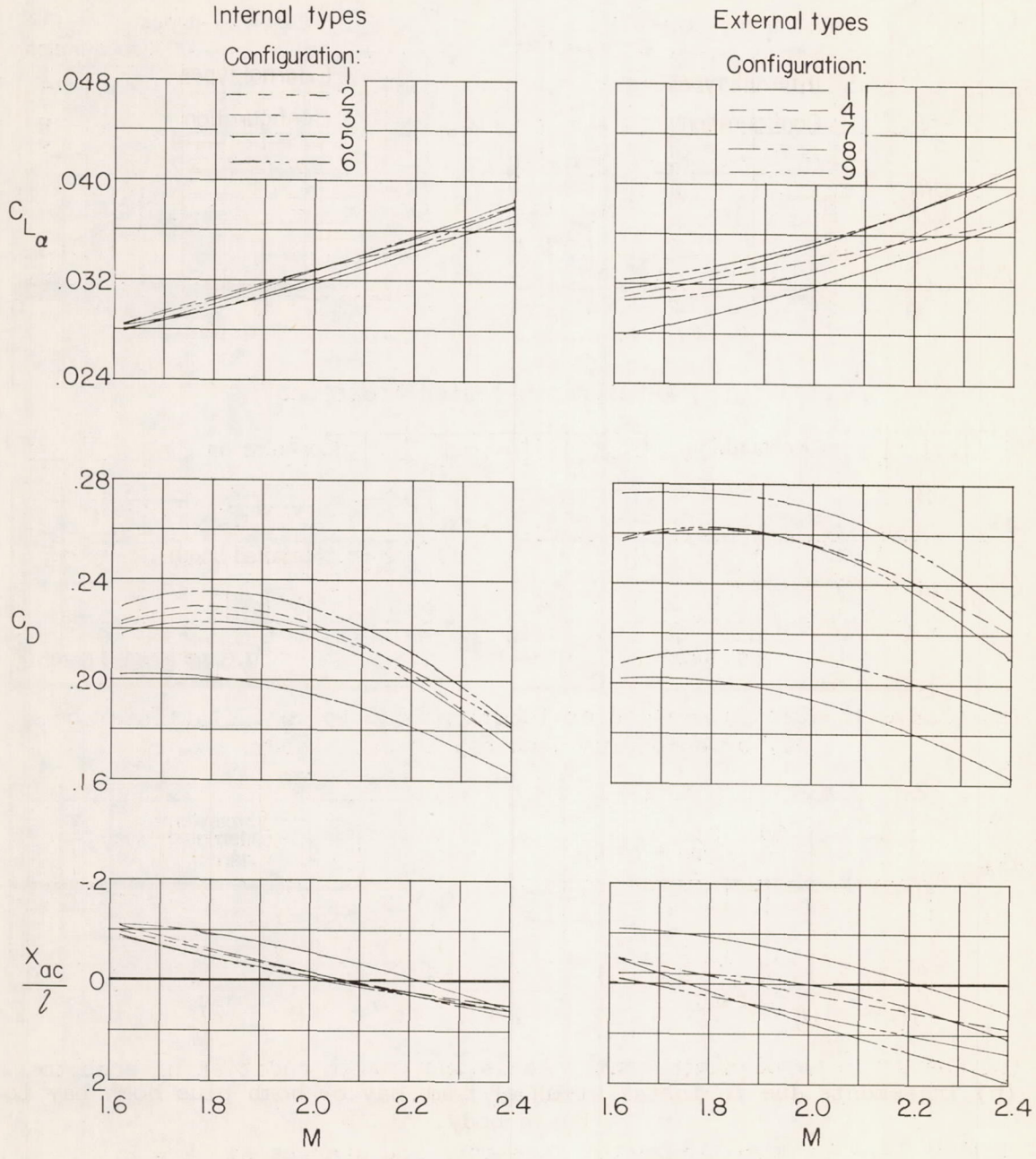

(a) Lift slope, drag, and aerodynamic-center locations.

Figure 15.- Pertinent measured results at $\alpha = 0^\circ$ for various Mach numbers.

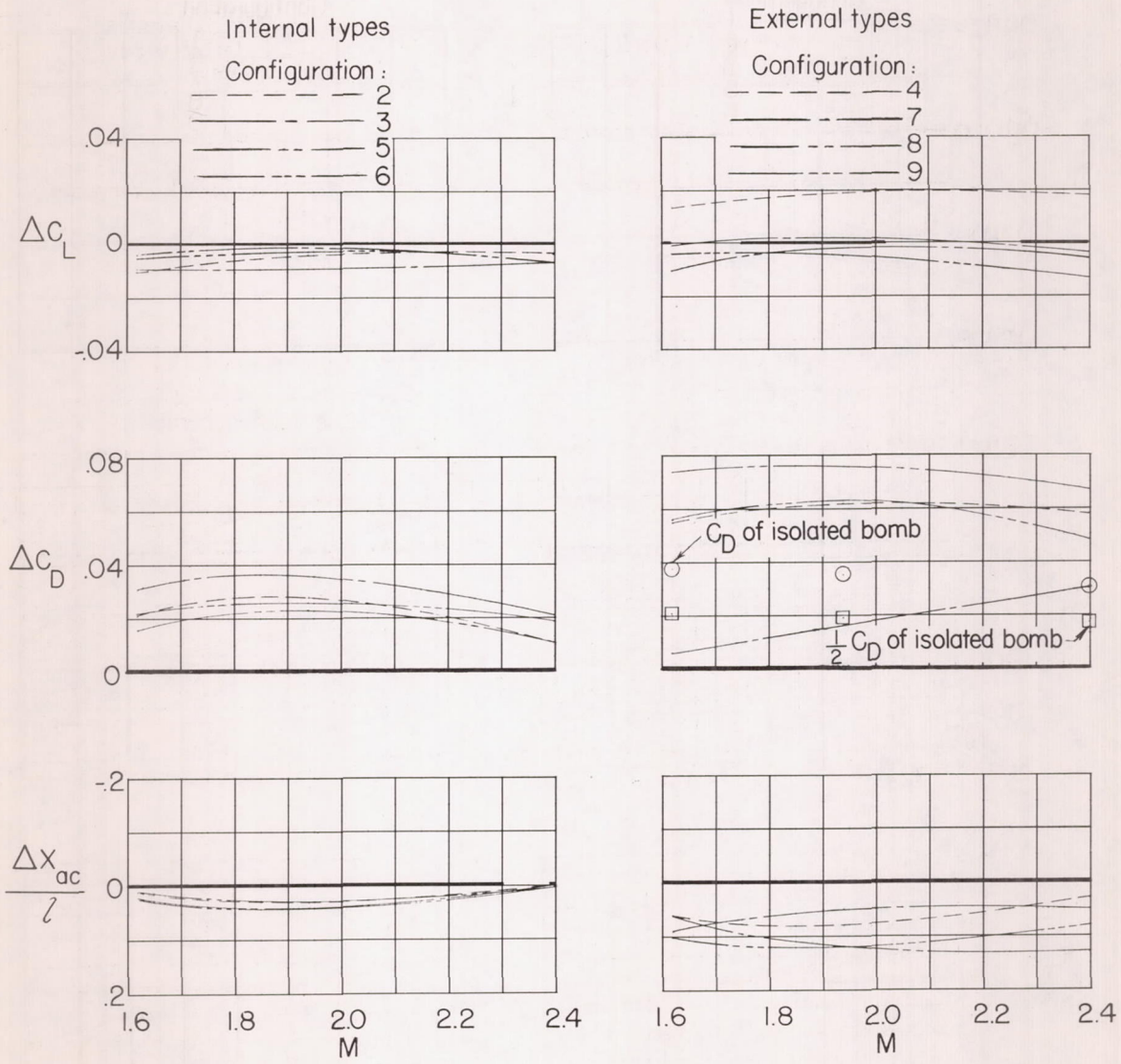

(b) Increments due to installation of bomb bay or bomb plus bomb bay to basic body.

Figure 15.- Continued.

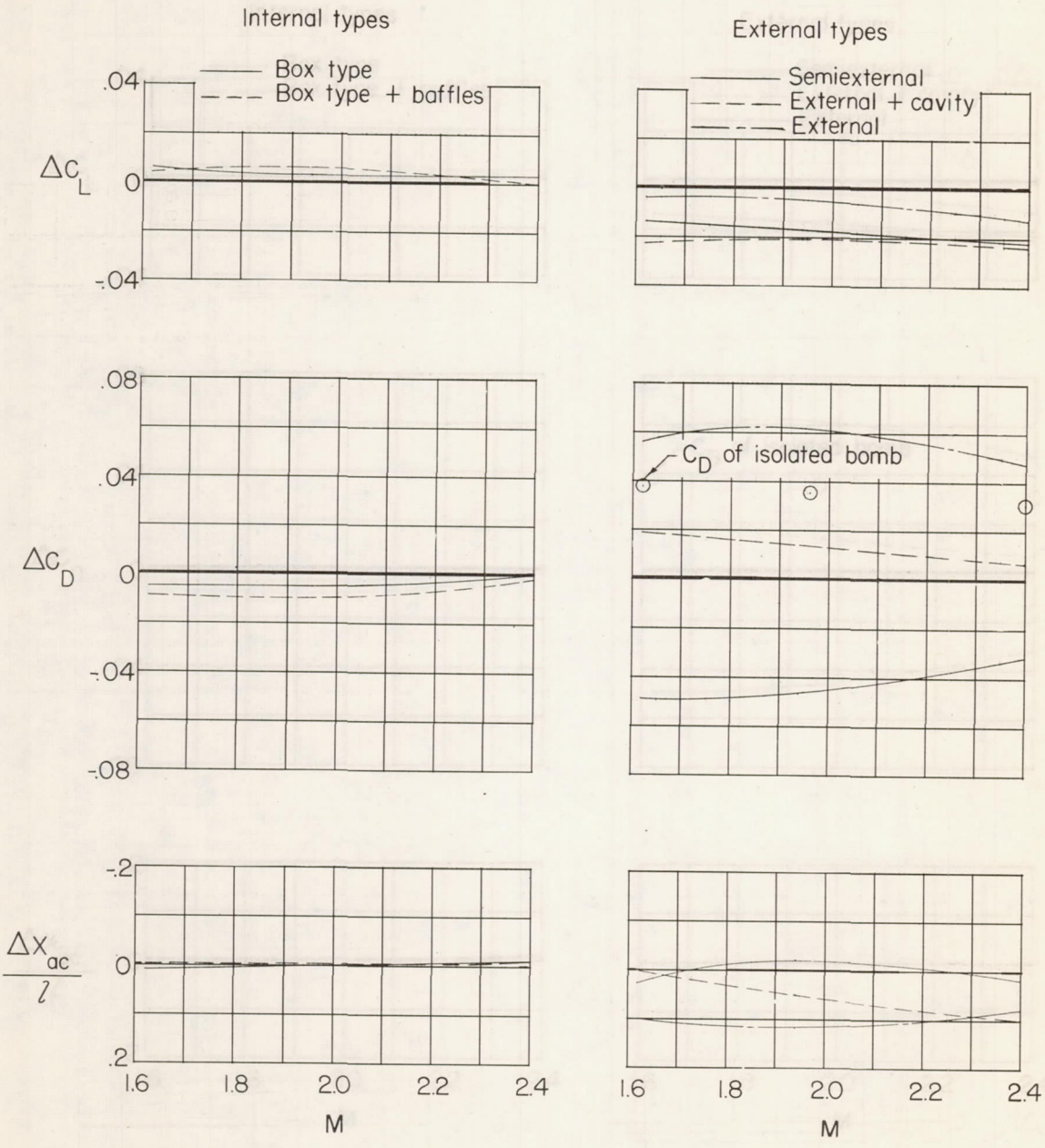

(c) Increments due to addition of bomb to bomb bay.

Figure 15.- Concluded.

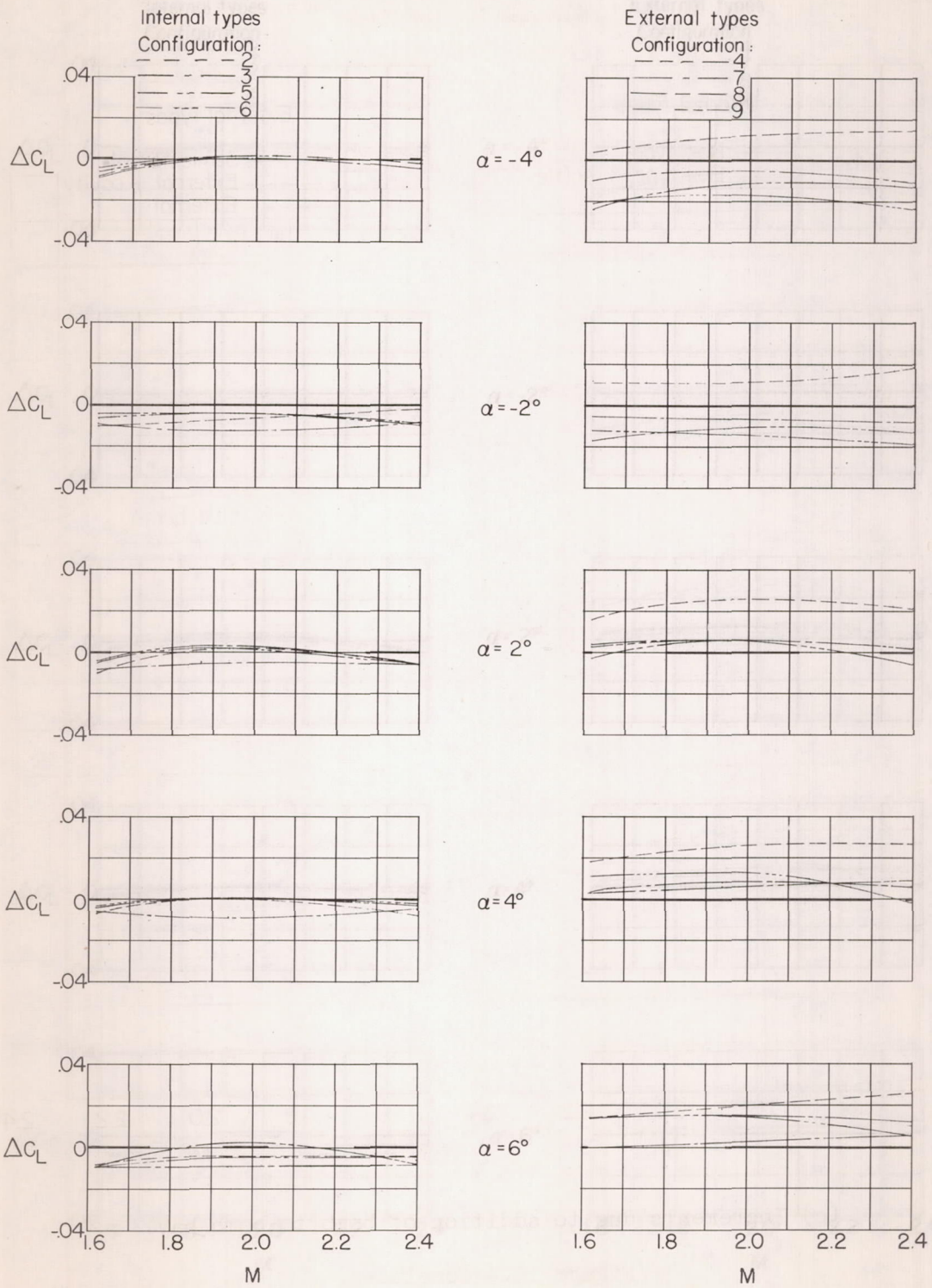

(a) Due to installation of bomb bay or bomb plus bomb bay to basic body.

Figure 16.- Incremental lifts at various Mach numbers at $\alpha \neq 0°$.

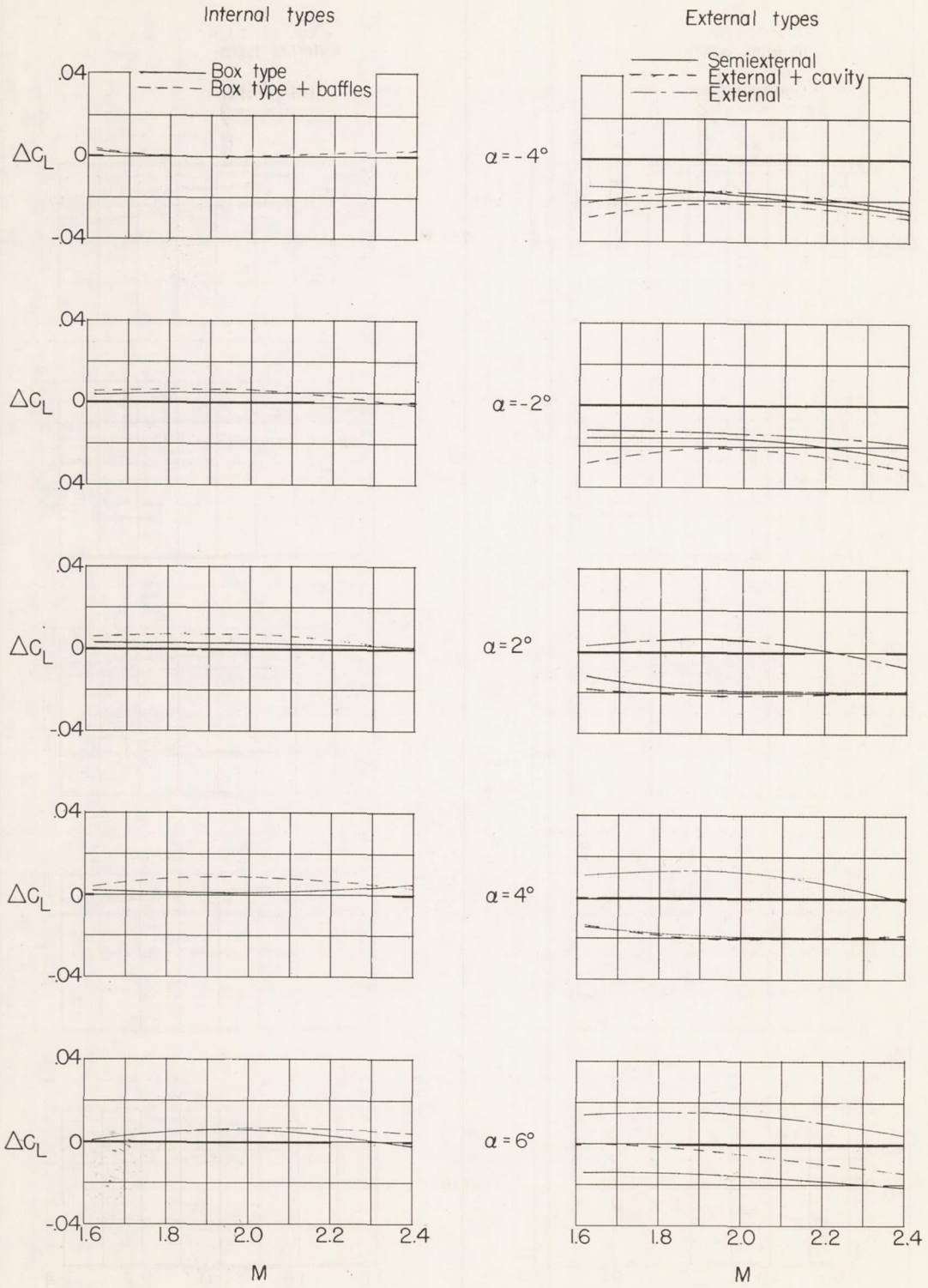

(b) Due to addition of bomb to bomb bay.

Figure 16.- Concluded.

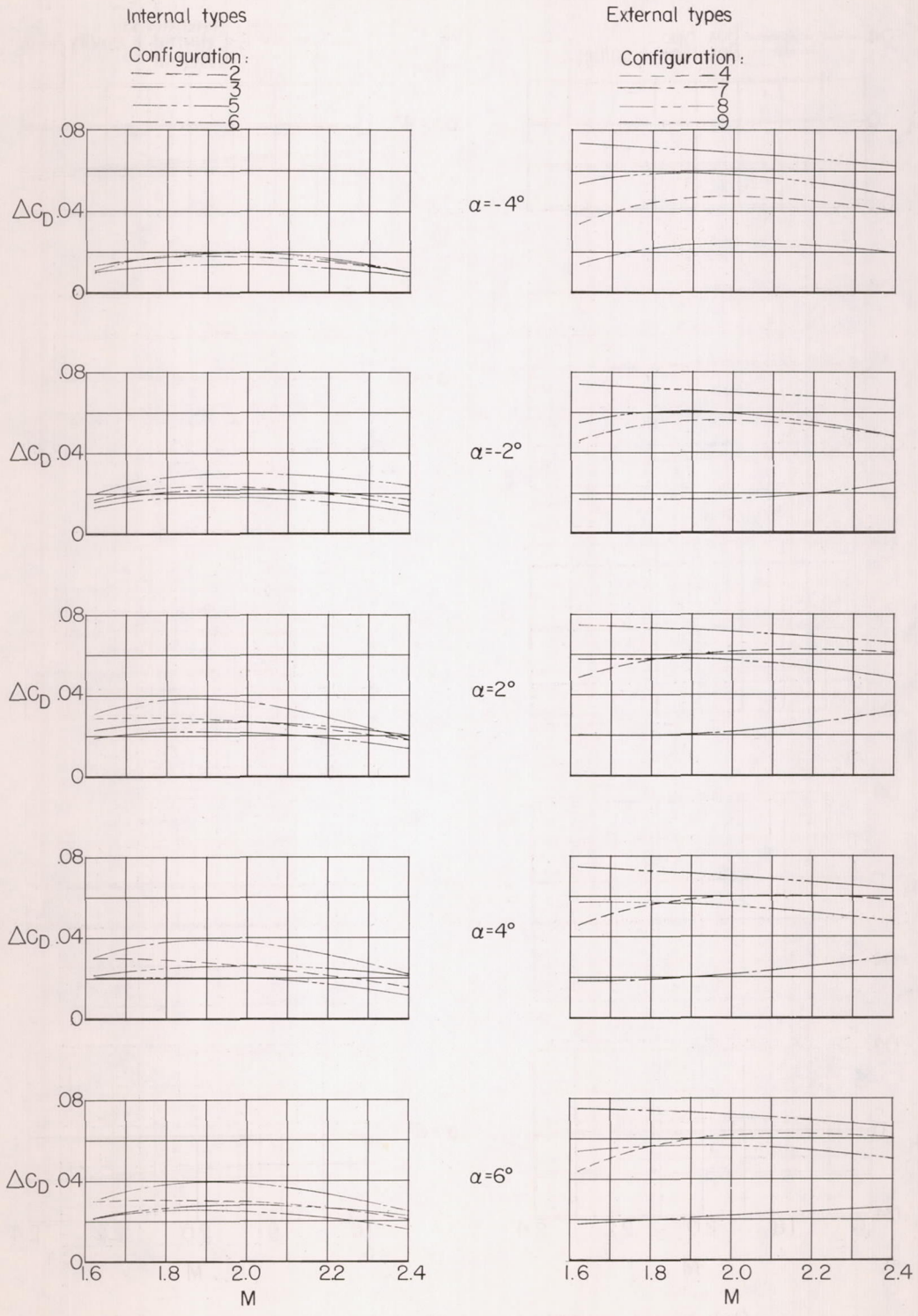

(a) Due to installation of bomb bay or bomb plus bomb bay to basic body.

Figure 17.- Incremental drags at various Mach numbers at $\alpha \neq 0^\circ$.

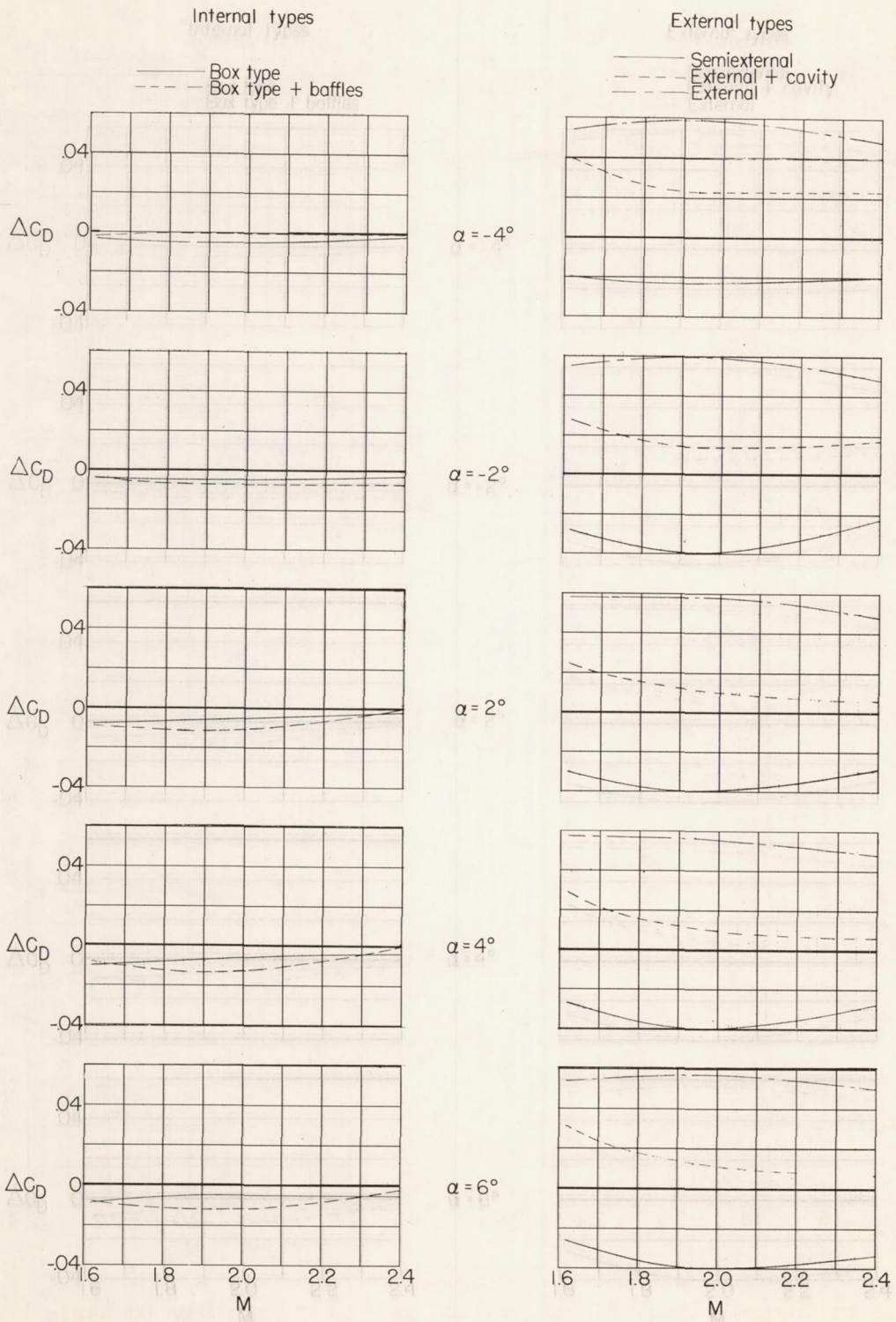

(b) Due to addition of bomb to bomb bay.

Figure 17.- Concluded.

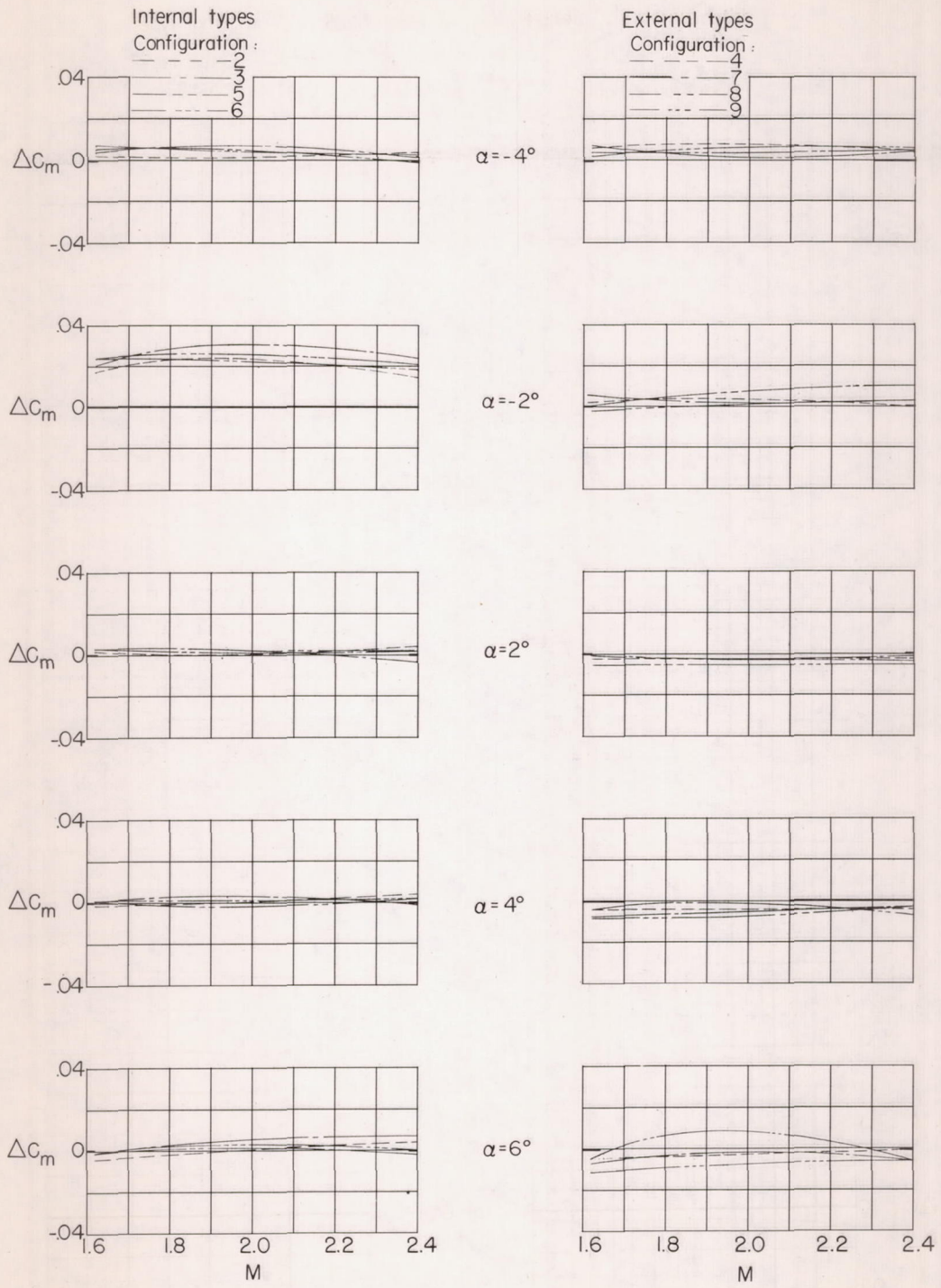

(a) Due to installation of bomb bay or bomb plus bomb bay to basic body.

Figure 18.- Incremental pitching moments at various Mach numbers at $\alpha \neq 0°$.

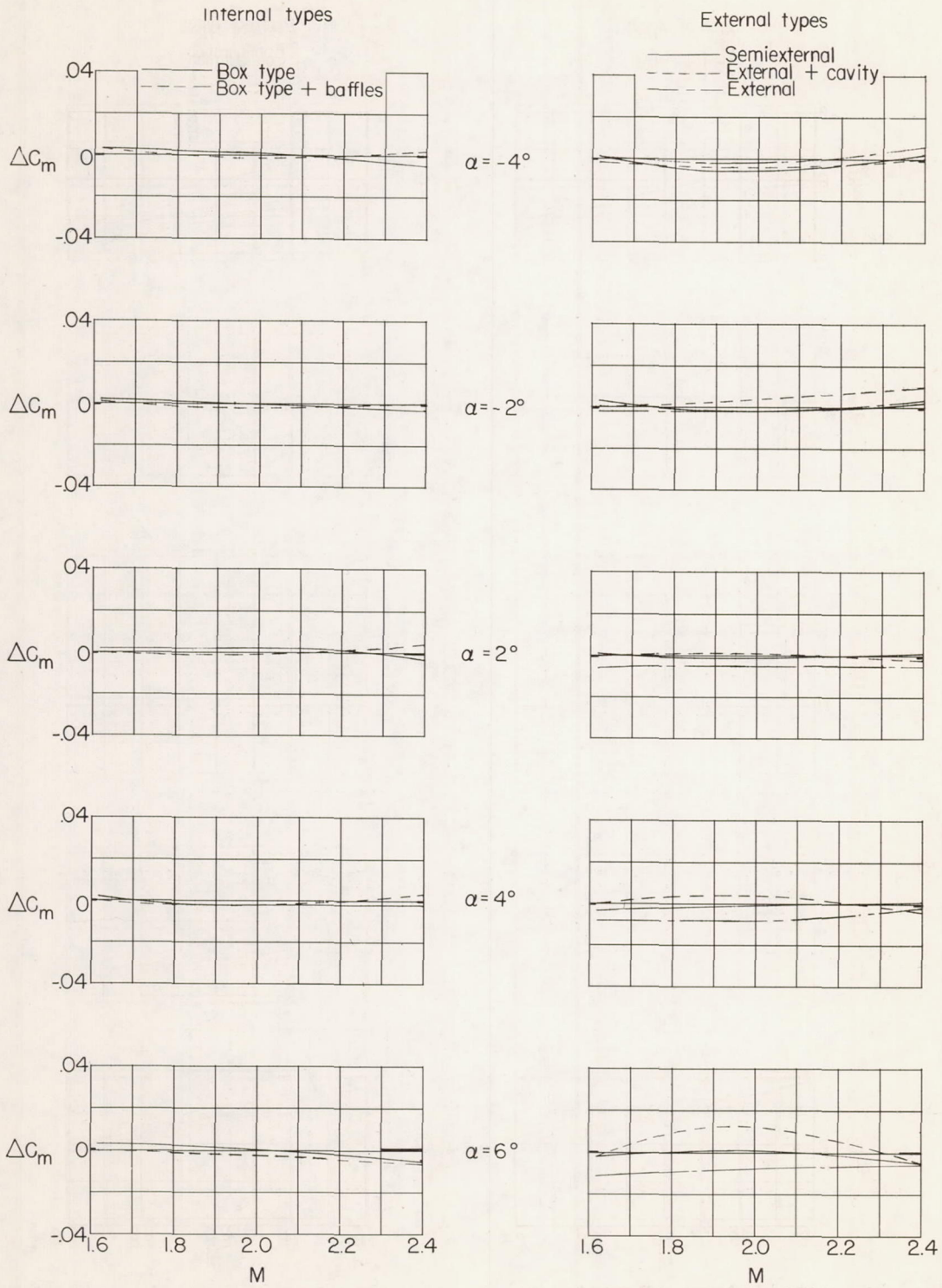

(b) Due to addition of bomb to bomb bay.

Figure 18.- Concluded.

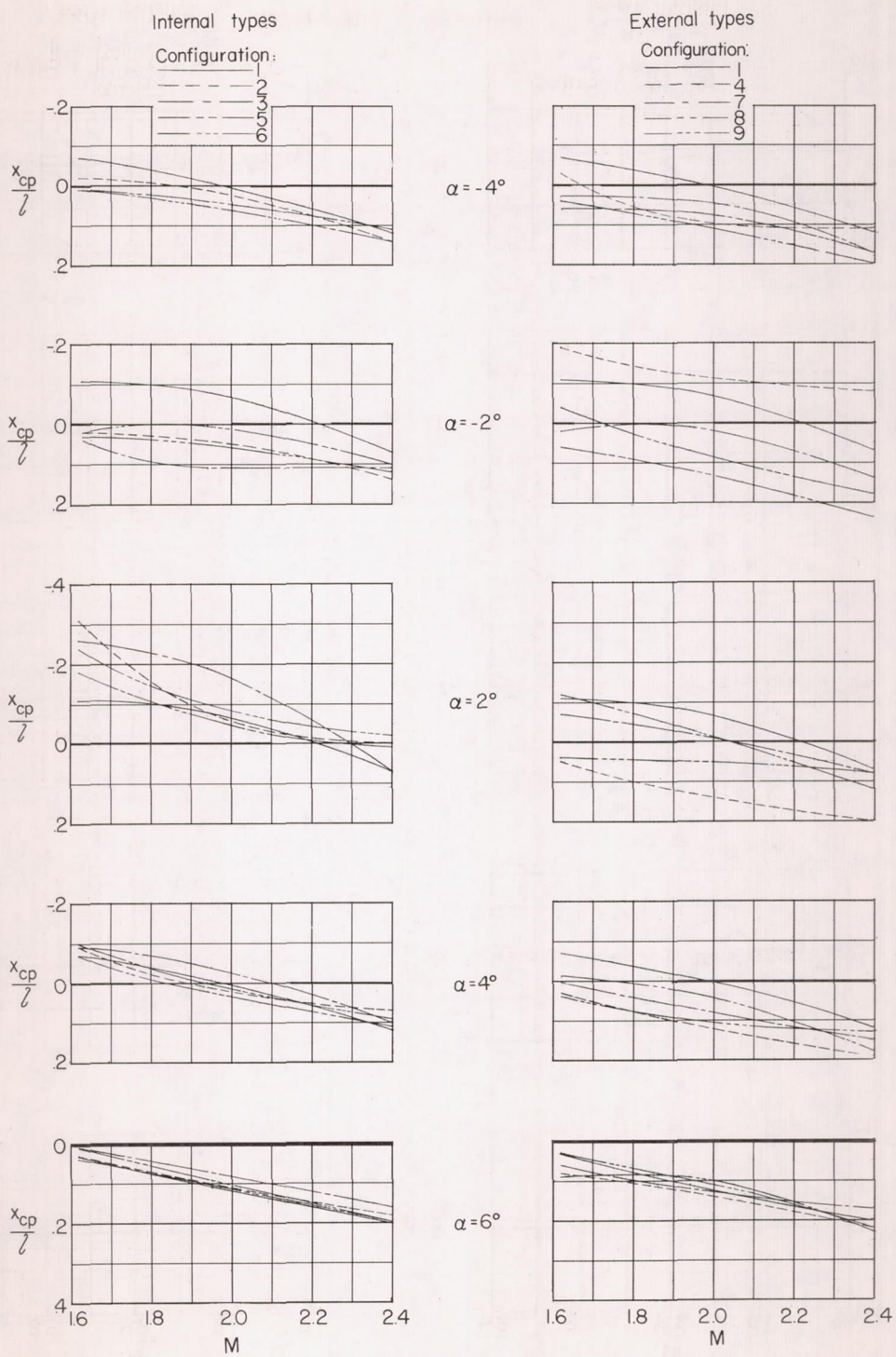

(a) Center-of-pressure locations.

Figure 19.- Center-of-pressure locations and changes at various Mach numbers at $\alpha \neq 0^{\circ}$.

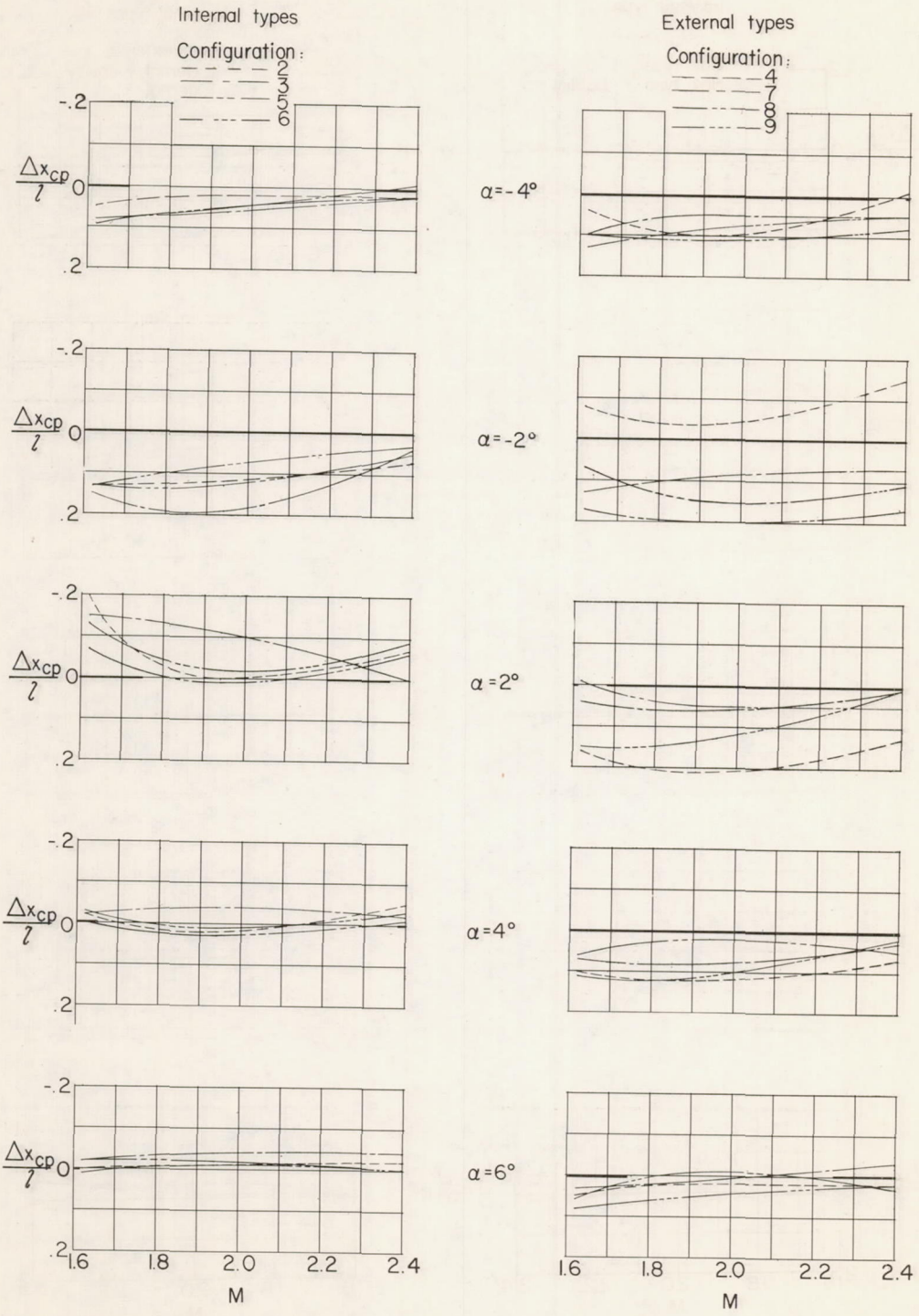

(b) Change in center-of-pressure locations due to installation of bomb bay or bomb plus bomb bay to basic body.

Figure 19.- Continued.

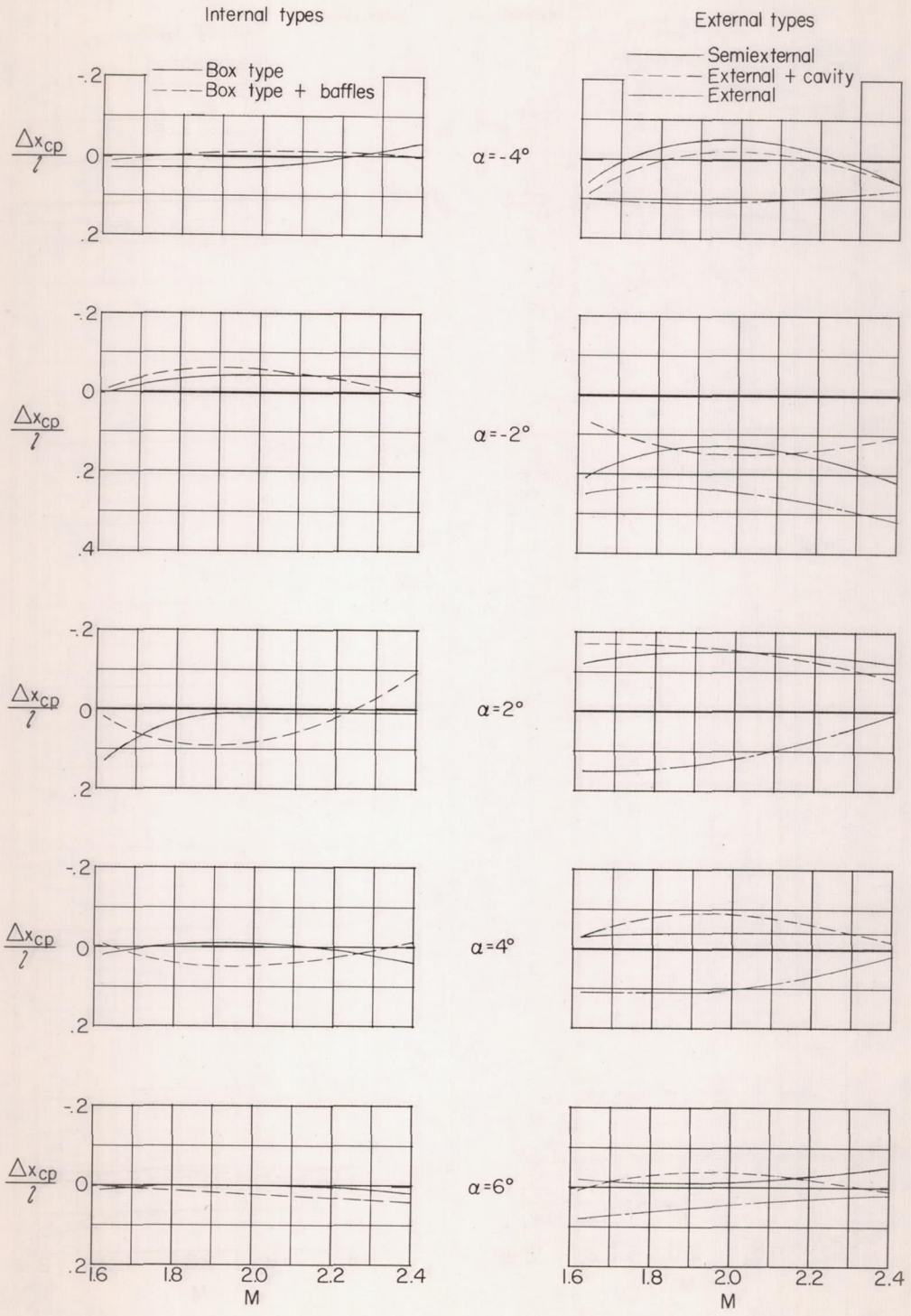

(c) Change in center-of-pressure locations due to addition of bomb to bomb bay.

Figure 19.- Concluded.

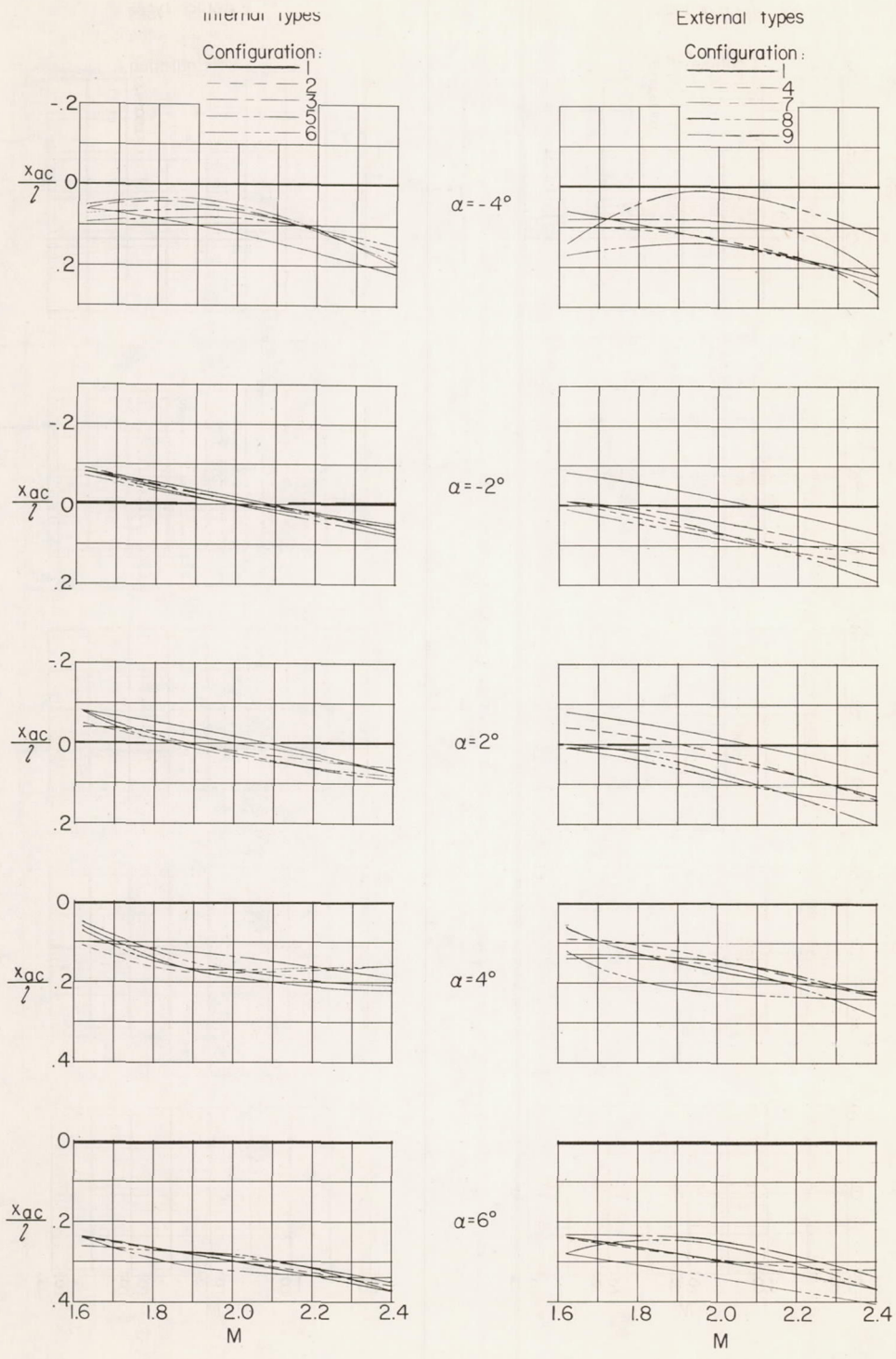

(a) Aerodynamic-center locations.

Figure 20.- Aerodynamic-center locations and changes at $\alpha \neq 0^{\circ}$ at various Mach numbers.

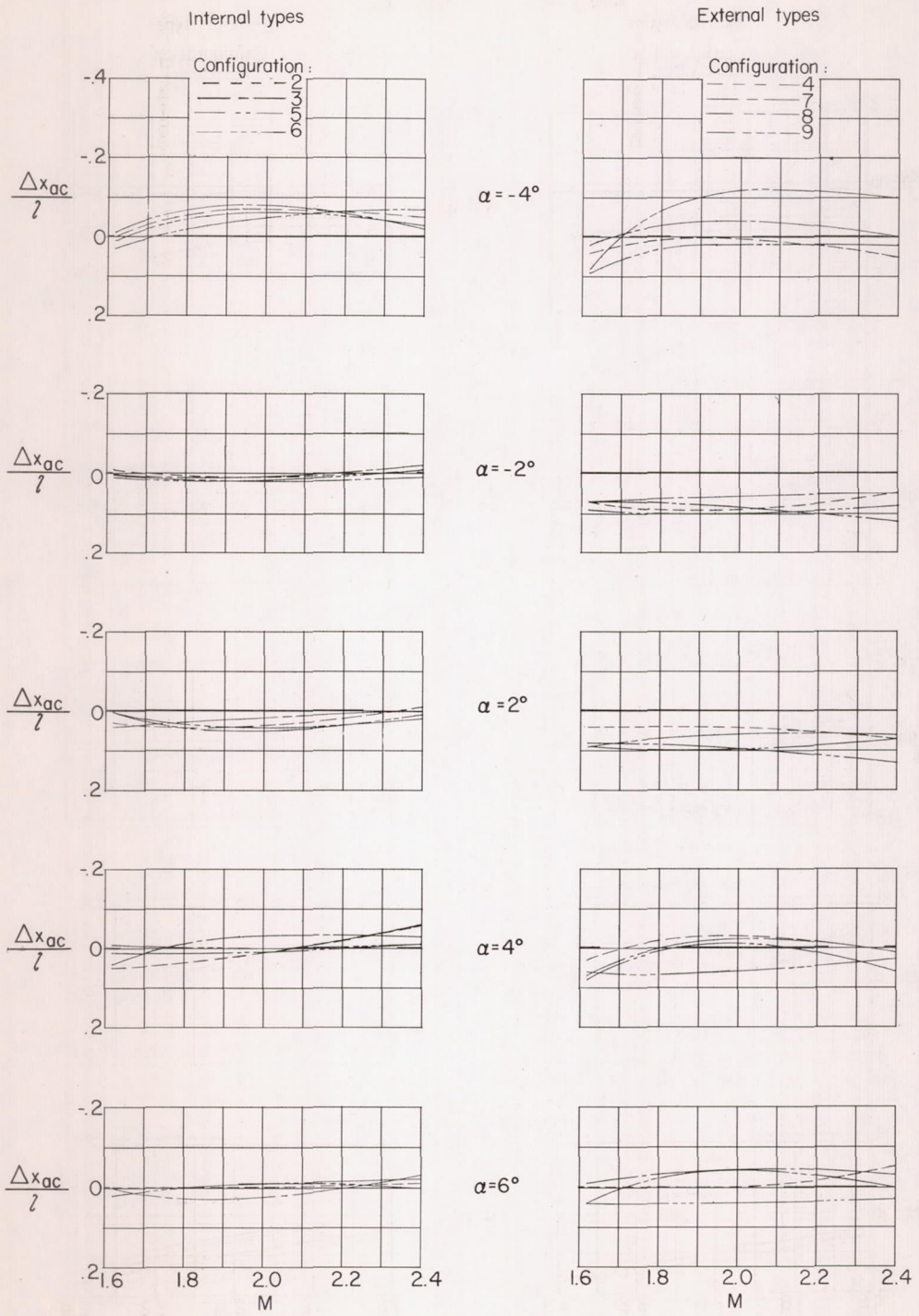

(b) Change in aerodynamic-center location due to installation of bomb bay or bomb plus bomb bay to basic body.

Figure 20.- Continued.

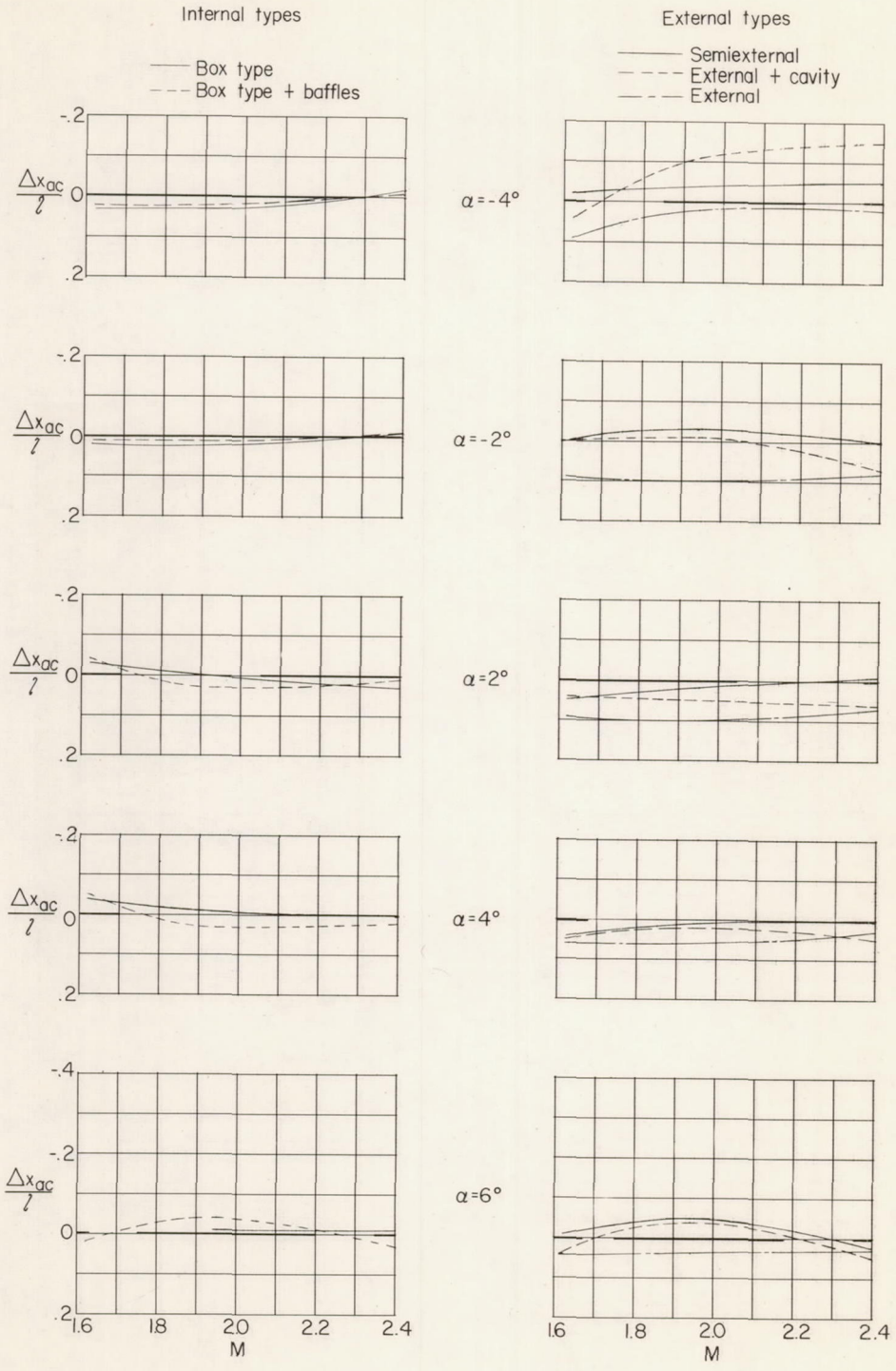

(c) Change in aerodynamic-center location due to addition of bomb to bomb bay.

Figure 20.- Concluded.

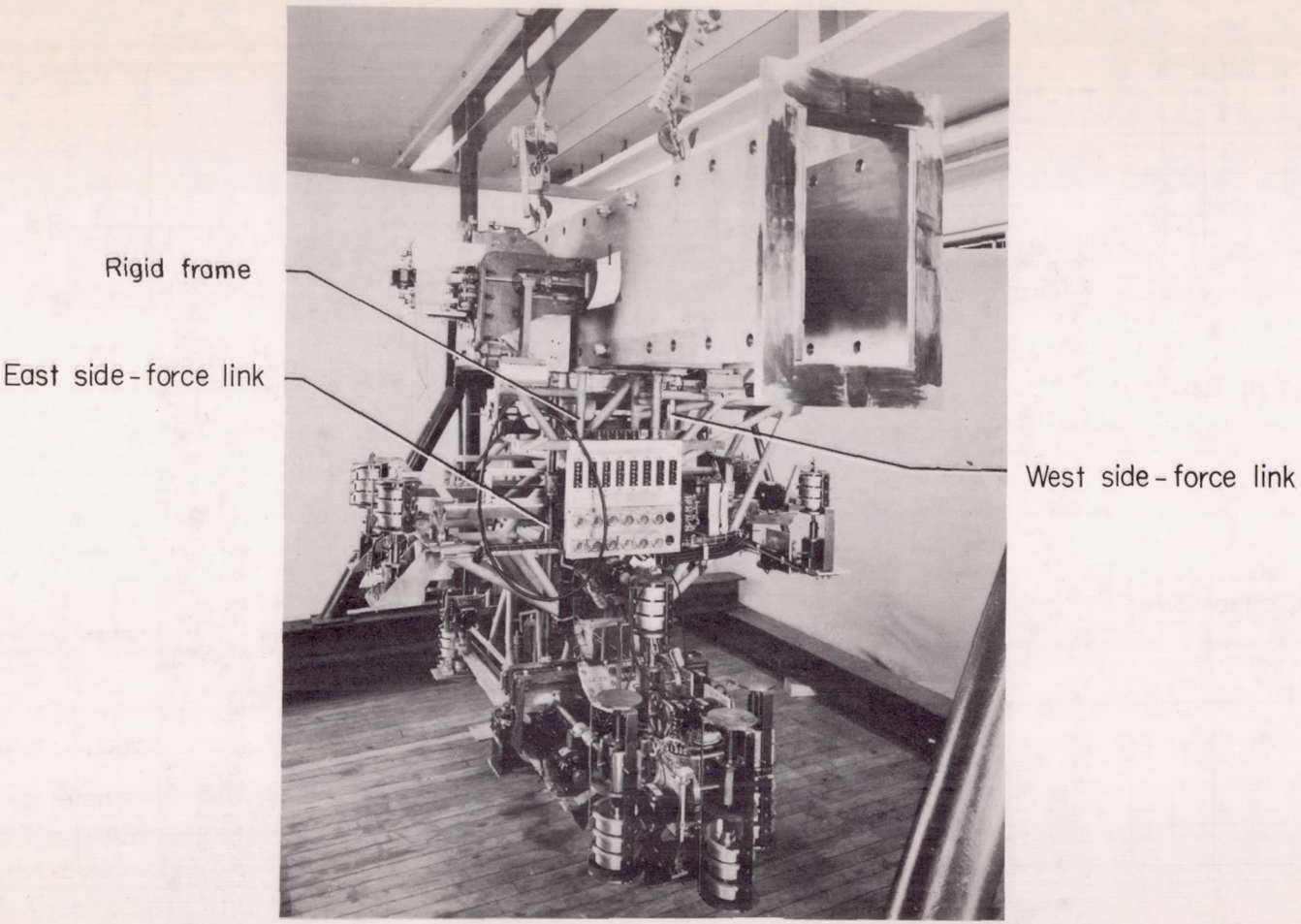

(a) Downstream, east view. L-79443.1

Figure 21.- The six-component-balance assembly at the Langley 9-inch supersonic tunnel (box removed).

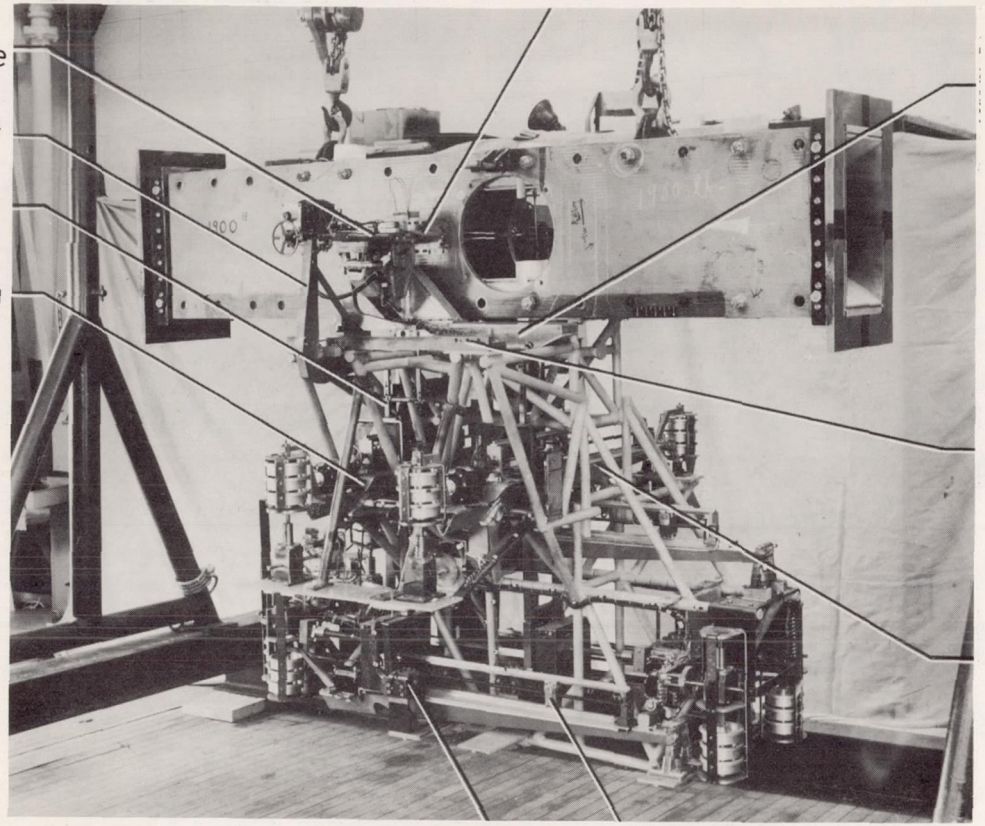

L-79446.1

(b) Upstream, west view.

Figure 21.- Continued.

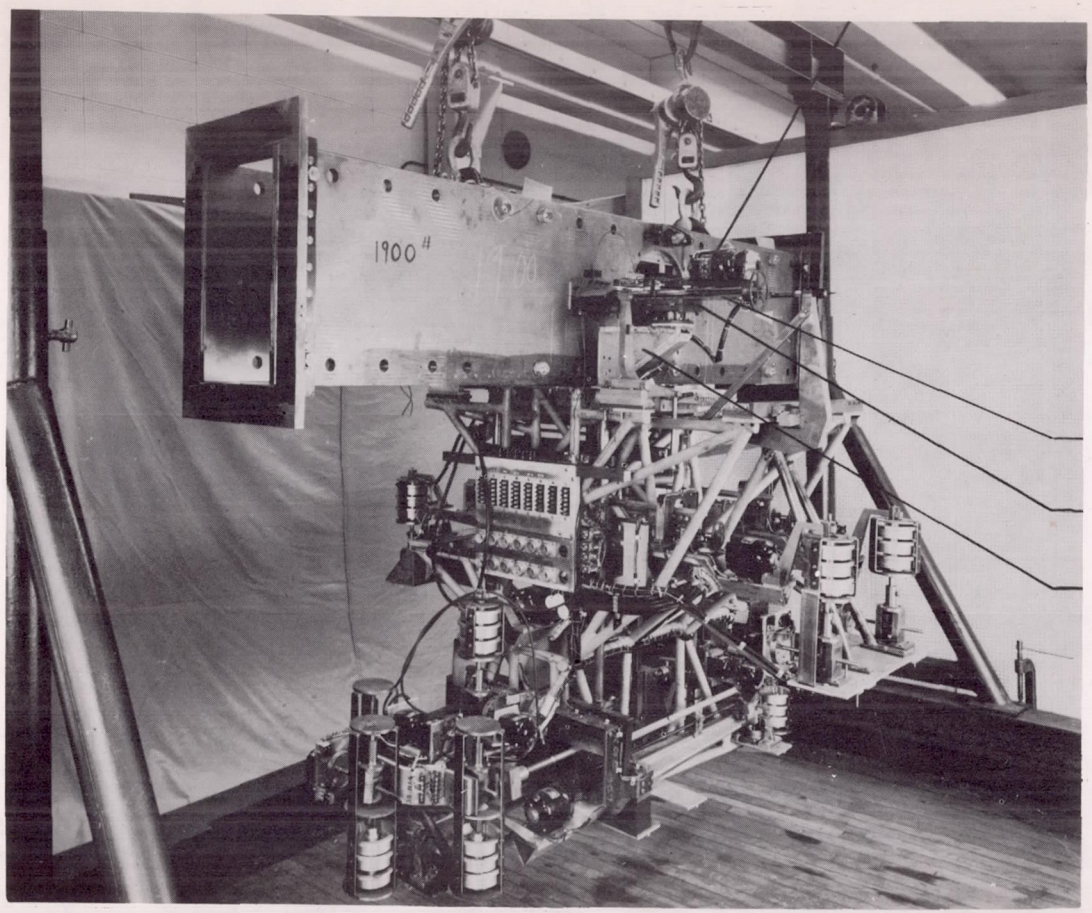

L-79444.1

(c) Downstream, west view.

Figure 21.- Continued.

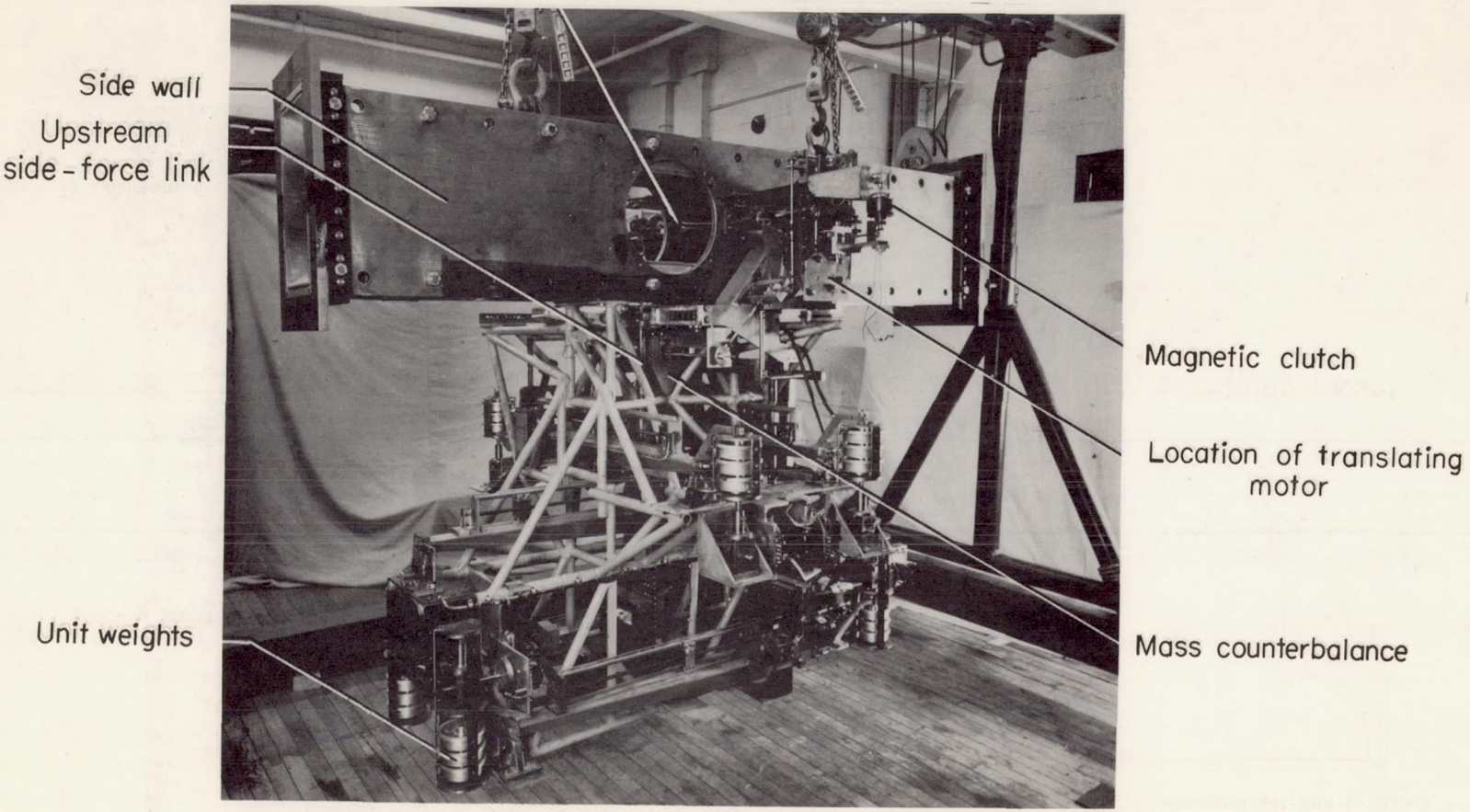

L-79445.1

(d) Upstream, east view.

Figure 21.- Continued.

CONFIDENTIAL

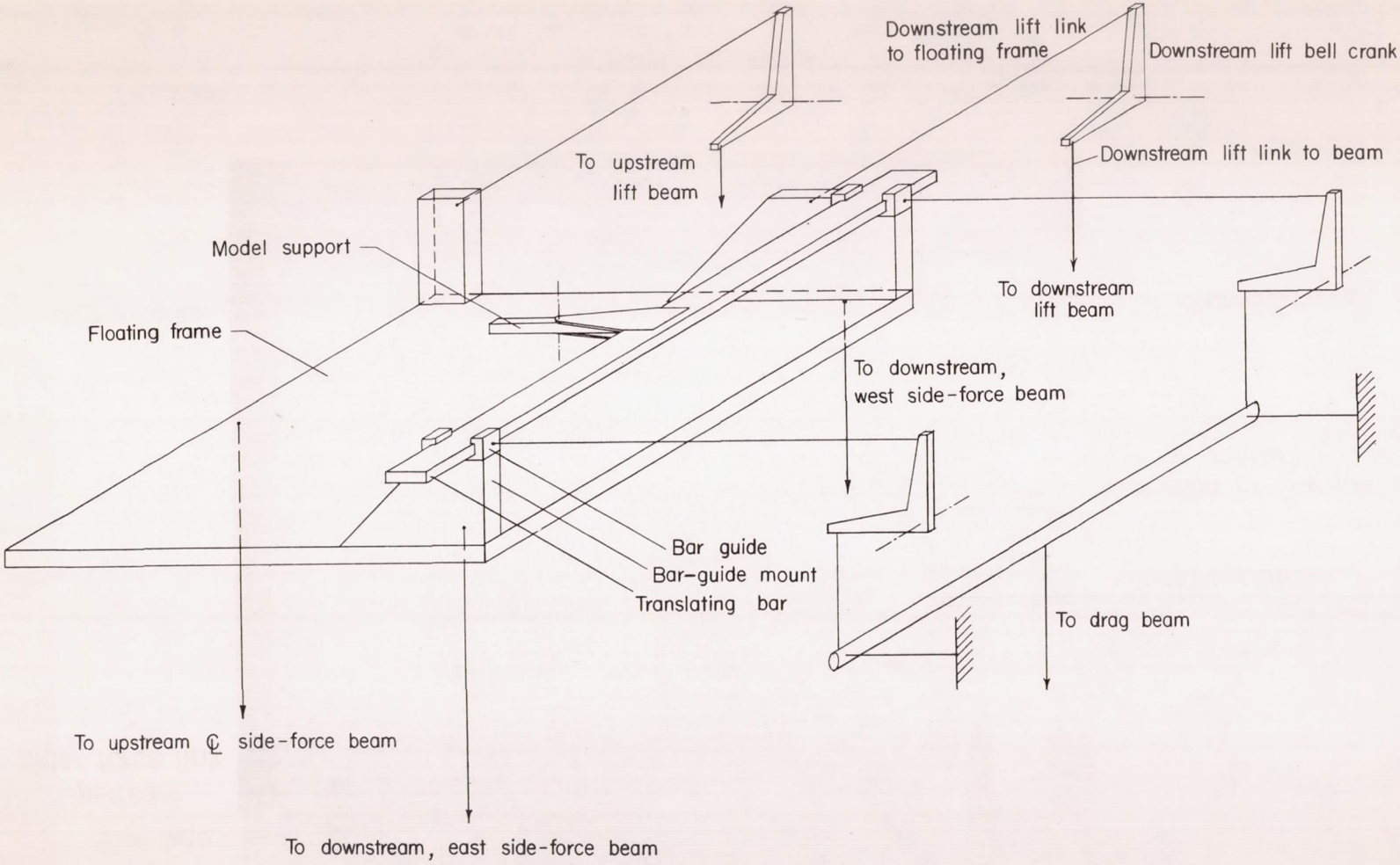

(e) Isometric drawing of major components.

Figure 21.- Concluded.